

N71-31421
NASA CR-119317

Final Report-Phase I

**ANALYSIS OF ATS PHOTOGRAPHS USING
A SPECIALLY DESIGNED ELECTRONIC CONSOLE**

Prepared for:

GODDARD SPACE FLIGHT CENTER
GREENBELT, MARYLAND 20771

CASE FILE
COPY



STANFORD RESEARCH INSTITUTE
Menlo Park, California 94025 · U.S.A.



STANFORD RESEARCH INSTITUTE
Menlo Park, California 94025 · U.S.A.

Final Report-Phase I
(8 October 1969 - 8 October 1970)

ANALYSIS OF ATS PHOTOGRAPHS USING A SPECIALLY DESIGNED ELECTRONIC CONSOLE

By: ROY H. BLACKMER, Jr.
ELDON J. WIEGMAN
SIDNEY M. SEREBRENY
REX G. HADFIELD

Prepared for:

GODDARD SPACE FLIGHT CENTER
GREENBELT, MARYLAND 20771

Contracting Officer: HENRY ARISTA
Technical Monitor: WILLIAM E. SHENK

CONTRACT NAS5-21086

SRI Project 8244

Approved by:

R. T. H. COLLIS, *Director*
Aerophysics Laboratory

RAY L. LEADABRAND, *Executive Director*
Electronics and Radio Sciences Division

ABSTRACT

The objective of this study has been to demonstrate the capability of the SRI/NASA Electronic Display System as an aid in the analysis and interpretation of ATS cloud data, and evaluation of the limitations in obtaining useful information on cloud motion imposed by oblique viewing and/or resolution of the ATS camera. This System applies the techniques of electronic scanning, storage, display, and data processing to the analysis of cloud imagery. A closed-circuit TV yielding time-lapse viewing, plus electronic cursors to track and measure cloud motion, are some of the prime advantages of the equipment.

Capability was assessed in three diverse tasks, as follows:

- (1) Identification of cloud-height and measurements of cloud displacements at large angles of view (using only ATS cloud photographs) were evaluated through the use of the equipment and compared to the evaluation made by a second investigator of the same data, using ATS photographs and concomitant ESSA satellite photographs.
- (2) The distribution of cloud types and heights, determined from cloud-motion measurements of ATS III photographic data, was compared to the cloud cover viewed by Apollo 6 between the east coast of the U.S. and the west coast of Africa on 4 April 1968.
- (3) Growth rates and movements of cumulonimbus anvils were evaluated and compared to the occurrence and severity of the attendant weather and with the wind shear at appropriate levels.

CONTENTS

ABSTRACT. iii

LIST OF ILLUSTRATIONS vii

LIST OF TABLES. xi

ACKNOWLEDGMENT. xiii

I INTRODUCTION 1

 A. Objectives. 1

 B. Research Tasks. 1

 C. SRI/NASA Electronic Display System. 2

II MEASUREMENT CAPABILITY AT VARIOUS ANGLES OF VIEW 5

 A. Method of Measurement 7

 B. Effect on Cloud Motion Measurements 11

III CLOUD IDENTIFICATION AND MEASUREMENT 15

 A. Comparison of Cloud Height Estimates
 Using ATS and ESSA Photographs. 15

 B. Comparison of Cloud Motions Measured
 by Different Investigators. 29

 1. Magnitude of Differences 29

 2. Location of Differences. 31

 C. Comparison of Cloud Data and Rawinsonde Data. 38

 1. Cloud Motions and Wind at Level of Best Fit. 38

 2. Observed Cloud Types and Level of Best Fit 40

 D. Summation 46

IV COMPARISON OF APOLLO 6 AND ATS III DATA. 49

 A. Synoptic Situation and Cloud Types. 50

 B. Cloud Measurements. 55

C.	Summation	65
V	COMPARISON OF CLOUD GROWTH RATES WITH OBSERVED SEVERE STORM ACTIVITY.	67
A.	Measurement of Cloud Growth	68
B.	Discussion of Days Studied.	69
C.	Cloud Size and Time Changes in Cloud Size Related to Severity of Associated Weather	84
D.	Cloud Motion and Growth Related to Wind Shear	90
E.	Summation	90
	REFERENCES.	95

ILLUSTRATIONS

Figure 1	SRI/NASA Electronic Display System	3
Figure 2	Block Diagram of Data Processing Procedure . .	4
Figure 3	Geometric Relationships Concerning Angle of View.	5
Figure 4	ATS III Grid with Angles of View (in Degrees) Superimposed.	6
Figure 5	Earth Distance per Cursor Unit at Various Latitudes and Angles of View	8
Figure 6	Effect on Cloud Measurement Comparison through Unit Cursor Variation (selected data).	12
Figure 7	Selected Cloud Data, 12 April 1968	16
Figure 8	Selected Cloud Data, 18 April 1968	18
Figure 9	Selected Cloud Data, 23 April 1968	20
Figure 10	Selected Cloud Data, 28 April 1968	22
Figure 11	Selected Cloud Data, 29 April 1968	24
Figure 12	Selected Cloud Data, 30 April 1968	26
Figure 13	Differences (direction and speed) between Independent Measurements of Same Clouds	30
Figure 14	Location of Compared Measurements (66 cases) .	32
Figure 15	Comparison of Cloud Motion with Wind at Level of Best Fit	41

Figure 16	Differences between Cloud Motion and Rawin as a Function of Angles of View.	42
Figure 17	Cumulative Frequency of Differences between Cloud Motion and Wind at Level of Best Fit.	43
Figure 18	Level of Best Fit and Nearest Reported Cloud Cover for 43 Cases within 60 nmi of Rawinsonde Station.	45
Figure 19	Synoptic Situation at 1200 GMT on 4 April 1968 and Locations of Clouds Measured Along Track of Apollo 6.	52
Figure 20	ATS III View of Cloud Cover Along Track of Apollo 6.	54
Figure 21	Comparison of Cloud Elements Shown by Apollo 6 ATS III Photographs.	56
Figure 22	Cloud Motions Superimposed over Selected Sections of Apollo 6 Mosaics	58
Figure 23	Details of Cumulus Cell Distribution	62
Figure 24	Details of Motion in Multiple Layers	64
Figure 25	Cloud Cover on 28 April 1968	72
Figure 26	Cloud Cover on 17 and 18 April 1968.	74
Figure 27	Cloud Cover on 19 April 1968	76
Figure 28	Cloud Cover on 30 April 1968	77
Figure 29	Cloud Cover on 23 April 1968	79
Figure 30	Time Changes in Cloud Areas and Severity of Associated Weather on 23 April 1968	86
Figure 31	Weather Categories Associated with Cloud Elements of Various Sizes.	88

Figure 32	Comparison of Direction of Cloud Motion and Direction of Wind Shear.	91
Figure 33	Comparison of Cloud Growth and Speed of Wind Shear.	92

TABLES

Table 1	Distance from Satellite Subpoint (expressed in degrees of latitude) for Various Angles of View . .	6
Table 2	Distance in Nautical Miles per Cursor Unit at Selected Latitudes and Angles of View.	10
Table 3	Average Cloud Motion Change Through Unit Cursor Variation.	13
Table 4	Frequency of Levels of Best Fit (43 cases).	39
Table 5	Mean Differences between Cloud Motions and Wind at the Levels of Best Fit	44
Table 6	Cloud Distributions Along Track of Apollo 6	53
Table 7	GMT Times of Photographs Used in Cloud Growth Study.	68
Table 8	Weather Category Associated with Measured Cloud Elements.	71

ACKNOWLEDGMENT

The authors wish to acknowledge the contributions of R. M. Trudeau, Meteorological Associate, and A. G. Burris, Meteorological Assistant, of the Aerophysics Laboratory, Electronics and Radio Sciences Division, Stanford Research Institute, for their efforts in data processing and report preparation.

I INTRODUCTION

Serebreny, et al. (1967) reported on the development and operation of an electronic system that applies the techniques of electronic scanning, storage, display, and data processing to the analysis of cloud imagery obtained from Applied Technology Satellites. This system, known as the SRI/NASA Electronic Display System, was designed and constructed at SRI under NASA Contract NAS5-11652.

This system has since been used for a number of investigations in which the measurement of cloud displacement has been compared to the wind flow. Because of the experience and results achieved in those studies, NASA has supported the present investigation to examine the capabilities of the system in a wider variety of cloud studies.

A. Objectives

The objectives of this investigation have been to:

- (1) Demonstrate the capability of the SRI/NASA Electronic Display System to further the analysis and interpretation of ATS cloud data.
- (2) Evaluate the limitations in obtaining useful information on cloud motion imposed by oblique viewing and/or resolution of the ATS camera.

B. Research Tasks

The research tasks have been as follows:

Task 1--(a) Make measurements of cloud displacement at large angles of view, using only ATS cloud photographs, and compare them with measured winds; (b) independently make similar comparisons using both the same data sample of ATS cloud photographs and concomitant cloud photographs from ESSA polar-orbiting satellites and correlate the comparisons in (a) and (b).

Task 2--Evaluate the distribution of cloud types and heights of the cloud population using measurements of cloud motion observed on ATS-III photographs for 4 April 1968 over the same area viewed by the Apollo 6 between the east coast of the U.S. and the west coast of Africa on this date.

Task 3--Measure the growth rates and movements of cumulonimbus anvils occurring on six days during April 1968 and relate these to the severity of the attendant weather (hail, wind, tornadoes, etc.). [Three-dimensional radar precipitation echoes will be used as an aid in assessing storm severity.] Compare the growth rates and movements of the anvils with wind and wind shear at appropriate levels.

C. SRI/NASA Electronic Display System

The SRI/NASA Electronic Display System has been described fully elsewhere;¹ in brief, it consists of three separate but interconnected units, as shown in Figure 1. On the far right is a high-quality Vidicon

¹A complete description of the SRI/NASA Electronic Display System is given in Evans and Serebreny (1969).



FIGURE 1 SRI/NASA ELECTRONIC DISPLAY SYSTEM

camera, used as an input TV scanner of ATS photographic transparencies; the center console contains two magnetic disc memories and a television picture display, including electronically generated cross hairs (cursors); at the far left is a teletypewriter and paper tape punch, which provides both hard copy and machine-readable logging of data. These data are subsequently used as input for a computer program to derive the motion parameters.

The complete data processing procedure is indicated in Figure 2.

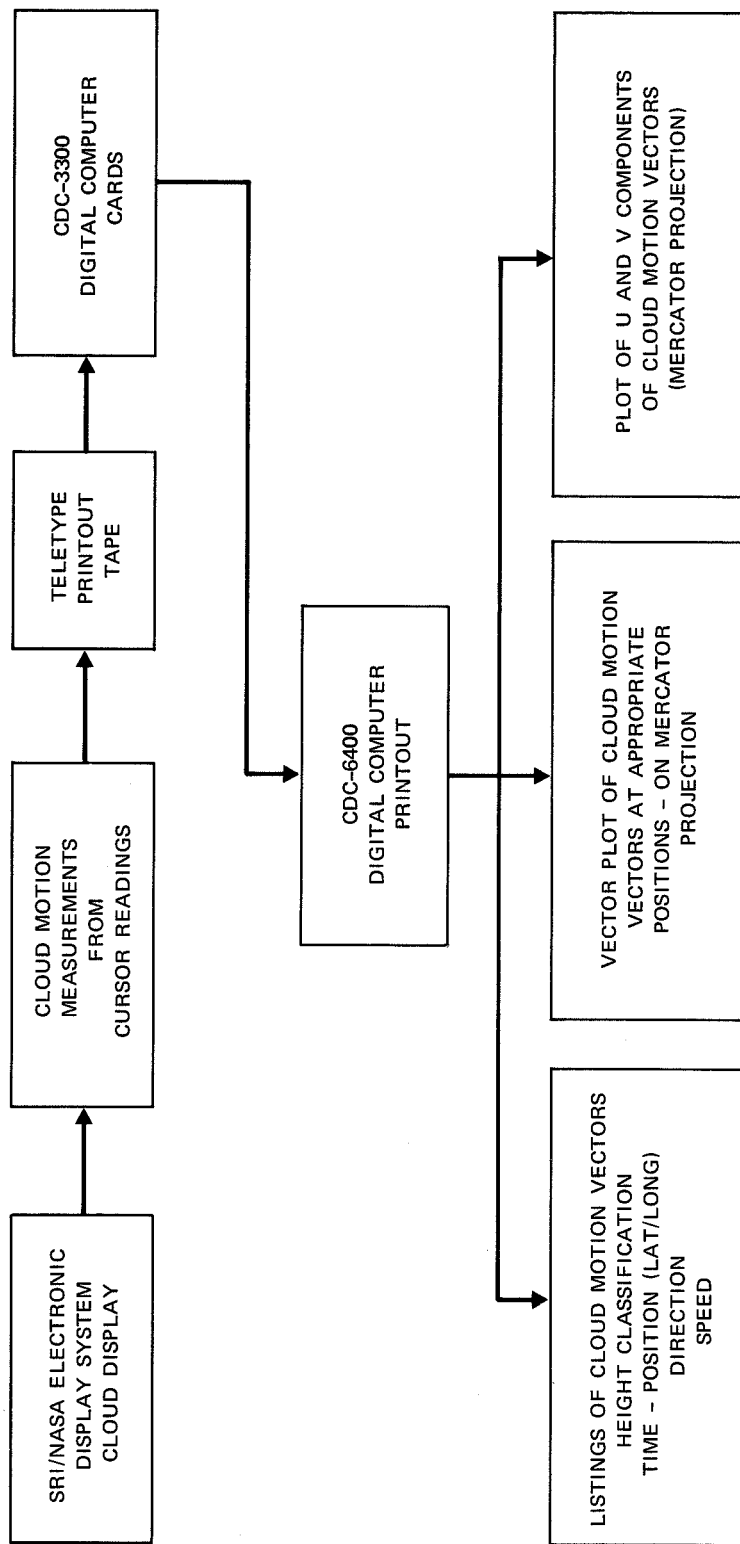
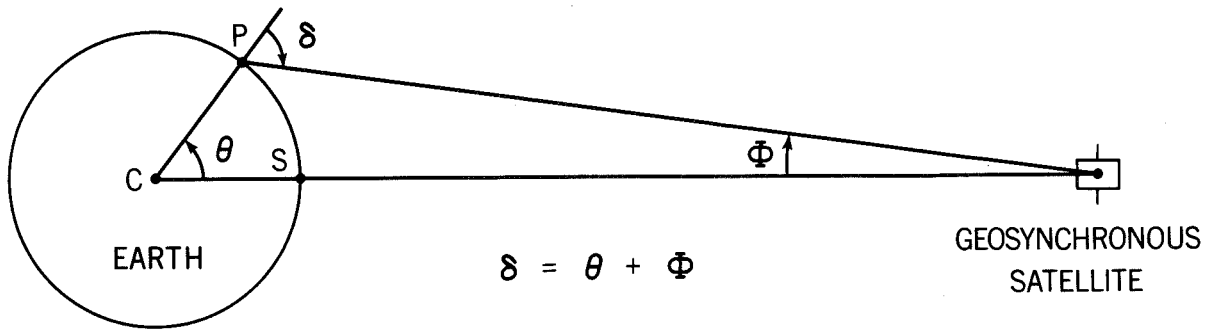


FIGURE 2 BLOCK DIAGRAM OF DATA PROCESSING PROCEDURE

II MEASUREMENT CAPABILITY AT VARIOUS ANGLES OF VIEW

Identification and measurement of clouds in an ATS photograph are affected by the geometrical relationships that exist between the earth and the satellite. Figure 3(after Shenk and Kreins, 1970) illustrates



Nadir angle Φ , local zenith angle δ (angle of view), and great circle arc θ for a satellite positioned in a geosynchronous orbit. Point P is an arbitrary point along the great circle, Point S is the subsatellite point, and Point C is at the center of the earth.

FIGURE 3 GEOMETRIC RELATIONSHIPS CONCERNING ANGLE OF VIEW

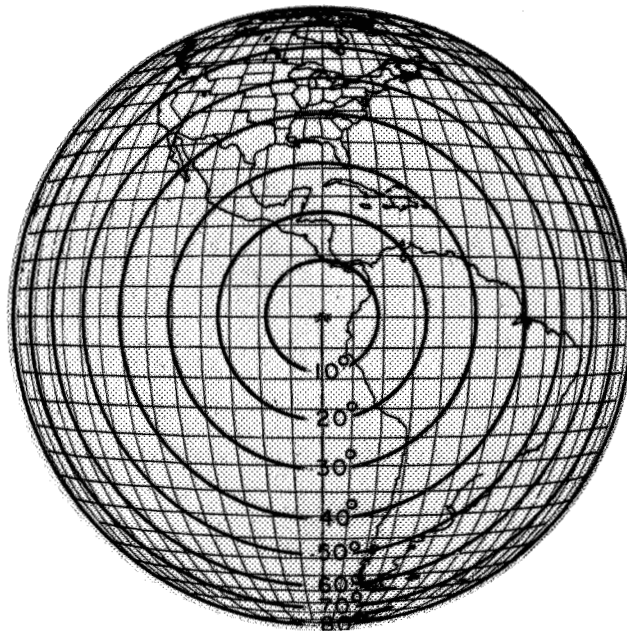
the geometric relations along a great circle passing through the subsatellite point between local zenith angle δ (which can be termed the angle of view), nadir angle Φ , and great circle arc θ . The change in angle of view expressed in degrees of latitude from the satellite subpoint is given in Table 1.

The overall effect of this change in the angle of view over an ATS picture is shown in Figure 4, from which it can be seen that the spacing between the viewing angles decreases as the latitude increases. For example, the spacing between angles of view of 60° and 70° is only half

Table 1

DISTANCE FROM SATELLITE SUBPOINT (EXPRESSED IN DEGREES
OF LATITUDE) FOR VARIOUS ANGLES OF VIEW

Angle of View (degrees)	Latitude from Satellite Subpoint (degrees)
10	8.5
20	17.0
30	25.5
40	34.5
50	43.5
60	52.5
70	62.1
80	71.5
90	81.3



Subpoint 0.0°N, 84.0°W

FIGURE 4 ATS III GRID WITH ANGLES OF VIEW (IN DEGREES) SUPERIMPOSED

that between 10° and 20° ; between 80° and 90° , the spacing is only one-tenth of that between 10° and 20° . This results in a great visual compression of cloud detail and spacing. Obviously, as the distance from the subsatellite point increases, cloud cover is viewed more obliquely, and greater difficulty may be encountered in accurately identifying and tracking a cloud.

A. Method of Measurement

The SRI/NASA Electronic Display System uses electronically generated x and y cursors as the basic measuring device. Cursor values, taken at the initial and final location of a cloud, define the specific distance a cloud element moves during a given time period. Since the number of x or y cursor positions are fixed at 400 and 490 intervals, respectively, the distance corresponding to a cursor unit on the displayed ATS photograph can differ, depending both on the size of the displayed photograph and on the angles of view of that portion of the photograph being viewed.

At the center of the ATS photograph, where a given picture distance covers a relatively small earth distance (small angle of view), a change of one cursor unit in an east-west or north-south direction corresponds to a relatively small earth distance. Close to the horizon (large angle of view) a small distance on the ATS photograph covers many earth miles, so that the distance represented by a change of one cursor unit also becomes greatly increased.

Figure 5 shows the latitudinal variation of the distance represented by one x or one y cursor unit at various longitudes from the satellite subpoint. For example, at the equator, a change of one y cursor unit does not vary with longitude until near the horizon; out to about 70° longitude from the satellite subpoint, one y cursor unit corresponds to

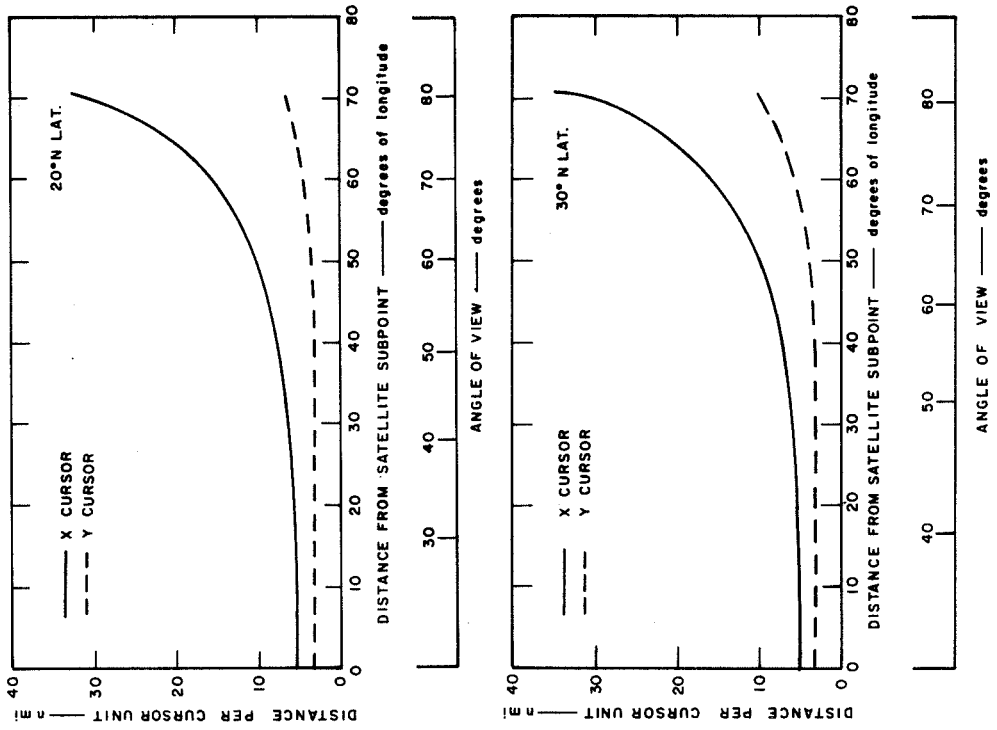


FIGURE 5 EARTH DISTANCE PER CURSOR UNIT AT VARIOUS LATITUDES AND ANGLES OF VIEW

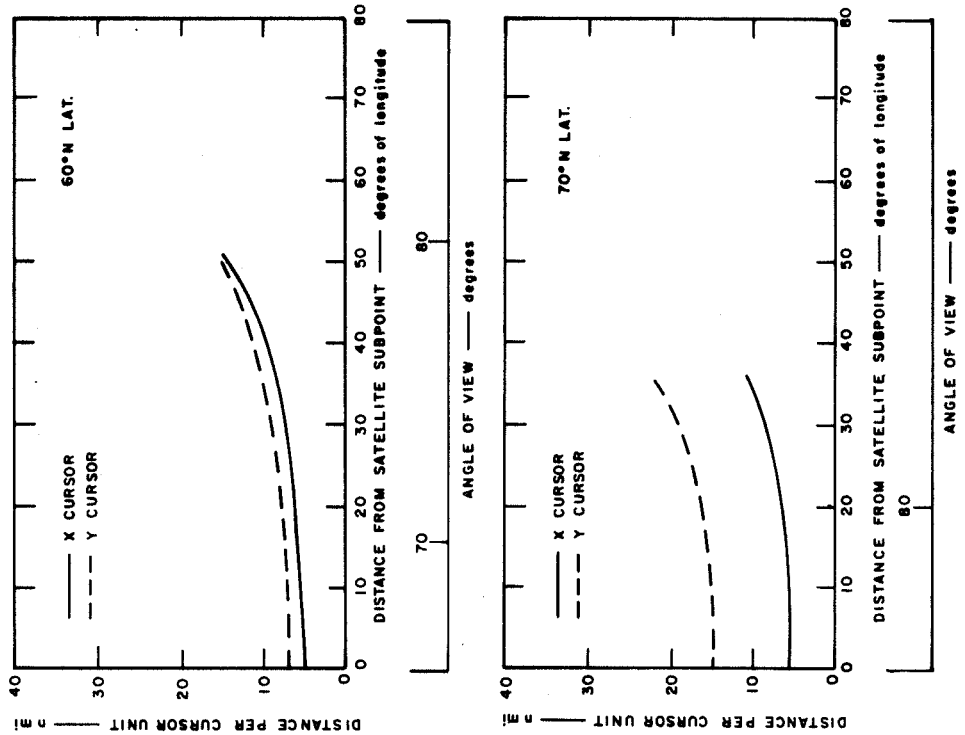


FIGURE 5 EARTH DISTANCE PER CURSOR UNIT AT VARIOUS LATITUDES AND ANGLES OF VIEW (Concluded)

a distance value of 3 nmi. One x cursor unit, however, represents a distance that can vary from 5 nmi (at the satellite subpoint) to more than 30 nmi (at 70° longitude from the subpoint).

At 50°N, the distances corresponding to a change of one x or y cursor unit are nearly equal until about 40° longitude from the satellite subpoint, beyond which the values diverge. At 70°N, the distance corresponding to a change in one y cursor unit substantially exceeds that corresponding to a change of one x cursor unit over the entire range of longitude from the satellite subpoint. A summation of the graphs in Figure 5 is presented in Table 2.

Table 2

DISTANCE IN NAUTICAL MILES PER CURSOR UNIT
AT SELECTED LATITUDES AND ANGLES OF VIEW

Latitude in Degrees	Angle of View in Degrees											
	30°		40°		50°		60°		70°		80°	
	x	y	x	y	x	y	x	y	x	y	x	y
0	5.5	3.0	6.5	3.0	8.0	3.0	10.5	3.0	18.0	3.0	30.0	3.0
10	5.5	3.0	6.0	3.0	7.5	3.0	10.5	3.0	16.0	3.0	30.0	4.0
20	5.0	3.0	6.0	3.0	7.5	3.0	10.0	3.5	15.5	4.0	30.0	6.0
30			5.0	3.0	6.5	3.0	8.0	3.5	13.5	5.0	30.0	9.5
40					5.0	4.0	7.0	4.0	11.5	6.0	25.0	10.5
50							5.5	5.0	9.0	6.5	21.5	14.5
60									6.0	7.0	16.5	17.5
70											6.5	16.5

The values shown in Figure 5 were computed with the console's TV camera lens set at maximum magnification (about 14.4 times the original ATS viewing positive) and would increase as the magnification was decreased.

B. Effect on Cloud Motion Measurements

Figure 6 illustrates the effect of applying the values shown in Table 2 to three sets of measurements in the latitude band from 45°N to 55°N. Each of these measurements was varied by one cursor unit. In this selected sample, the greatest difference between rawin speed and cloud speed at the level of best fit² is 6 knots; between rawin direction and cloud direction it is 21°. Comparison of measured cloud motions with rawin values shows that a substantial number of the directions and speeds are within the range of uncertainty that would result from a difference of one x or one y cursor unit. Time differences and/or distance between rawin station and location of measured clouds, however, could account for some of the lack of agreement. Errors can accrue from the length of time a given cloud can be tracked. This is particularly serious if the tracking time is short (e.g., 20 minutes), since the motion can equal the magnitude of the measurements uncertainty. As a matter of practice, a minimum tracking time of one hour is recommended.

Table 3 (based on the total sample of 240 cloud motion measurements) shows the average effect on speed and direction that could have been made by a variation of a cursor setting of one unit determining the initial or final position. Obviously, the effect on measurement certainty, particularly in terms of direction, can be substantial at angles of view of 50° or greater. In fact, these average values of direction and speed difference encompass a significant proportion of the measurement differences obtained by the two different investigators (see Section III-B).

²The minimum vector difference between the observed wind and the cloud motion vector.

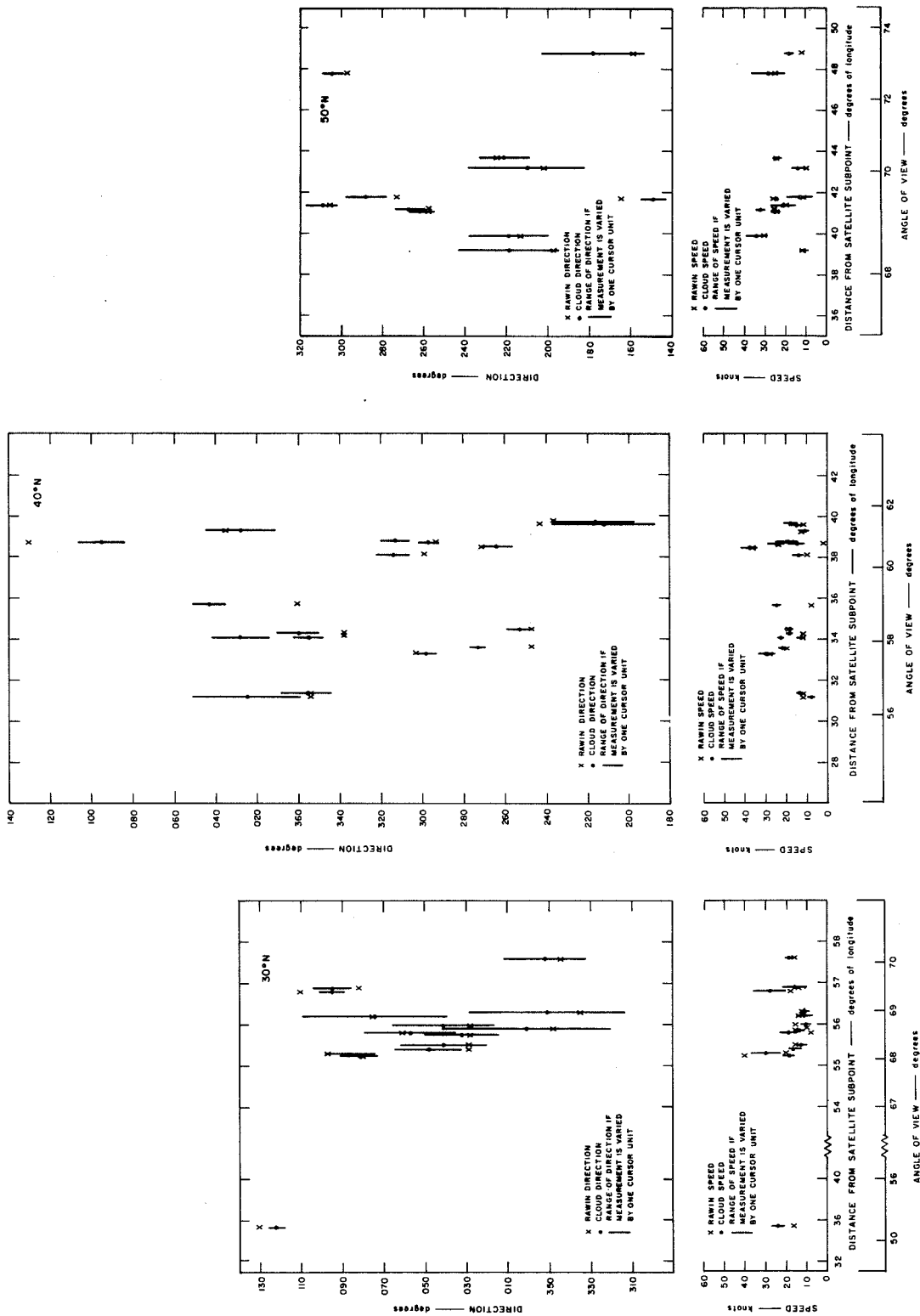


FIGURE 6 EFFECT ON CLOUD MEASUREMENT COMPARISON THROUGH UNIT CURSOR VARIATION (SELECTED DATA)

Table 3

AVERAGE CLOUD MOTION CHANGE THROUGH UNIT CURSOR VARIATION

Angle of View (degs)	Latitude Range														
	25.1°N-35.0°N					35.1°N-45.0°N					45.1°N-55.0°N				
	Cases	ΔD (degs)	$\overline{\Delta D}$ (degs)	ΔS (kts)	$\overline{\Delta S}$ (kts)	Cases	ΔD (degs)	$\overline{\Delta D}$ (degs)	ΔS (kts)	$\overline{\Delta S}$ (kts)	Cases	ΔD (degs)	$\overline{\Delta D}$ (degs)	ΔS (kts)	$\overline{\Delta S}$ (kts)
35.1 to 45	7	2-5	3.9	2-2	2.0										
45.1 to 55	8	4-27	12.6	2-3	2.6	9	3-23	6.3	2-3	2.2					
55.1 to 65	15	8-32	14.9	2-7	2.8	57	2-26	9.1	1-8	3.0	12	4-21	14.0	0-5	2.7
65.1 to 75	42	5-41	19.2	0-11	3.5	22	2-42	13.0	1-7	4.2	49	2-41	15.9	0-7	3.0
>75	2	14-18	16.0	1-2	1.5	4	9-21	13.5	4-6	5.0	13	2-29	16.5	0-8	3.8

This would indicate that certain measurement cursor settings, as determined by each investigator, were quite close even at high angles of view, but even this degree of agreement yielded marked direction and speed differences.

The values in Table 3, based on the 240 measurements, are applicable to that set of data alone. Not all possible directions of the compass were obtained in these measurements, nor was the distribution of measurements uniform over the grid quadrant. Therefore, the values can not be considered to be equivalent to values that might be obtained in a general solution of unit cursor variation using a complete spectrum of directions, speeds, and locations.

In certain instances, however, it is evident that over measurement or under measurement by even a unit cursor setting, can lead to significantly erroneous estimates of cloud height when these values are used to search for a level of best fit. Multiple levels of best fit sometimes result from a measurement variation, particularly in cases where the rawinsonde profile possesses small increases of wind speed or small wind direction changes with height. Because of these possibilities, resultant

levels of best fit should be compared for compatibility with the types of cloud being reported in the area of interest, if such data exist. Also, multimeasurements of the same cloud--or of seemingly similar clouds in the immediate area--can be of assistance in deriving a "most likely" level of best fit.

III CLOUD IDENTIFICATION AND MEASUREMENT

A. Comparison of Cloud Height Estimates Using ATS and ESSA Photographs

The basic task was to assess the ability of an experienced meteorologist to identify clouds at large angles of view, at least to the minimal degree of distinguishing "low" cloud from "high" cloud. To do so, a sample of six days (12, 18, 23, 28, 29, and 30 April 1968) were selected for cloud motion measurement. Both ATS III and ESSA III photographs were available for these days, although the ATS picture quality had become degraded during April 1968 by some loss of sensor sensitivity. Although this loss was not severe enough to preclude cloud identification, it may have contributed to measurement difficulties.

Measurements were confined to the northwestern quadrant of the ATS photograph. At this time the satellite subpoint was located near 84°W longitude, thus providing good coverage of the western United States and the eastern Pacific to about 145°W longitude.

The cloud cover for the six selected days in April is shown by ATS III and ESSA III photographs in Figures 7 through 12. (The ESSA III photographs selected for illustration are nearest in time to the illustrated ATS data and view most of the area in which clouds were measured. In all cases this was less than one hour of difference.) The ATS data show a series of frontal cloud bands, either in the eastern Pacific or along the west coast. Post-frontal cloudiness is patchy and cellular in appearance. Stratiform cloud patches of varying extent are present off the lower California coast.

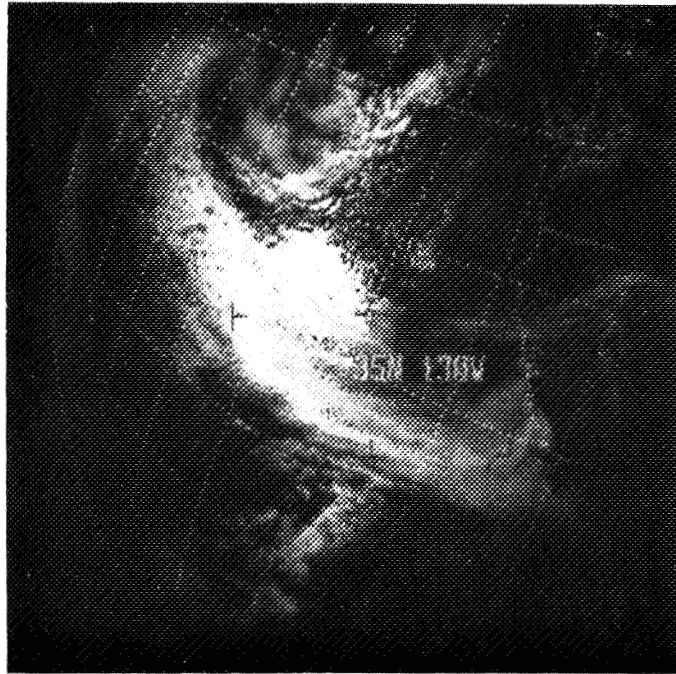
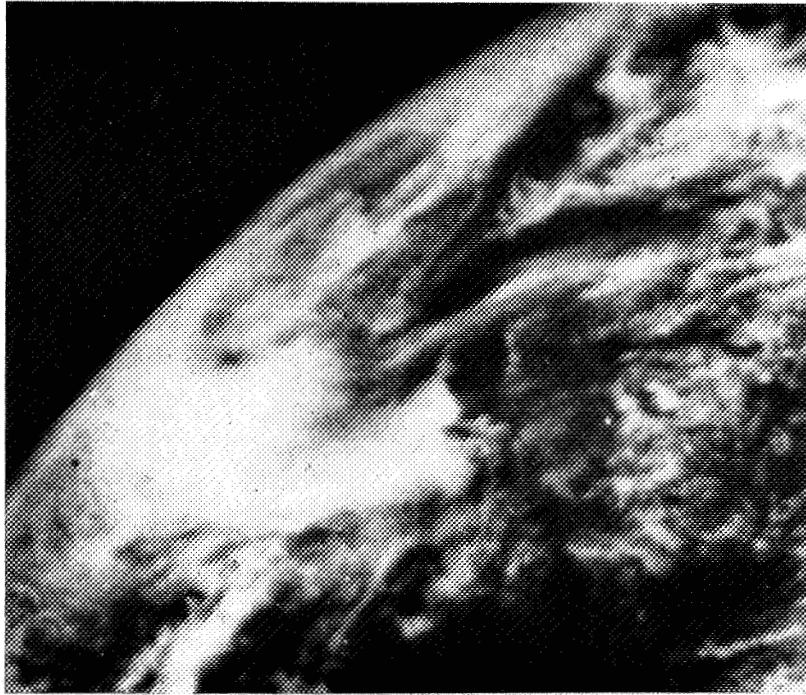
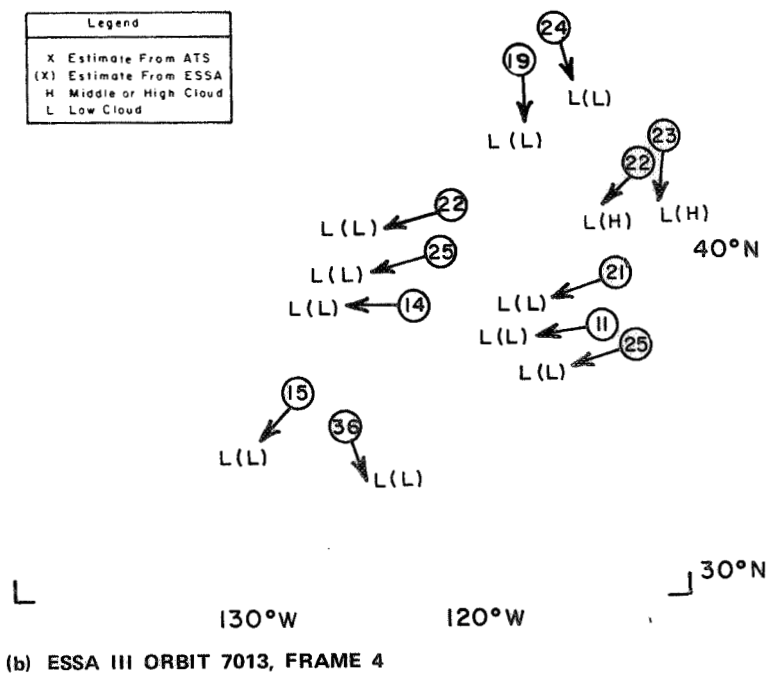
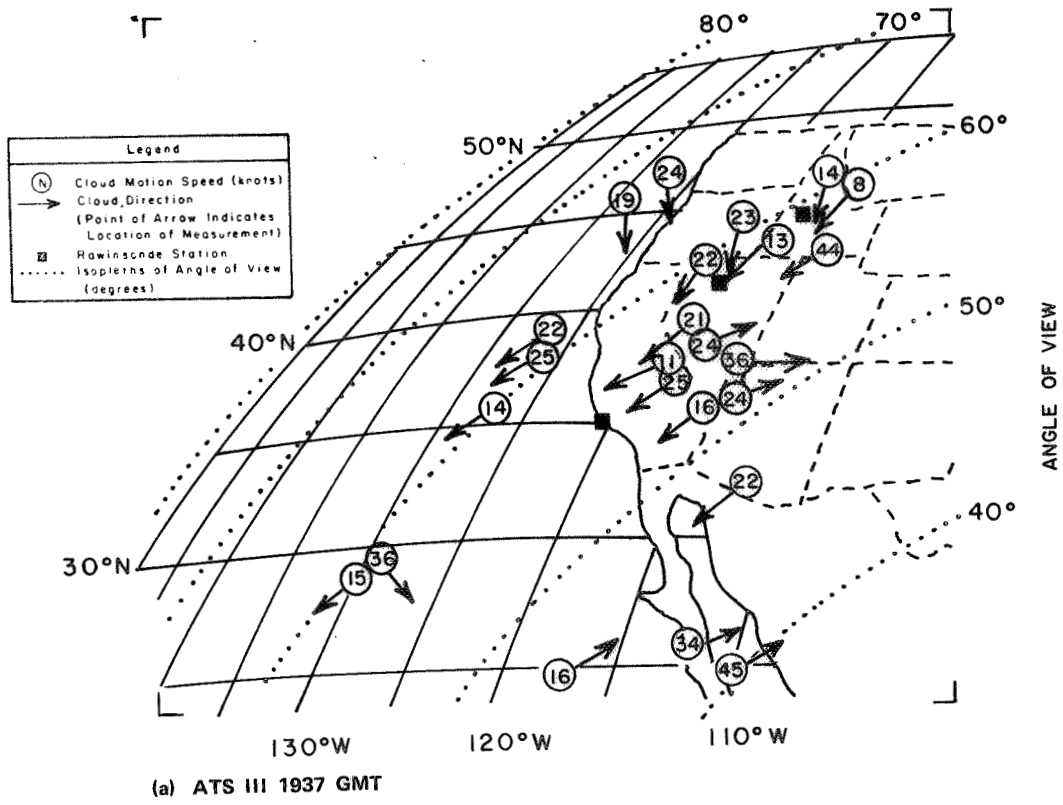
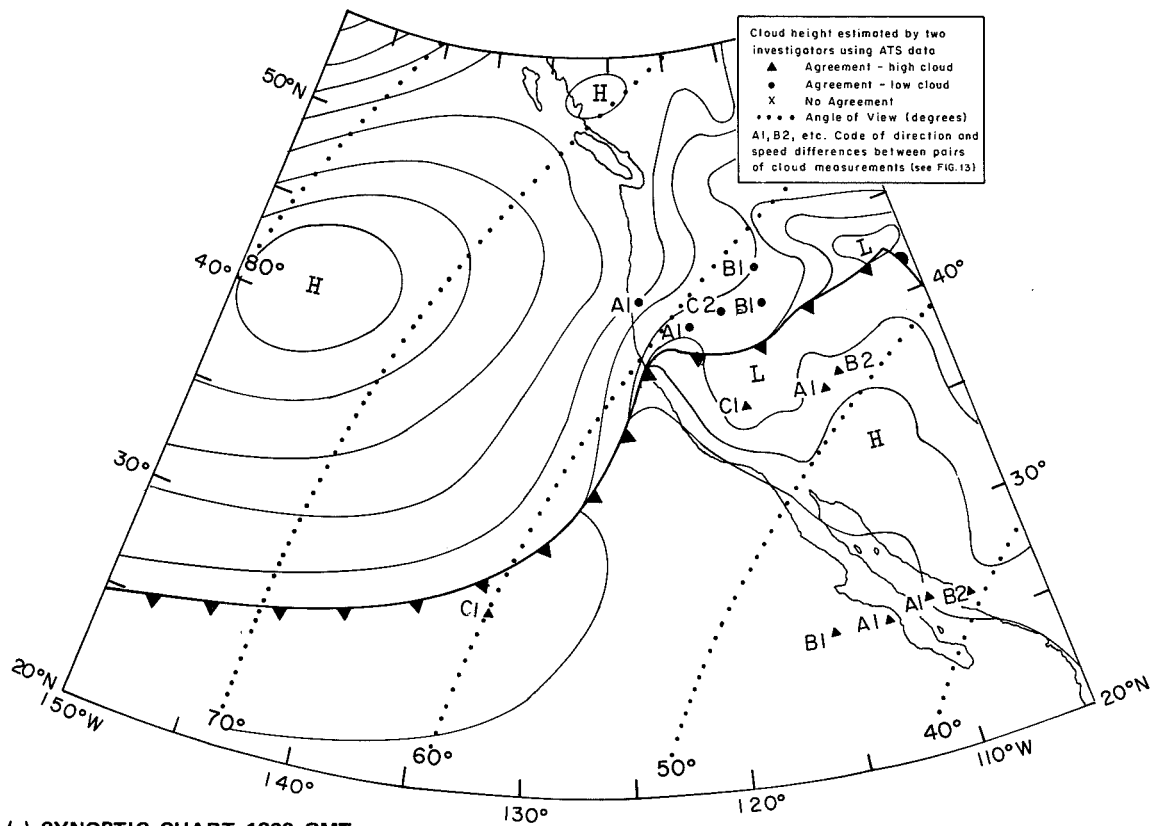


FIGURE 7 SELECTED CLOUD DATA, 12 APRIL 1968





(d) DESCRIPTION

No cloud features were measured over the area in excess of approximately 62° angle of view since this region of the ATS photograph displayed a rather uniform cloud cover with indistinct edges. The cloud cover located at less than 62° of angle of view possesses sharper edges and has more features capable of being tracked. A frontal cloud band is visible, beginning near 38°N , 125°W . The measured clouds are in the southeast portion of high-pressure cell. An examination of clouds common to the areas viewed by ATS and ESSA shows that measurements were obtained from edges of huge cloud clusters and bands or exceptionally large cells. Note the small-cell cloud cluster near the center of the ESSA photograph. This cloud pattern dissolves to a uniform-appearing, rather featureless, cloud sheet in the ATS photograph.

Comparison of cloud height estimates using the ESSA photograph indicates good agreement. All the cases were estimated to be "low" cloud, except for two cases near 42°N , 120°W .

FIGURE 7 SELECTED CLOUD DATA, 12 APRIL 1968 (Concluded)

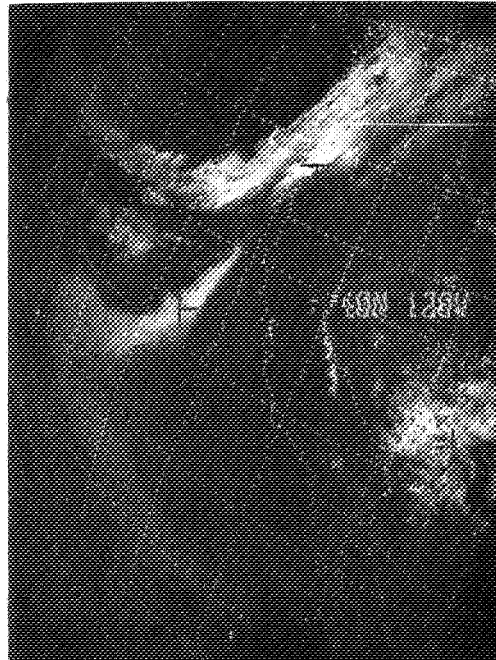
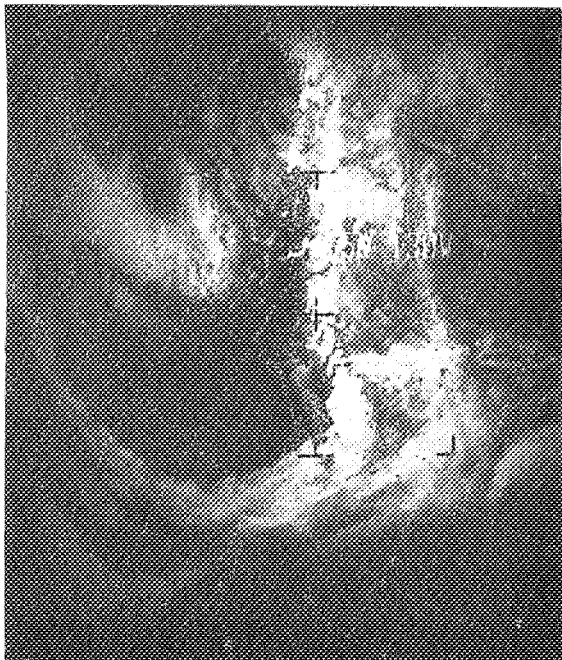
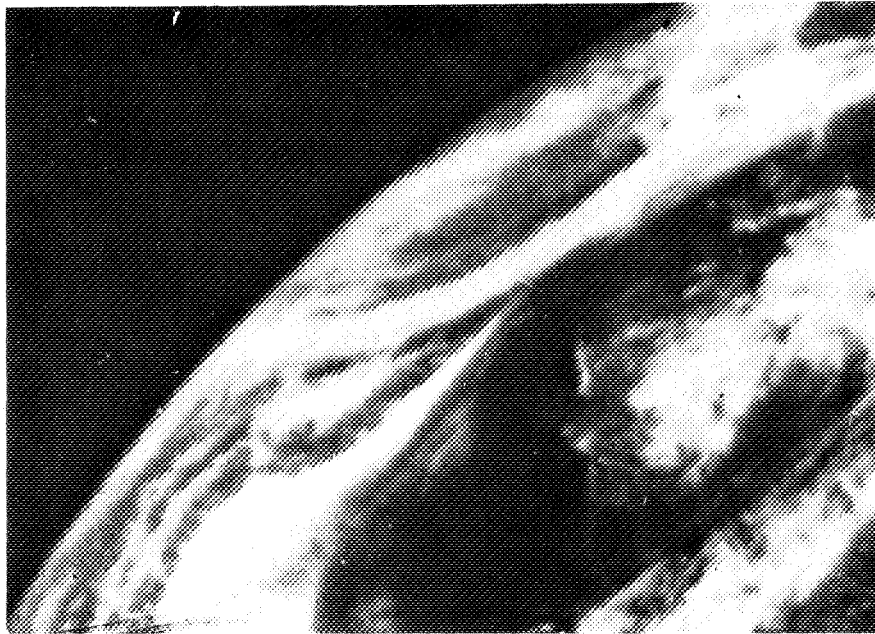
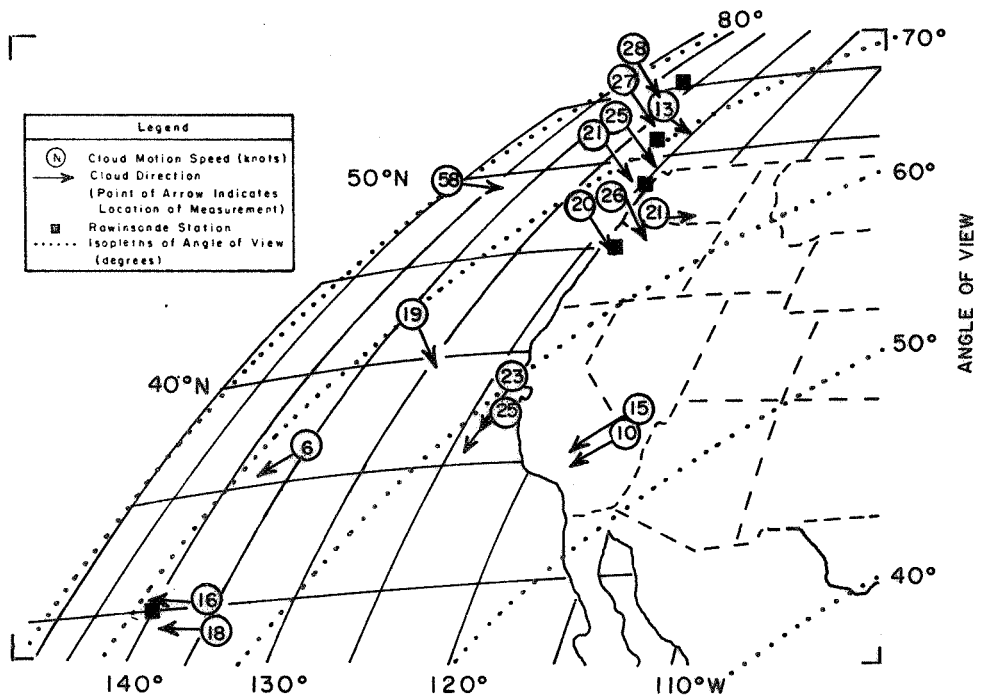
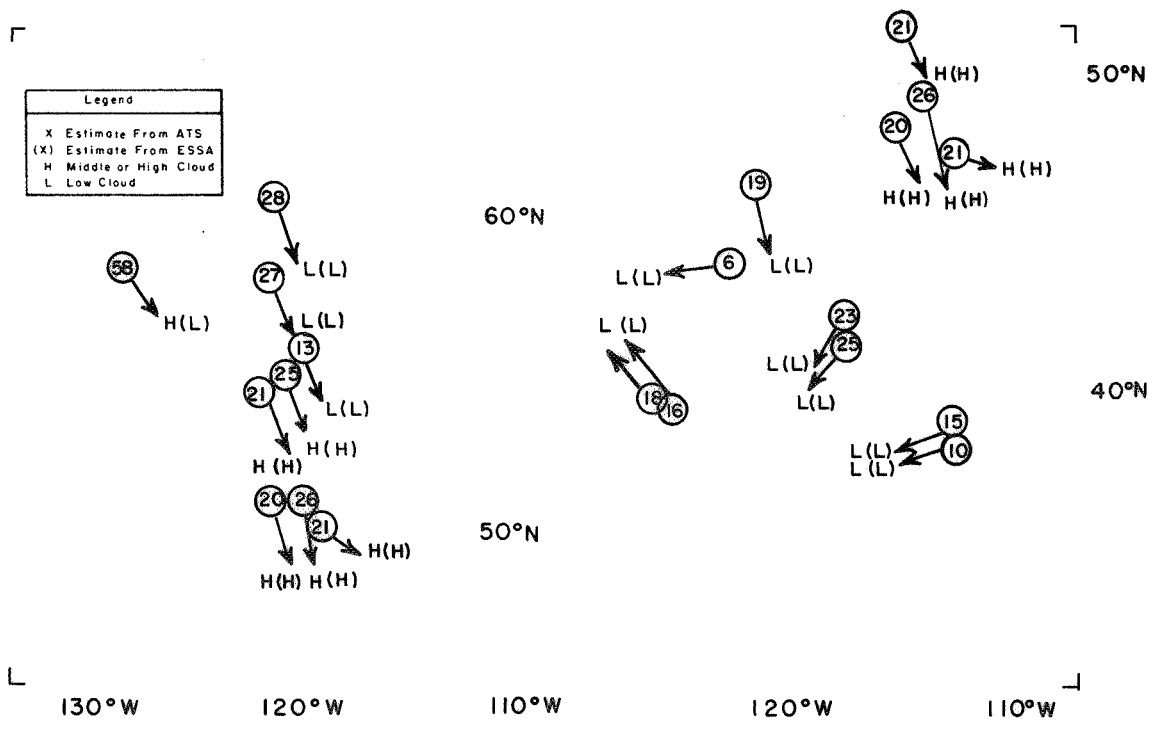


FIGURE 8 SELECTED CLOUD DATA, 18 APRIL 1968

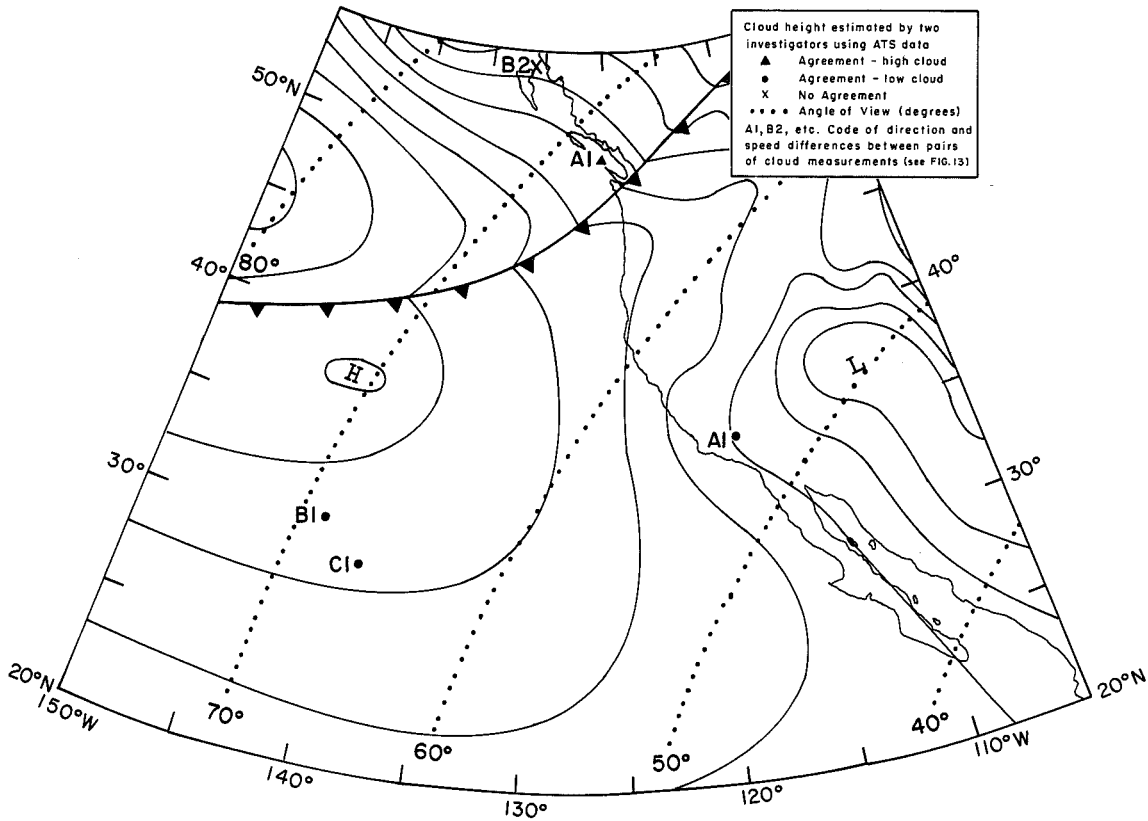


(a) ATS III 1916 GMT



(b) ESSA III ORBIT 7088, FRAME 3

(c) ORBIT 7088, FRAME 4



(c) SYNOPTIC CHART 1800 GMT

(d) DESCRIPTION

The ATS photograph on this date shows a well-defined cloud band associated with a cold front through the eastern North Pacific. There is a large post-frontal clear area, followed by a cloud band on the edge of the photograph. South of the frontal cloud band there are large sheets of cloud in broad patches and rows.

All motions, except one, were taken at angles of view of 70° or less. The two ESSA photographs cover the area seen by the ATS photographs. A comparison of the estimates of cloud height show excellent agreement for both "high" and "low" categories. One exception is the measurement near 49°N , 139°W (angle of view $\approx 75^\circ$) with a displacement value of 58 knots. Here the estimate from the ATS data is that of "high" cloud, while the estimate from the ESSA photograph is that it is "low" cloud, based on the evidence of tightly packed cells. Unfortunately, it is not possible to determine if the displacement value is reasonable, since there are no rawinsonde stations in the immediate vicinity.

FIGURE 8 SELECTED CLOUD DATA, 18 APRIL 1968 (Concluded)

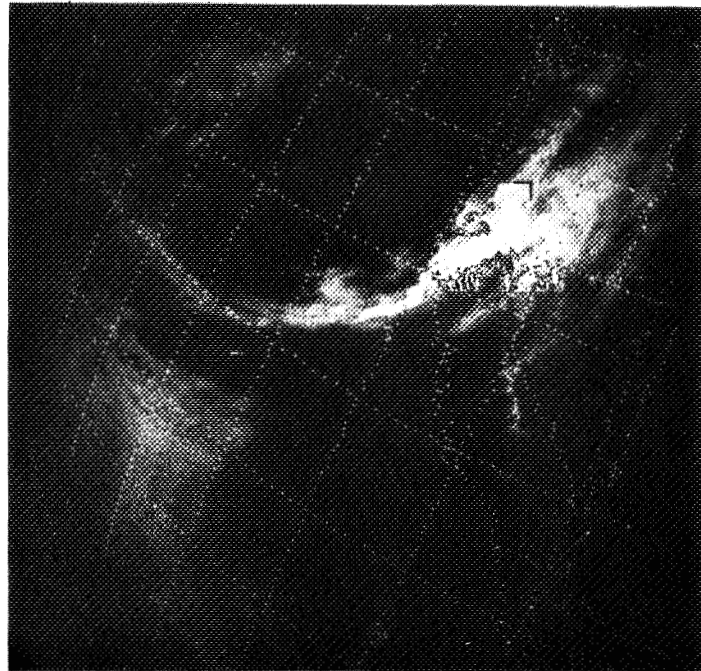
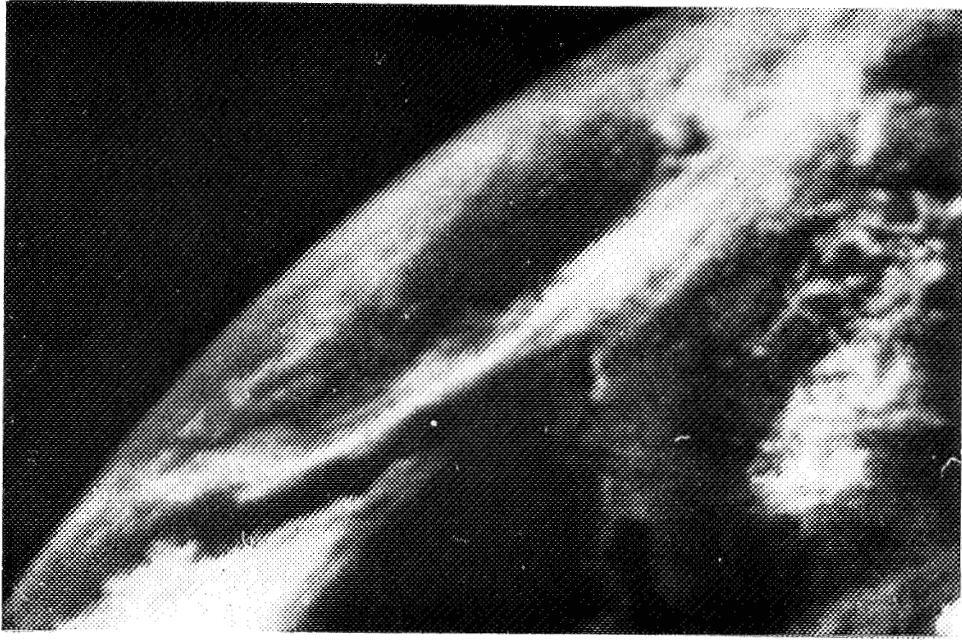
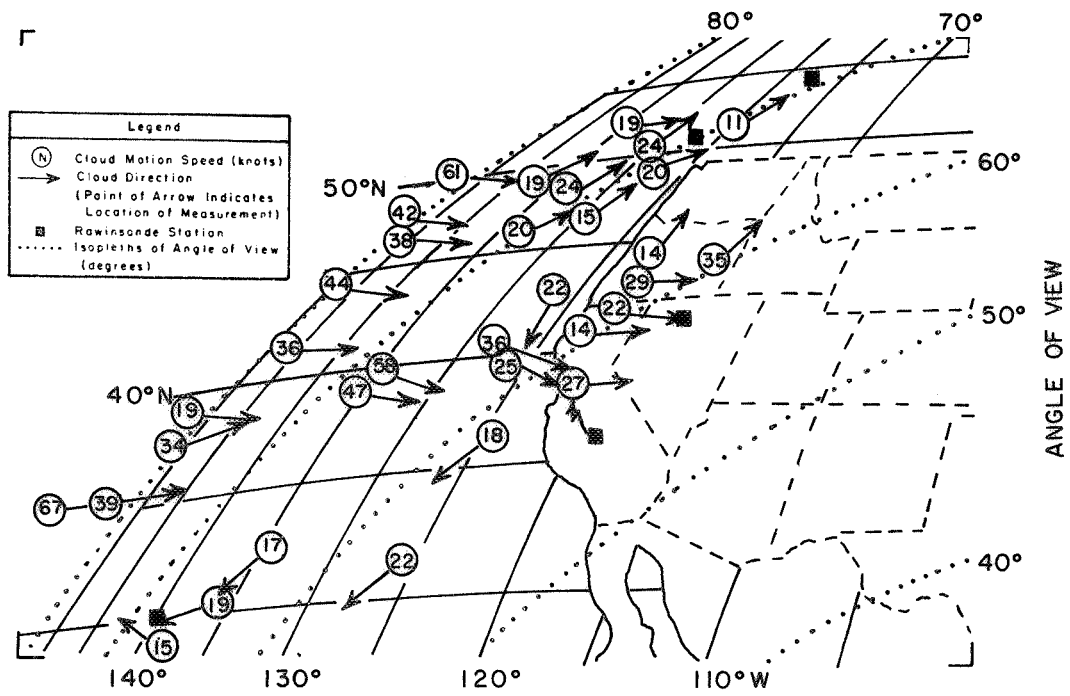
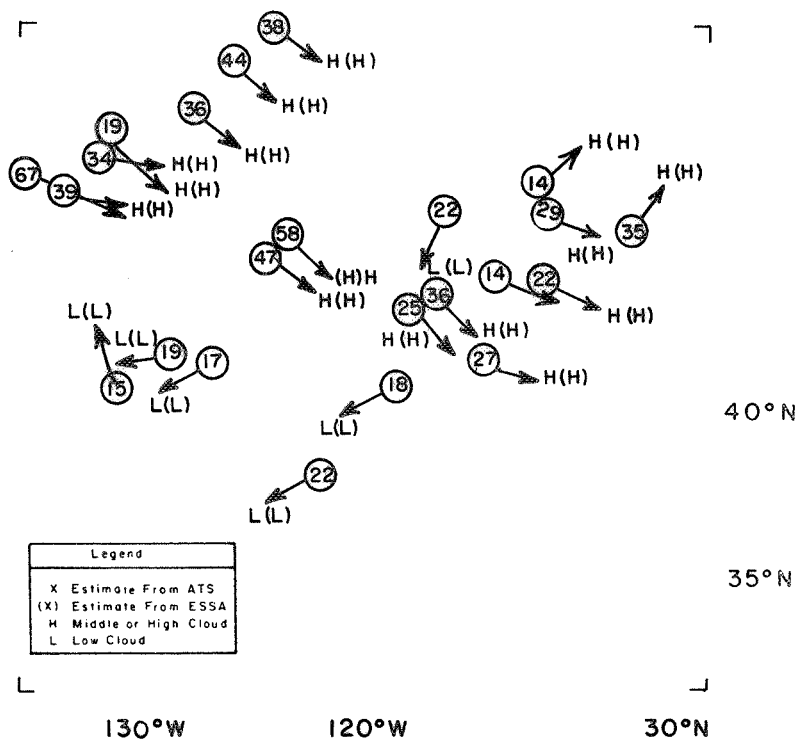


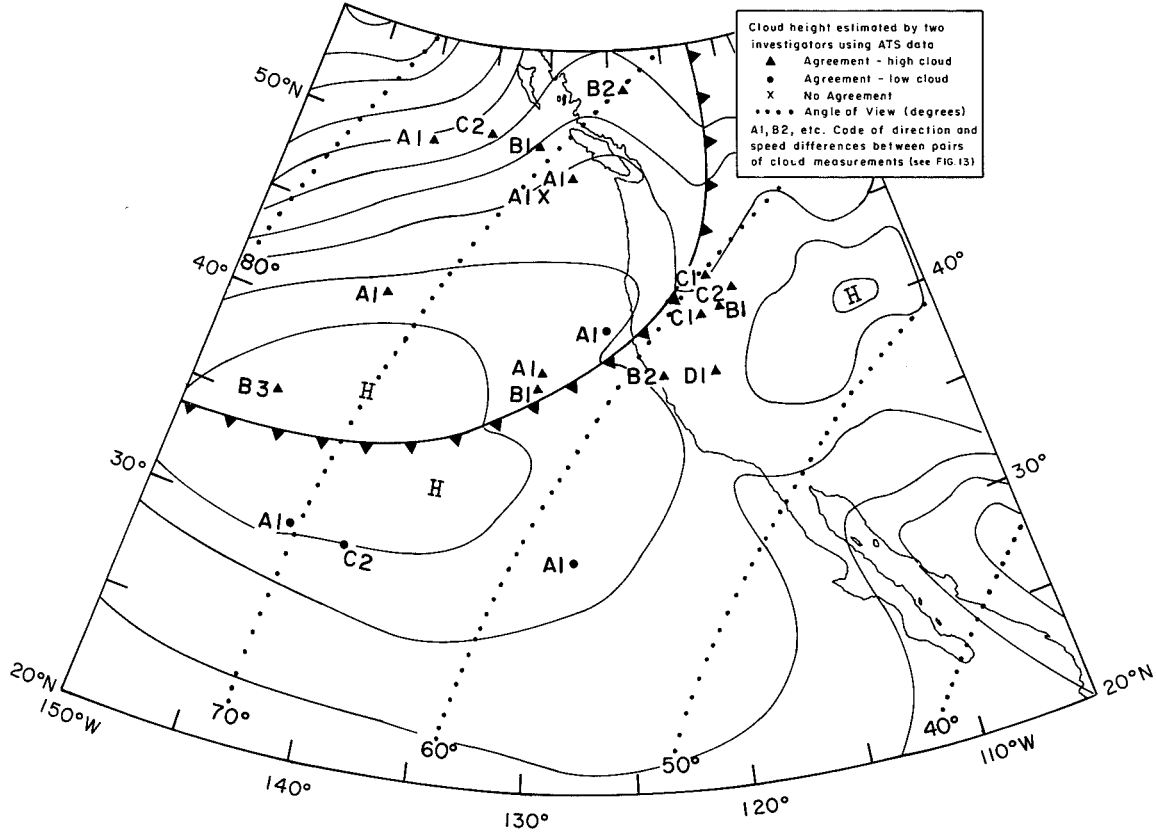
FIGURE 9 SELECTED CLOUD DATA, 23 APRIL 1968



(a) ATS III 1918 GMT



(b) ESSA III ORBIT 7151, FRAME 4



(c) SYNOPTIC CHART 1800 GMT

(d) DESCRIPTION

The ATS photograph shows a well-defined cloud band associated with a cold front extending from western Canada southwestward to 34°N, 150°W. Essentially clear skies prevail in the post-frontal area, south of the 50th parallel, to about 140°W. A patch of apparently stratiform clouds is visible south of the frontal cloud band. A broad band of cloud with rather indistinct edge covers the area to the west of 140°W.

The ESSA photograph views the Pacific region south of the 45th parallel, but the appearance of the clouds in the two satellite systems are quite disparate; the ATS view tends to brighten and solidify the cloud elements, at the expense of detail.

In this example, agreement on the identification of the cloud height classification, based on ATS cloud motion, was successful out to about an angle of view of 75°. The motions of the few "low" clouds match the sense of wind direction that is implied by the synoptic chart (see map), but most of the cloud height estimates for those measurements contained in the area of the ESSA photograph are of "high" cloud.

FIGURE 9 SELECTED CLOUD DATA, 23 APRIL 1968 (Concluded)

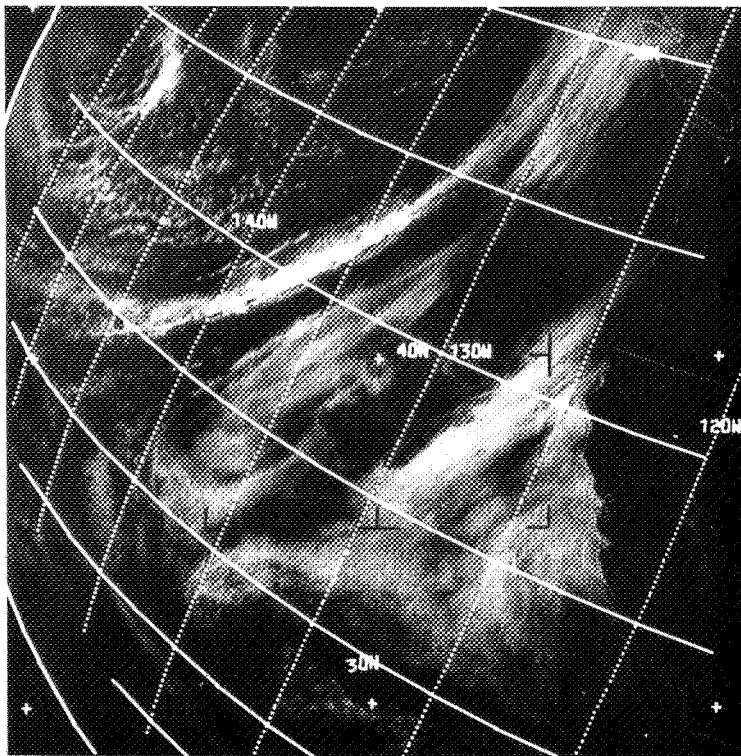
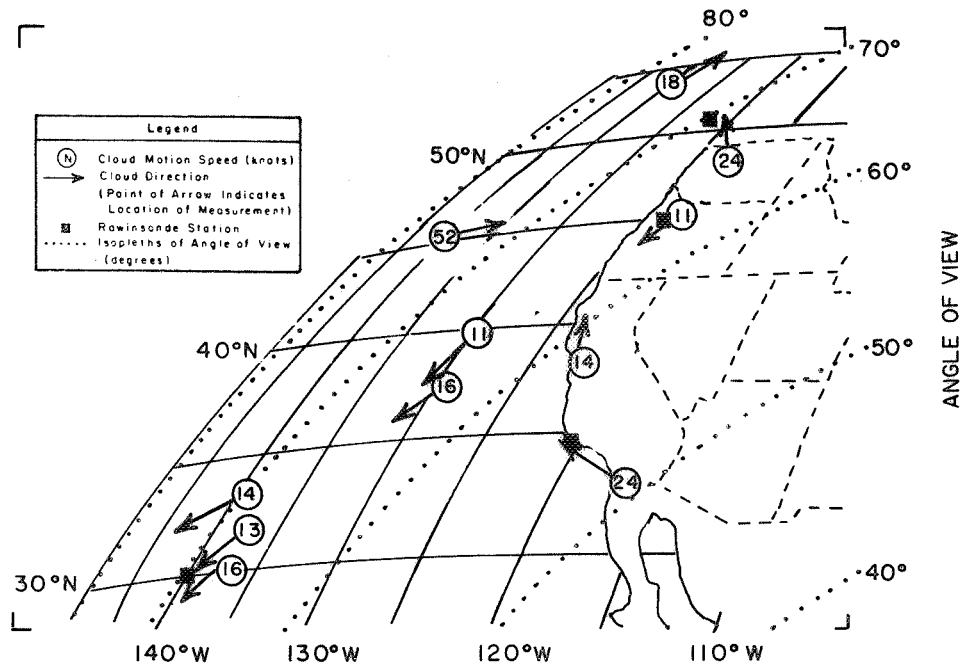
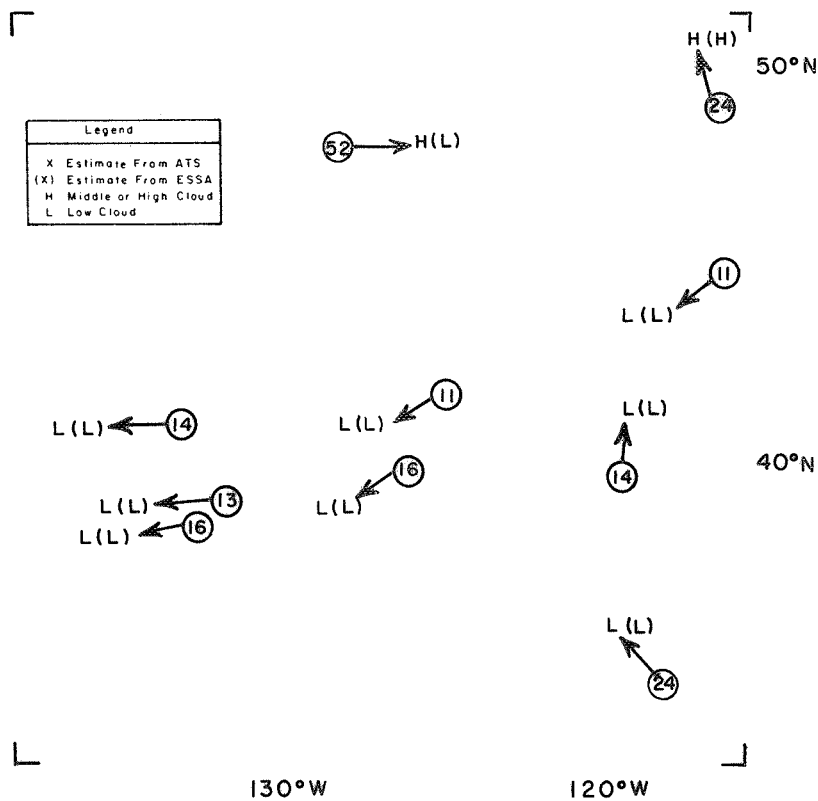


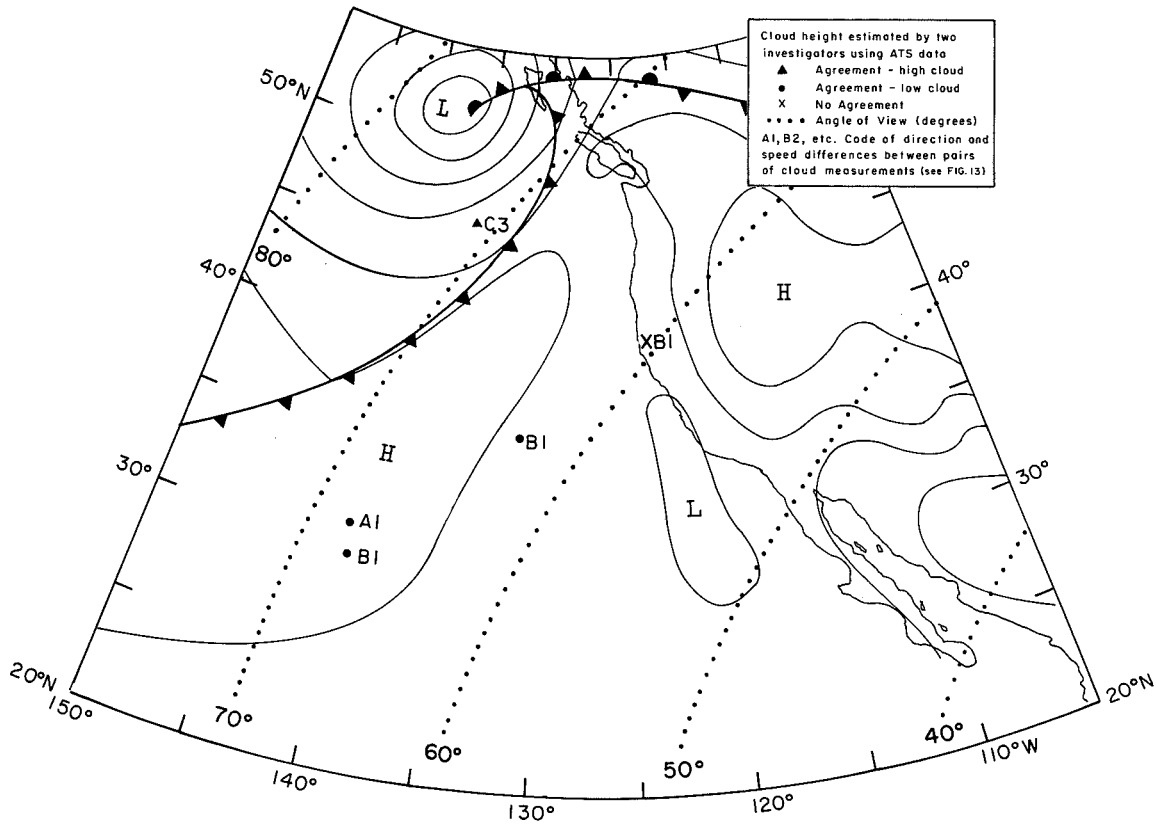
FIGURE 10 SELECTED CLOUD DATA, 28 APRIL 1968



(a) ATS III 2039 GMT



(b) ESSA III ORBIT 7214, FRAME 4



(c) SYNOPTIC CHART 1800 GMT

(d) DESCRIPTION

The ATS photograph shows a cloud band associated with a cold frontal system. Post-frontal clearing is present, followed by a rather cellular, but indistinct, cloud field. Extensive cloudiness prevails to the south and east of the front. The cloud cover appears rather dense, organized in huge patches and very diffuse-edged.

Measurements were taken in the pre-frontal and post-frontal areas and along the stratus edge on the west coast. The identification of the cloud types on the ATS and ESSA photographs agree, except for the single case near 45°N, 135°W, in the immediate post-frontal area. Because of the high angle of view in the ATS photograph, this latter region appears vastly different from the corresponding ESSA view. In the ESSA view identification of the cloud type is somewhat uncertain since the small-rod or half-cell appearance of the clouds can be that of altocumulus clouds or low-level cumulus.

FIGURE 10 SELECTED CLOUD DATA, 28 APRIL 1968 (Concluded)

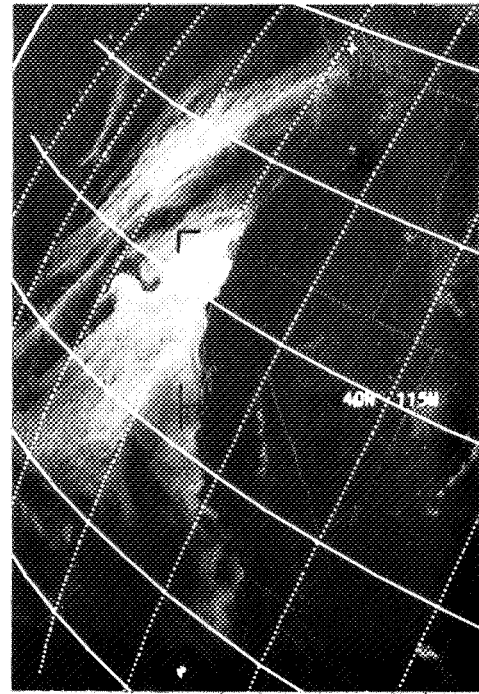
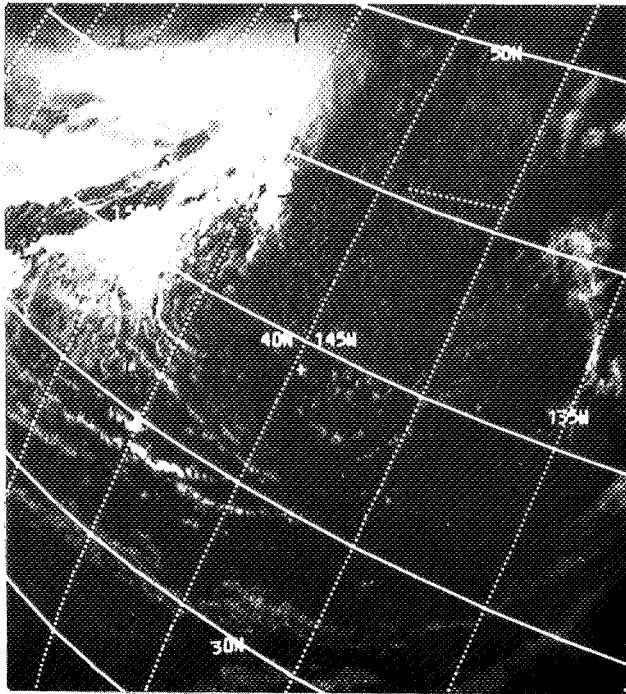
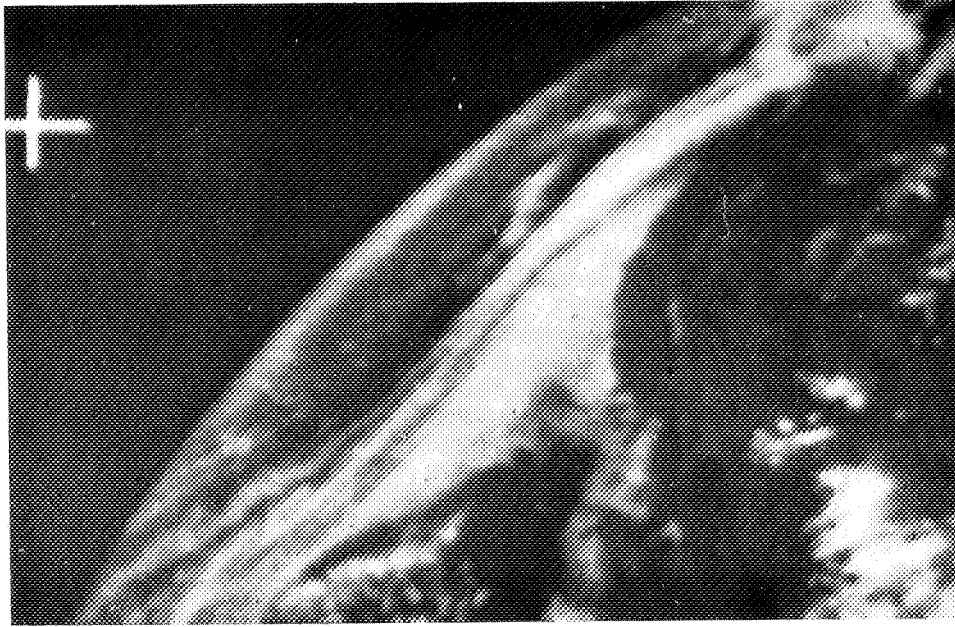
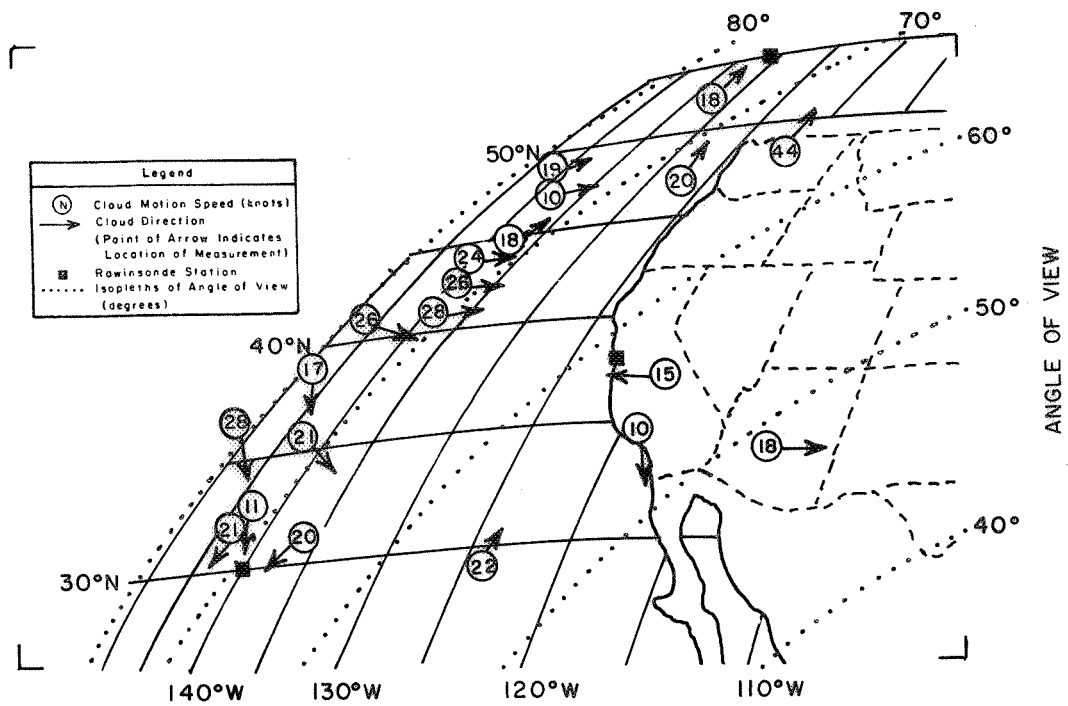
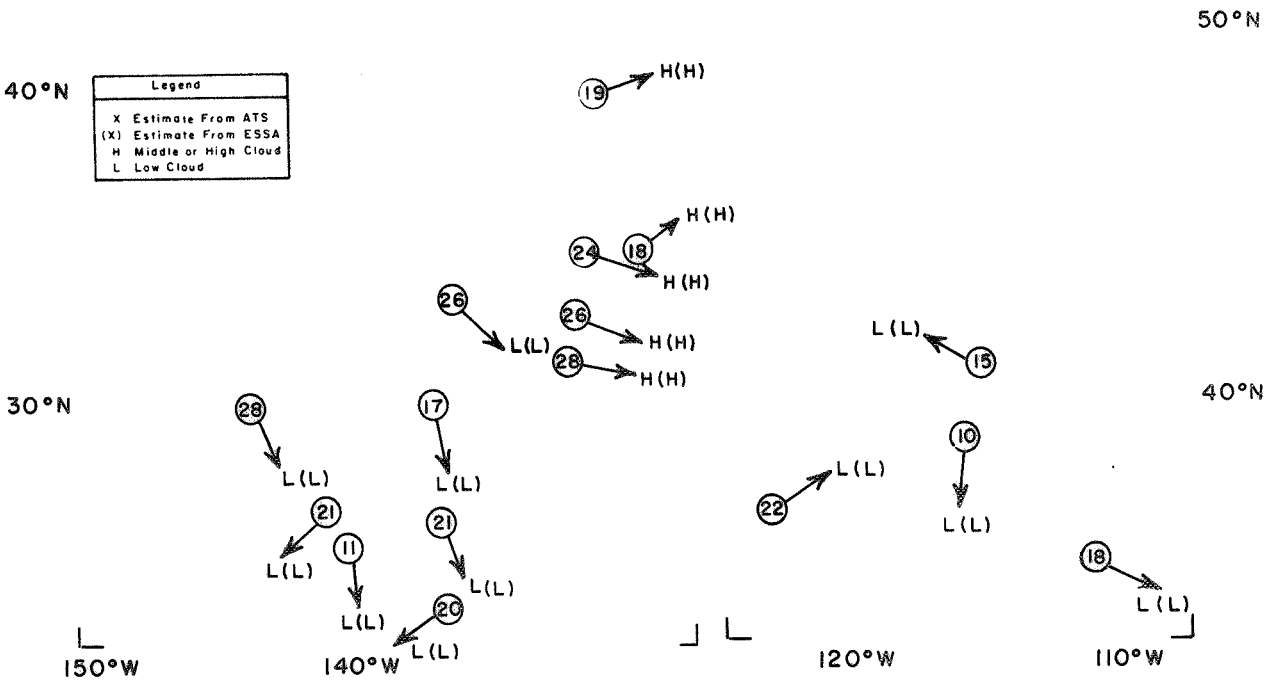
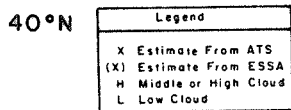


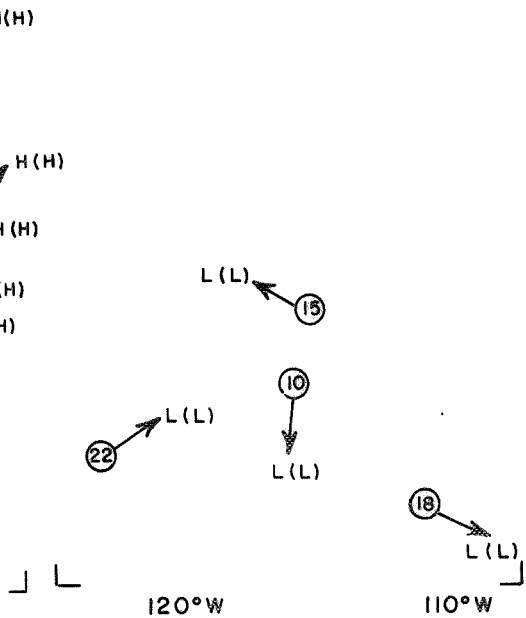
FIGURE 11 SELECTED CLOUD DATA, 29 APRIL 1968



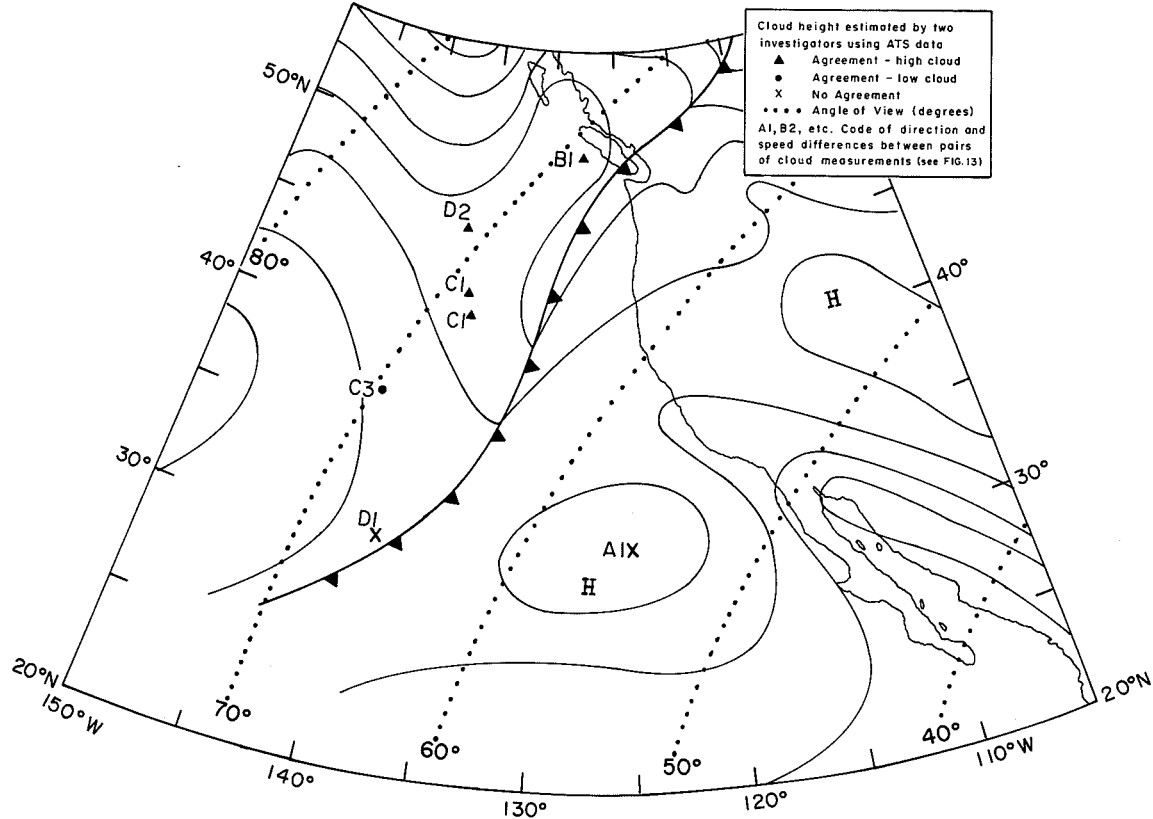
(a) ATS III 2130 GMT



(b) ESSA III ORBIT 7227, FRAME 4



(c) ESSA III ORBIT 7226, FRAME 4



(c) SYNOPTIC CHART 1800 GMT

(d) DESCRIPTION

The ATS photograph shows a frontal cloud band oriented NNE-SSW off the west coast of the United States. Compared to the previous day the clouds in the southern portion of the band have been eroded. The southerly flow ahead of the front has brought an extensive stratiform cloud cover along the west coast. The post-frontal area is occupied by numerous cloud elements with indistinct form with a rather solid appearing band of cloud visible on the western horizon.

The majority of the ATS measurements were of "low" clouds located in the post-frontal region, which the ESSA photograph shows to be occupied by very small cloud elements, rather widely-spaced. A comparison of the estimates of cloud identity shows them to agree. The clouds near 43°N, 135°W, identified as "high" cloud on the ESSA photograph, appear as a solid clump on the ATS photograph at an angle of 70°, as does the group of low clouds near 32°N, 142°N. The west-coast stratus and a portion of the frontal cloud band have a viewing angle less than 60° and the cloud identity estimates agree.

FIGURE 11 SELECTED CLOUD DATA, 29 APRIL 1968 (Concluded)

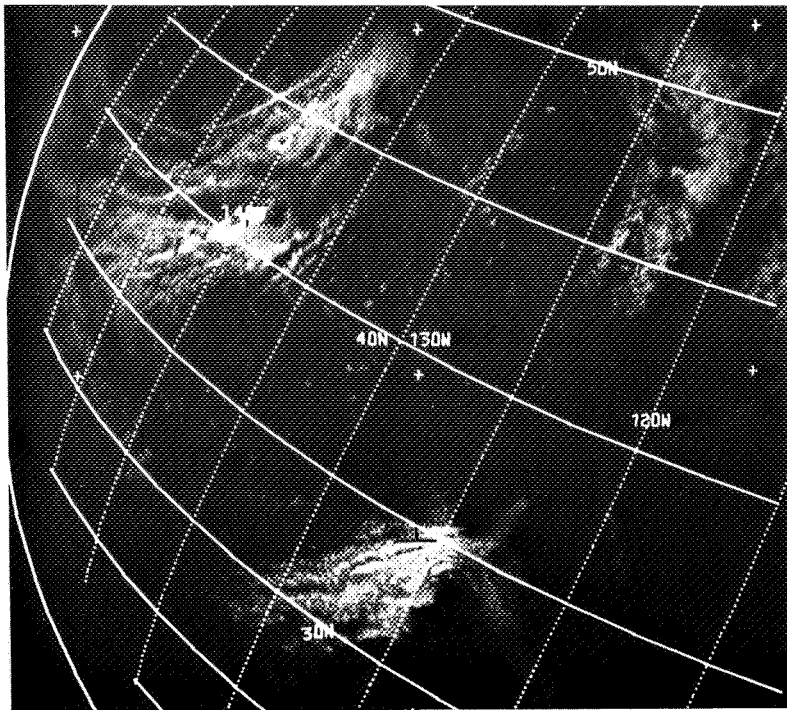
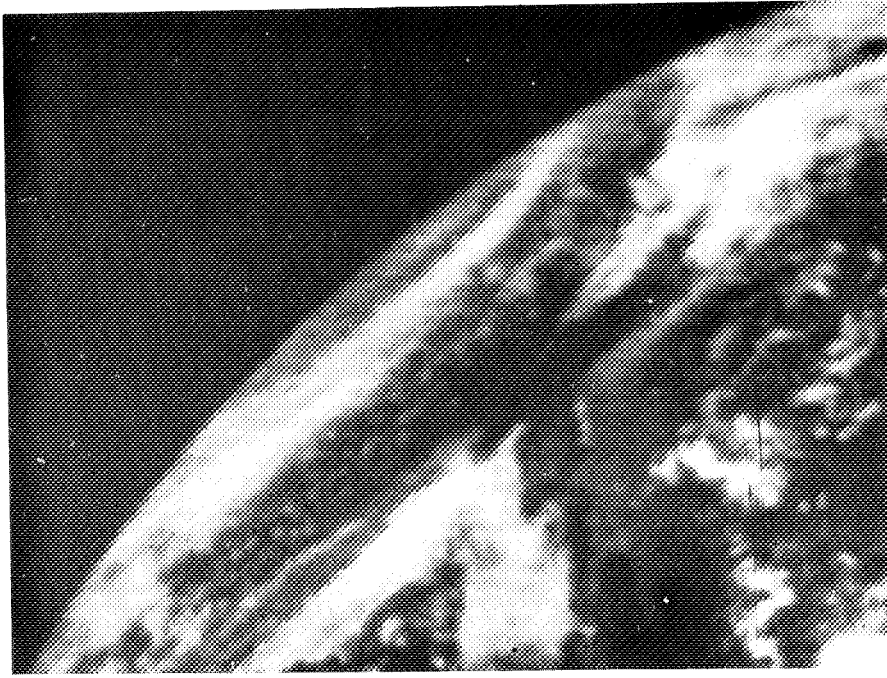
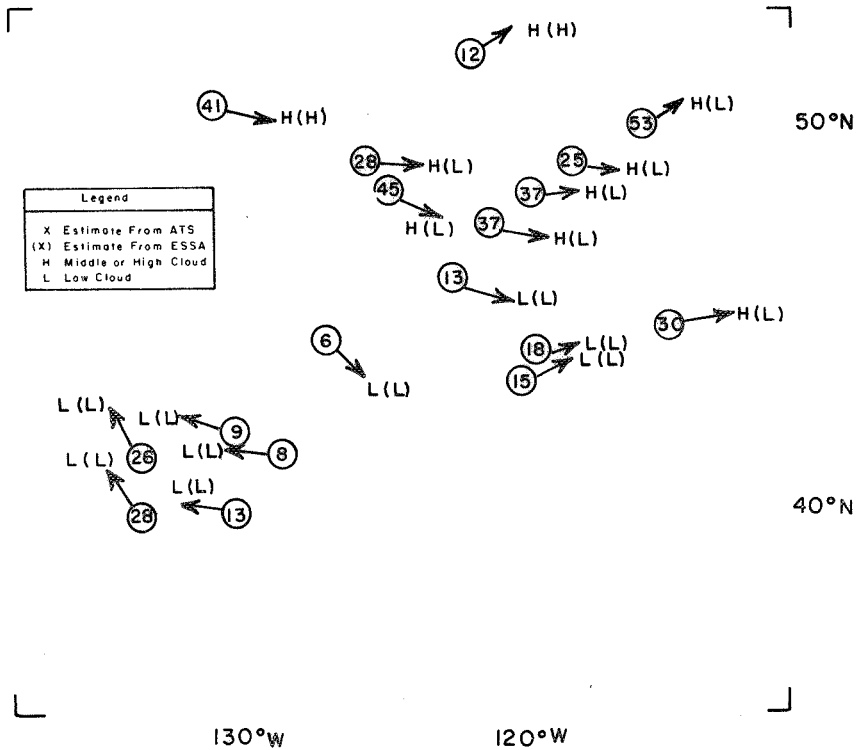
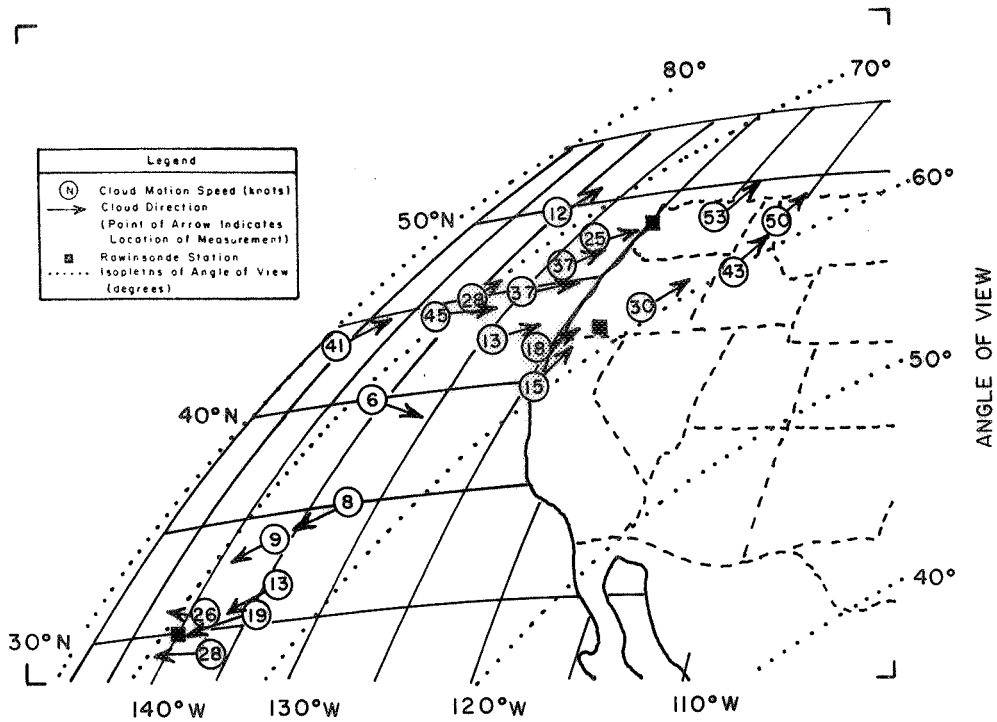
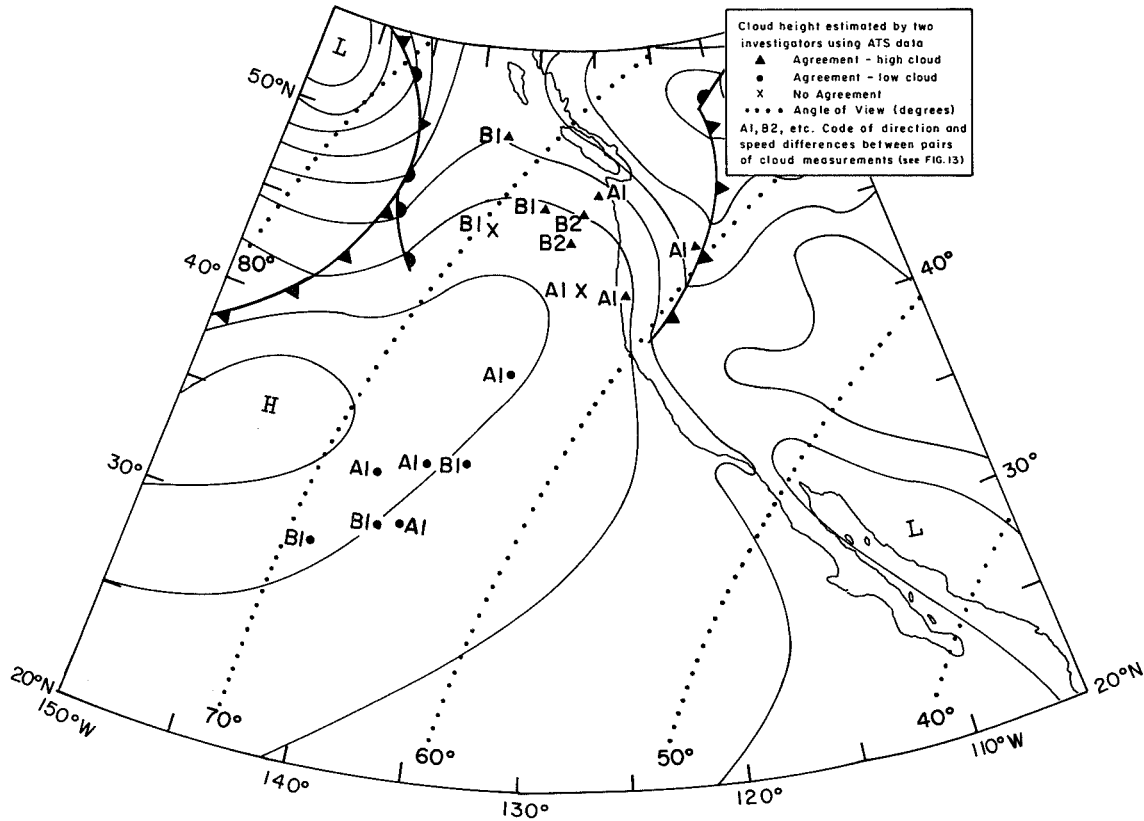


FIGURE 12 SELECTED CLOUD DATA, 30 APRIL 1968





(c) SYNOPTIC CHART 1800 GMT

(d) DESCRIPTION

On this day the front has moved inland, being followed by a ridge of high pressure. Residual cloudiness remains in the mountainous area of Washington and lower British Columbia; an extensive patch of stratiform clouds is seen in the Pacific just south of 36°N . Near the limb a new frontal cloud system is visible, with marked post-frontal clearing.

Most of the measurements were taken of clouds having angles of view less than 75° . Estimates of cloud height for the group of ATS motions near 30°N , 140°W (angle of view 70°) are in agreement, although the clouds on the ATS photograph appear as rather large "globules" whereas they appear quite small and indistinct on the ESSA photograph.

The principal area of disagreement occurs in the region between 44°N and 50°N , 135°W to 120°W . In the ESSA photograph, clouds in this region appear small and almost obliterated, leading to an estimate of "low" clouds. The ATS photograph shows considerably more cloudiness in this region and measurements of displacement values ranged from 28 to 45 knots, suggesting "high" clouds. These large speeds may result from the lack of a precise cloud edge or element to track and therefore may be somewhat excessive.

FIGURE 12 SELECTED CLOUD DATA, 30 APRIL 1968 (Concluded)

One analyst made 174 cloud identifications and measurements from the six-day period. These measurements were chosen at the discretion of the investigator and are random in location. As a result, the number of measurements vary on each of the six days, but, taken together, the measurements range over virtually all angles of view larger than 40° . Some of these (lack of space precluded the entire sample) are plotted on the ATS photos in Figures 7 through 12. Those cloud elements that were located within the area of the ESSA III photographs were identified by a second analyst using the ATS and ESSA photographs. The agreement between the identifications displayed on the ESSA photographs is rather good.

Perusal of Figures 7 through 12 indicates that the appearance of cloud bands and patches at varying angles of view had a decided effect on the ability to locate and track cloud features. This is clearly demonstrated by the varying locations and number of measurements taken on the individual days. Although all of the area contained in the ATS photographic quadrant was searched for cloud features that could be tracked, only under certain viewing conditions could measurement be obtained. Because of the absence of detail the estimate of "low" cloud using ATS data sometimes was based more on amount and direction of motion than on cloud appearance. This procedure was necessary in about one-third of the comparisons. In all cases the motion of the "low" clouds, and also most of the "high" clouds, agreed with the sense of the circulation implied by the surface and upper air charts, although no quantitative comparisons could be made.

B. Comparison of Cloud Motions Measured by Different Investigators

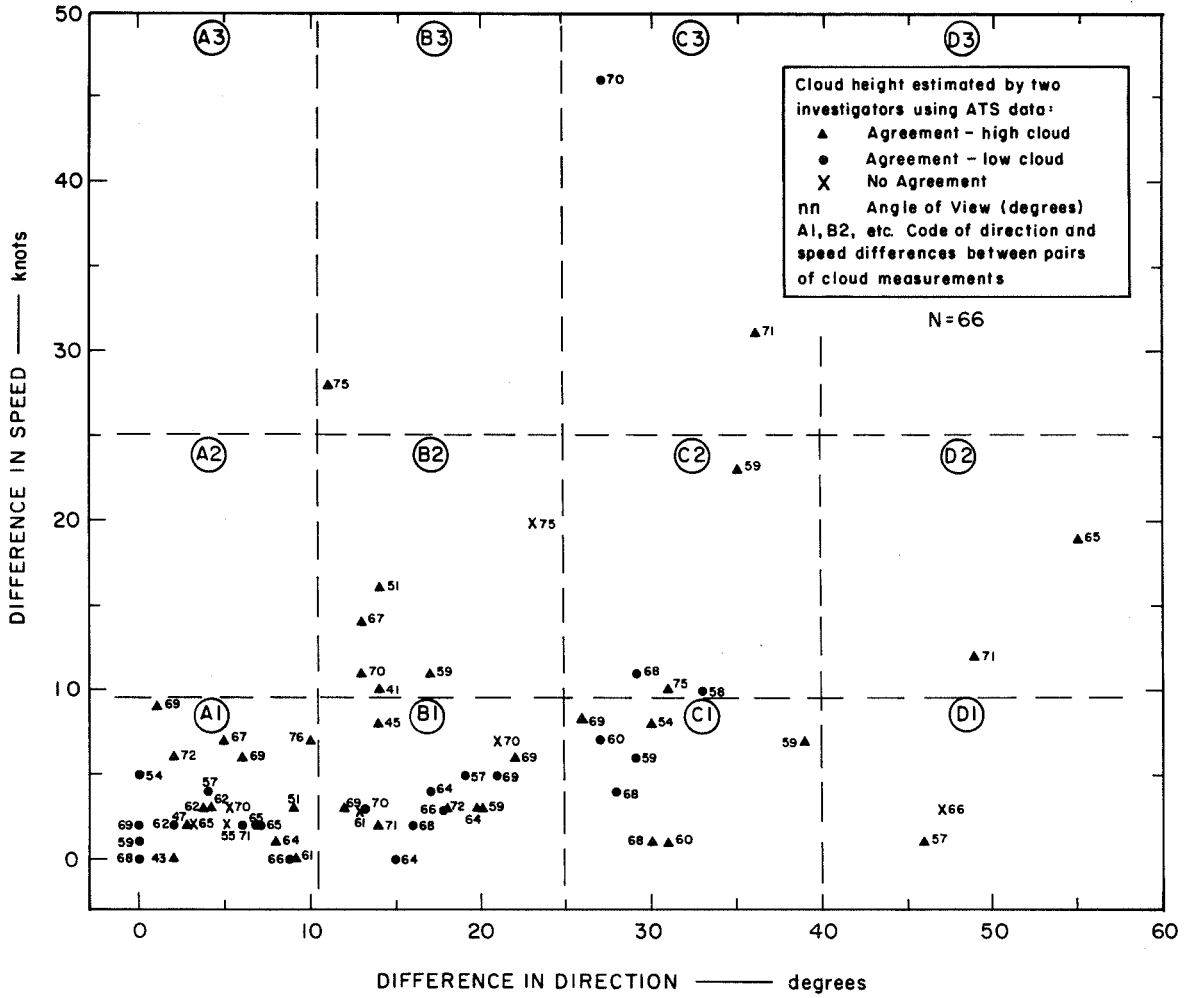
Part of Task 1 required a comparison of motion measurements as obtained by different investigators tracking the same cloud. Of the 174

measurements made by the initial investigator, 66 cases (approximately 40 percent, selected at random, were remeasured by a second investigator, yielding a total of 240 measurements. This selection included cases from each of the six days and covered a wide range of angles of view. While securing these cloud motion measurements both investigators also estimated the cloud "height" (either "high" for alto or cirro-form clouds and "low" for cumulus or stratus clouds) as an added test of the ability to identify clouds at large angles of view. In all comparisons the selected cloud was tracked through a minimum time span of one hour; about 88 percent of the cases were tracked through a two-hour time span.

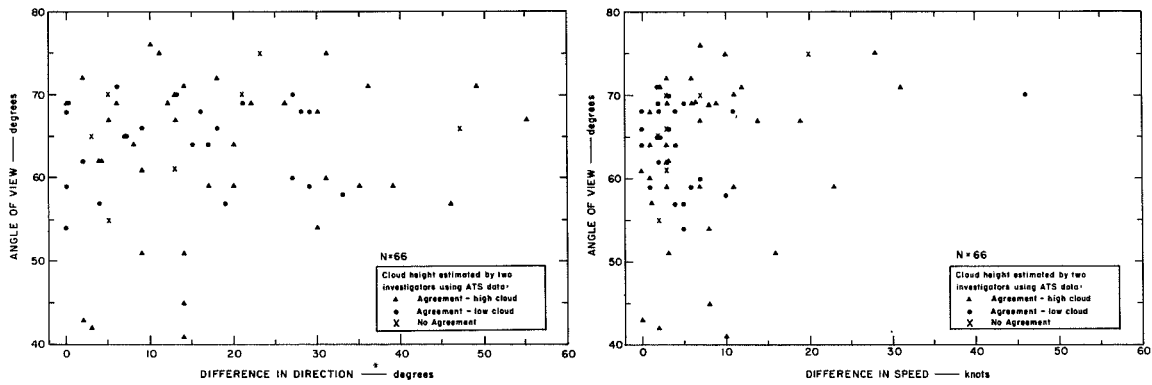
1. Magnitude of Differences

The distribution of speed and directional differences for the 66 pairs measured by the two investigators is given in Figure 13(a).³ The vast majority of comparisons (82 percent) yielded a speed difference of 10 knots or less between pairs; nearly 90 percent of the directional differences were less than 35°. The average speed difference was 6.76 knots, the average directional difference was 16.3°. Though absolute agreement was achieved in only two cases, differences within 10° in direction and 10 knots of speed were achieved in 25 comparisons (about 40 percent of the sample). Those categories indicating close measurement agreement (viz., A1, B1, B2) contain a wide range of angles of view; the largest disagreements (viz., D1, D2, C3) were associated only with large angles of view.

³As a convenience in categorizing the differences, the distribution [Figure 13(a)] was divided, subjectively, on the basis of occurrence and indicated by alphanumeric code. Agreement on the cloud height estimate is also indicated by code in Figure 13(a) and 13(b).



(a) CATEGORIES OF DIRECTION AND SPEED DIFFERENCES



(b) DIFFERENCES AS A FUNCTION OF THE ANGLE OF VIEW

FIGURE 13 DIFFERENCES (DIRECTION AND SPEED) BETWEEN INDEPENDENT MEASUREMENTS OF SAME CLOUDS

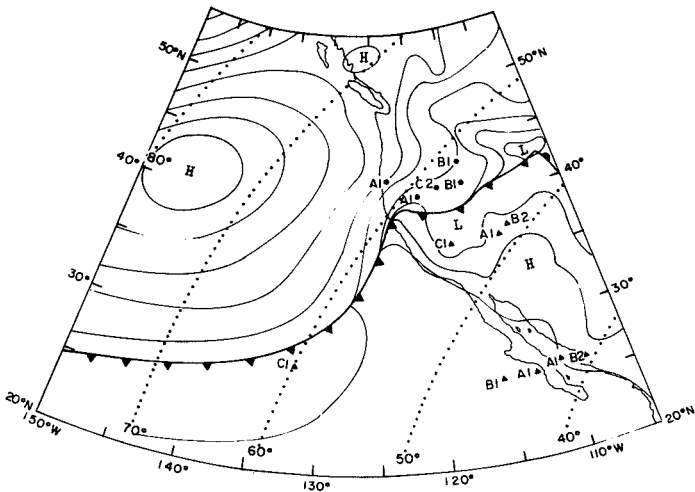
The distribution of direction and speed measurement differences by angle of view is shown in Figure 13(b). There is no (or only slight) tendency for increasing measurement difference values to occur with angles of view between 55° and 75° . These differences become marked for measurement values between angles of view of 40° and 55° . The sample size through the lower values of angle of view, however, is too small to make a definitive statement in this regard.

2. Location of Differences

Figure 14 shows the location (by days) of each of the 66 compared measurements.⁴ The distribution of these comparisons suggests that, in addition to the angle of view and tracking time, the "nature" of the cloud cover prevailing in a synoptic situation can have an important effect on the ability of two investigators to secure identical or near identical cloud motion measurements and cloud height identifications.

The word "nature," as used here, implies those factors of brightness, texture, and cloud type that influence visual detection and measurement. Stratiform clouds, which are thin, present a flat brightness gradient that leads to a visual appearance of ill-defined edges. Where cloud edges must be used for motion measurements in these circumstances (as may be necessary with a broad overcast cloud field), the measurements by two investigators are apt to differ. The situation is

⁴Code values for the various measurement difference categories and agreement on cloud height estimates are entered at the cloud location.

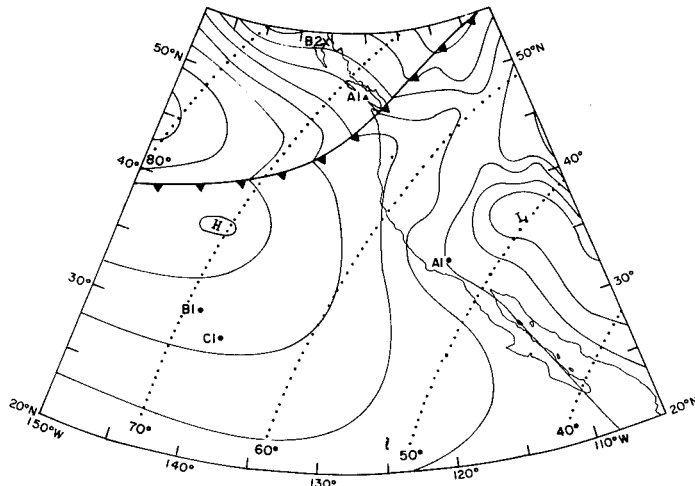


(a) 12 APRIL 1968

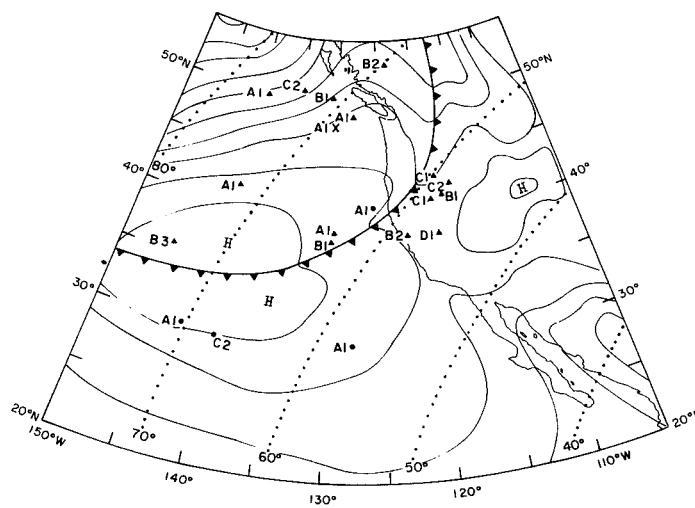
Cloud height estimated by two investigators using ATS data

- ▲ Agreement - high cloud
- Agreement - low cloud
- X No Agreement
- Angle of View (degrees)

A1, B2, etc. Code of direction and speed differences between pairs of cloud measurements (see FIG. 13)

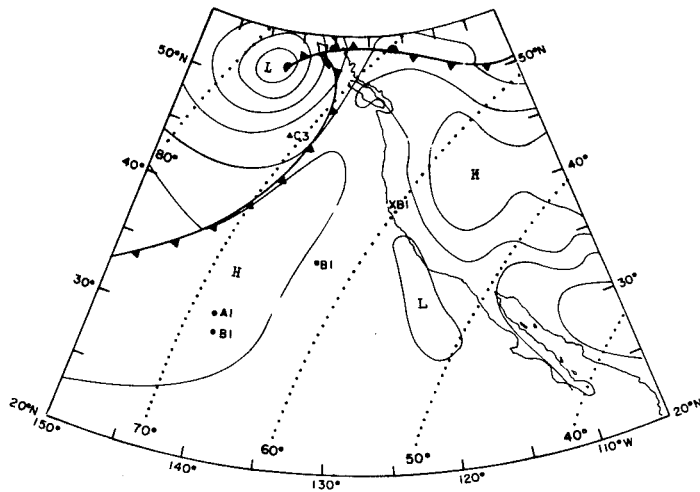


(b) 18 APRIL 1968

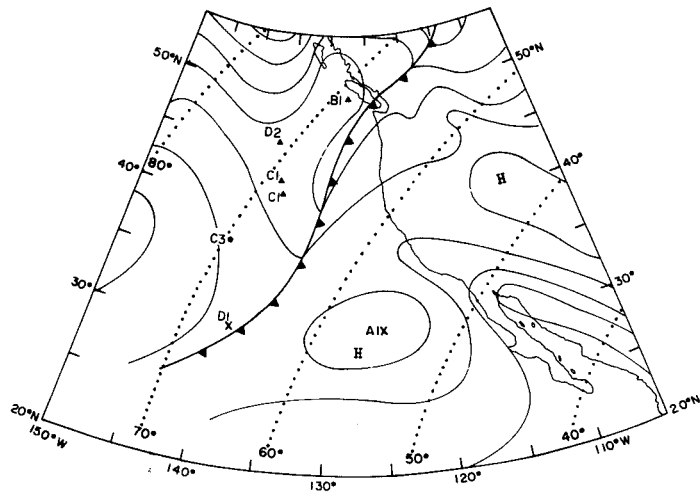


(c) 23 APRIL 1968

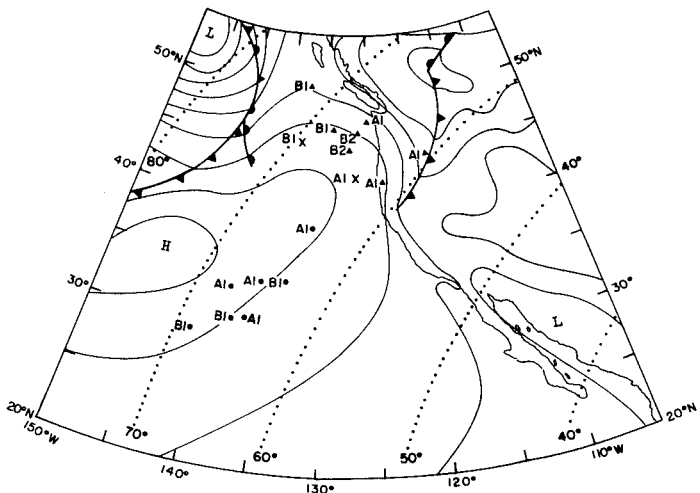
FIGURE 14 LOCATION OF COMPARED MEASUREMENTS (66 CASES)



(d) 28 APRIL 1968



(e) 29 APRIL 1968



(f) 30 APRIL 1968

FIGURE 14 LOCATION OF COMPARED MEASUREMENTS (66 CASES) (Concluded)

not so severe with cumulus clouds, since they usually appear as bright "blobs" with a comparatively "sharp" edge (marked brightness gradient). In all measurements use of the cloud mass centrum as a measuring point is to be preferred to use of cloud edges, if at all possible. Also, the length of the cloud tracking time should be as long as possible (a time span of one hour is about the minimum) to balance out the effect of mechanical measurement errors.

The group of cases between 55° and 60° angles of view on Figure 13 that show directional differences ranging from 25° to 45° were associated with measurements of prefrontal clouds located over the western states on 12 April and 23 April. With frontal situations the cloud appearance is often chaotic, with imprecise cloud edges, making it difficult to track clouds with certainty. Clouds with precise edges will be measured with more certainty.

The compared measurements, illustrated in Figure 14, can be described as follows:

12 April [Figure 14(a)]--The group of measurements situated just north of the cold front (angle of view 55° to 62°) yielded differences in the A1 or B1 category: Only one comparison shows a measurement difference as large as class C2. Both investigators estimated "low clouds." South of the front three comparisons yielded agreement on the identification of "high" clouds and speed but disagreed on direction.

Four cases are located in Lower California (angle of view 40° to 45°). The ATS photo showed these clouds to be small but with fairly precise edges. Both investigators identified the clouds as being in the "high" cloud category and measurements are in fair to good agreement (A1 to B2).

A single comparison (C1) is located near 28°N, 132°W, just ahead of the cold front. There is agreement on the estimate of "high" cloud; motion measurements show close agreement on speed but moderate difference in direction.

18 April [Figure 14(b)]--Two measurements were made in the post-frontal regime, both at rather high angles of view. The case at 75° angle of view located in British Columbia (B2) shows lack of agreement as to cloud height and a fair-sized difference in measurement. The ATS photo showed the cloud cover in this region to lack detail and resolution. Further south (68° angle of view) the identification and measurement (A1) are in good agreement. Here, the ATS photo showed the cold front cloudiness and the immediate post-frontal cloudiness with more clarity.

The two cases (B1, C1) near 30°N, 140°W (66° to 69° angle of view) are within the high-pressure cell. Both were identified as low cloud. Measurement agreement of speed can be considered as good but directional agreement was only fair. At these high angles of view, the cloud cover lacks sufficient visual detail to permit measurements with high confidence.

In lower California (54° angle of view), the comparison of identification and measurement was good (A1). The ATS photo showed cumuliform cloudiness in the area.

23 April [Figure 14(c)]--Numerous comparisons are distributed along the front extending from the west coast, through the high-pressure cell. Over the western states just ahead of the front both investigators estimated the clouds to be "high" clouds but there are moderate to large differences in measurement (B1 to D1), primarily in direction. The lack of a sharp brightness gradient between clouds and ocean makes the

measurement difficult, despite the comparatively moderate angle of view.

Along the front and in the post-frontal region, the cloud cover appears with a more precise edge and detail. The differences in measurement were generally A1 or B1 along the front and through the high cell with the exception of two cases (C2 and B3) near 30°N, 140°W and 35°N, 147°W, respectively.

Along 50°N latitude (post-frontal region) the investigators agreed in their estimation of "high" cloud, except for one case; measurement differences were small to moderate (A1 to C2).

Three cases were compared in the high-pressure cell ahead of the front; two of the three cases were in the A1 category and one was a C2. All three cases agree on cloud height identification.

28 April [Figure 14(d)]--All comparisons were made at angles of view greater than 60°. Of the five comparisons made, four were located within the high-pressure region, and yielded fair-to-good measurement agreement (A1 or B1). All cloud height estimates agree except one. The ATS photo shows the cloud cover to have rather distinct edges, though lacking in cloud detail.

The comparison near the front to the north yielded an agreement on cloud height estimation but large differences in motion measurement (C3). The angle of view is large and the ATS photo shows no cloud detail.

29 April [Figure 14(e)]--Most of the comparisons were located in the post-frontal region (angles of view between 65° to 72°). Cloud height estimates agreed but the pairs of measurements differed, moderately, yielding categories B1, C1, C3, and D2. The ATS photo shows diffuse cloud structures in the post-frontal region at these angles of

view. The one comparison quite near the front differed markedly in direction (D1) and in the estimates of cloud height.

The comparison in the center of the high cell yielded good agreement on motion (A1) but no agreement on the estimate of cloud height. This may be due to lack of resolution; the ATS photo shows small-sized cloud elements, which could be identified as cumulus or cirrus spissatus.

30 April [Figure 14(f)]--All comparisons were made of cloud elements in the high-pressure cell and ridge between 60° and 72° angles of view. The group of comparisons between 30°N and 35°N show good agreement on cloud height and motion. Most of the difference categories are A1 or B1. The ATS photo of this area shows small-sized cloud elements, well separated and with fairly precise edges.

The group of comparisons to the north (between 40°N and 50°N) yielded difference categories of A1, B1, and B2. There are two cases where the cloud height estimates did not agree. The ATS photo shows a broad area of clearing, filled with small-scale cloud elements. The cloud character and cloud edges seem not as distinct as those at the lower latitudes.

The data in Figures 13 and 14 show that 47 of the 66 cases (70 percent of the sample) fell into categories A1, B1, A2, and B2. These figures also show agreement on the cloud height estimates in 58 cases (88 percent of the sample). This includes 23 estimates of "low" cloud and 35 estimates of "high" cloud; 8 cases (12 percent of the sample) showed no agreement. Note, however, that these data are comparisons of the measurements of two investigators only; due to lack of reports they could not be compared to shipboard cloud observations for verification.

Considering all six days, these 47 cases ranged through virtually all angles of view from 45° to 70° and a wide variety of locations within a synoptic pattern. If these categories are assumed to represent fair to good agreement, then it can be said that, at least to 70° angle of view, the size of a cloud element, its detail, and sharpness of definition are important factors in accurate measurement and cloud height identification, since these qualities were more often met in these categories than in categories C1, C2, D2, and D1. In categories B3, C3, and D3, where speed and direction differences were very large, the angles of view were 70° or greater. Here, undoubtedly, the angle of view contributed to lack of sharpness of definition and detail with consequent inability to make a precise measurement.

C. Comparison of Cloud Data and Rawinsonde Data

1. Cloud Motions and Winds at Level of Best Fit

None of the ATS cloud motion measurements could be compared with wind reports at the exact position of the measurement. Nor could they be compared to measurements of the same cloud obtained from using ESSA III data because the ESSA III photographs did not overlap sufficiently in time or space to evaluate movements. However, some estimation of the measurement accuracy can be gained by comparing cloud motion to rawinsonde data, using the wind at the level of best fit (i.e., minimum vector difference between the observed wind and the cloud motion vector). This assumes that the wind at the level of best fit is equivalent to the wind at the cloud height and can be used in lieu of actual knowledge of the cloud height.

To do this, 43 motion measurements of cloud elements within 60 nmi of a rawinsonde station were available from the total sample of 174 initial measurements and 66 remeasurements. For these data the 1200

GMT and 0000 GMT hodographs were plotted using the rawin data that were available at 50-mb intervals. The measured cloud motion vectors were then plotted on these hodographs and the level of best fit noted.⁵ Table 4 lists the levels of best fit selected. Obviously, the majority of comparisons occurred at levels below the 500-mb level, suggesting that a preponderance of middle or low clouds were tracked.

Table 4

FREQUENCY OF LEVEL OF BEST FIT (43 CASES)

Level of Best Fit (mb)	Number of Cases
950	4
900	4
850	4
800	7
750	4
700	3
650	4
600	3
550	3
500	1
450	1
400	1
350	1
300	1
250	2

⁵ In selecting the level of best fit, the cloud motions were compared to both the 1200 GMT and 0000 GMT rawinsondes spanning the cloud motion time (which ranged from 1736 GMT to 2016 GMT). The smallest minimum difference that resulted from either of these comparisons was chosen for comparison. This procedure is based on the premise that the differences obtained in this manner would represent the optimum skill with which the system can be used.

A plot of cloud motion and the wind (considered separately in terms of direction and speed) at the level of best fit is shown in Figure 15. Agreement, of course, is fairly good considering the fact that some six hours of time difference separated the comparison, plus the fact that the minimum vector difference between the cloud motion and some winds could only be determined to the closest 50 mb. The direction of the cloud motions varied either side of the wind direction, but speeds of the cloud motion were generally somewhat greater than the speed of the wind at the level of best fit.

A plot of the differences in direction and speed between the measured cloud motion and the wind at the level of best fit as a function of the angle of view is given in Figure 16. In about 75 percent of the cases the differences in direction were less than 17° ; speed differences were less than 5 knots and the minimum vector differences were less than 8 knots.

A graph of these differences expressed as a cumulative percentage frequency is given in Figure 17.

A tabulation of the mean differences for the sample is given in Table 5. These values pertain to angles of view greater than 50° . In a previous study by Serebreny, et al. (1970), where the angle of view was less than 40° , the results show differences of smaller magnitude, particularly direction differences. This suggests, as did the data in Figure 14, that measurements at large angles of view possess somewhat greater direction uncertainties.

2. Observed Cloud Types and Level of Best Fit

It must be noted that the comparisons of cloud motion with rawinsonde data (Figures 15 through 17 and Table 4) were based upon the

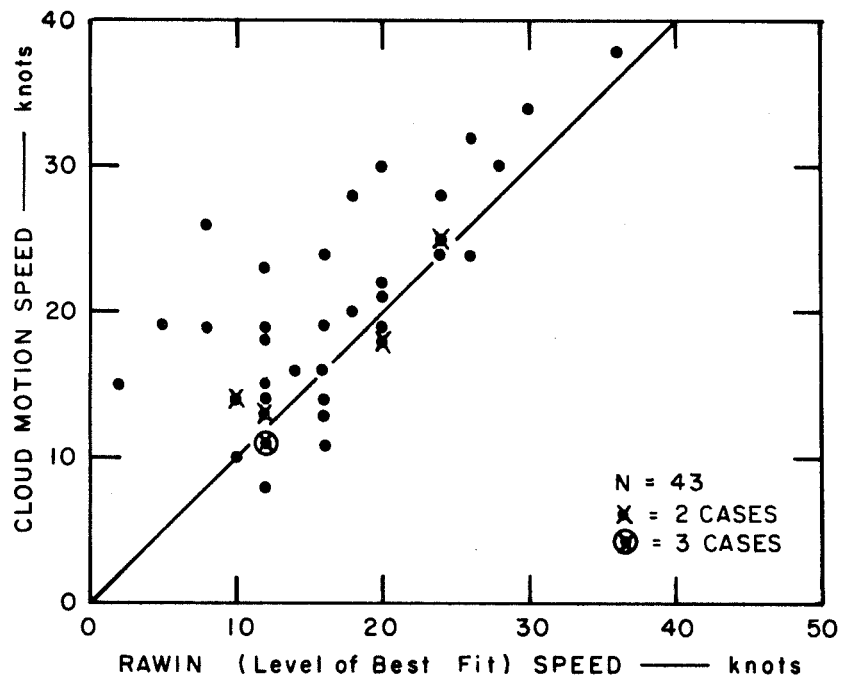
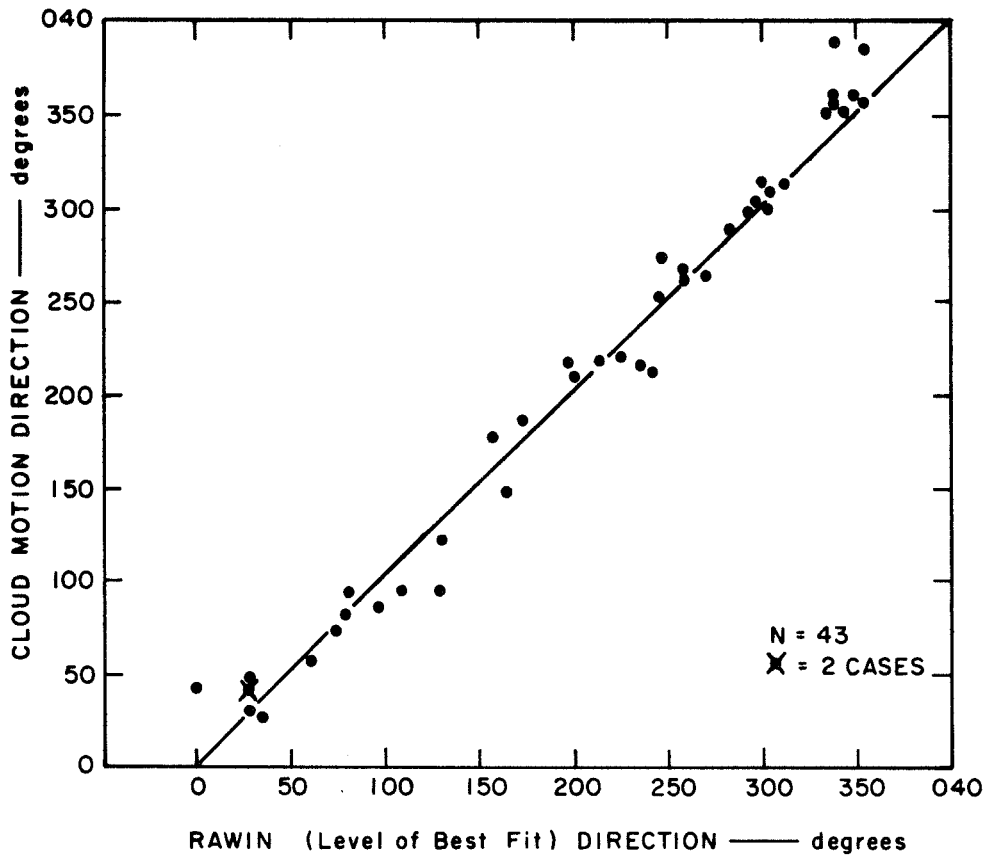


FIGURE 15 COMPARISON OF CLOUD MOTION WITH WIND AT LEVEL OF BEST FIT

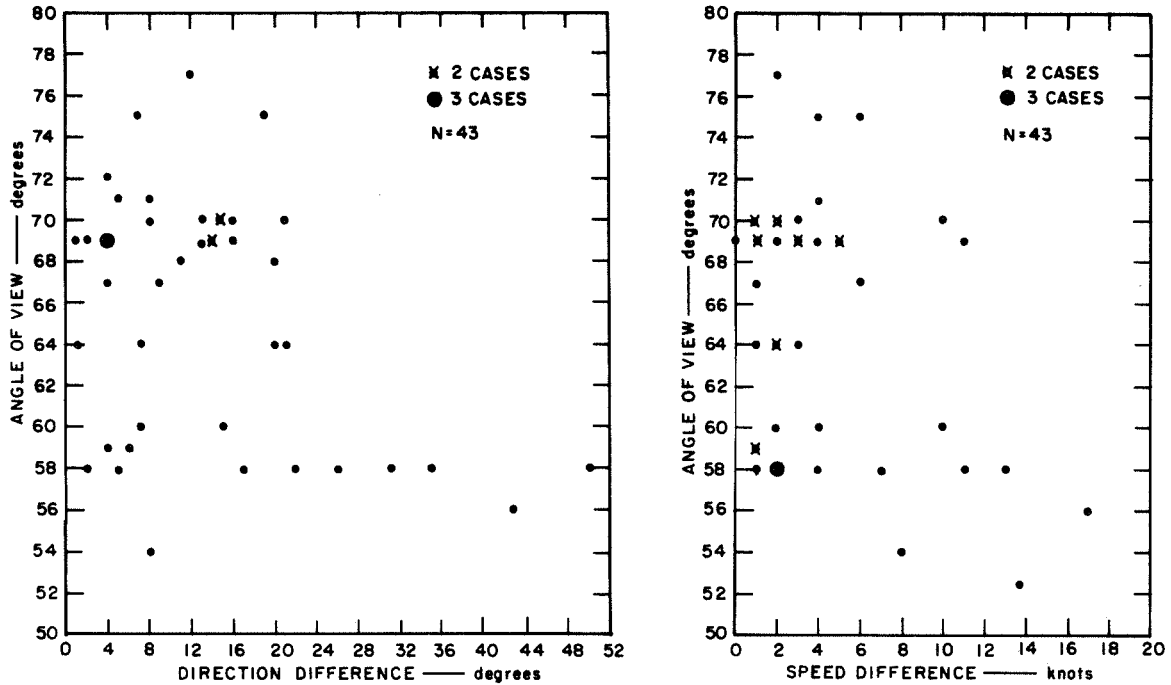


FIGURE 16 DIFFERENCES BETWEEN CLOUD MOTION AND RAWIN AS A FUNCTION OF ANGLES OF VIEW

wind found at the level of best fit. The level of best fit, however, is only an inferential estimate of the cloud height for which the motion was measured; the choice of the level of best fit itself is highly sensitive to the accuracy of the measured cloud motion. If this motion is "incorrect" with respect to actual values, the level of best fit will be incorrect (i.e., not equivalent to the true height of the measured cloud), even though the comparison may yield a rather small direction and speed or vector difference. If these errors are large it can lead to instances where the level of best fit would be "incompatible" with the type of cloud actually observed.

Surface cloud observations, nearest in space and time to the 43 cloud motions, were checked for compatibility with the type of cloudiness to be expected from the values of the levels of best fit. These observations were based on "hourlies" and the comparisons did not

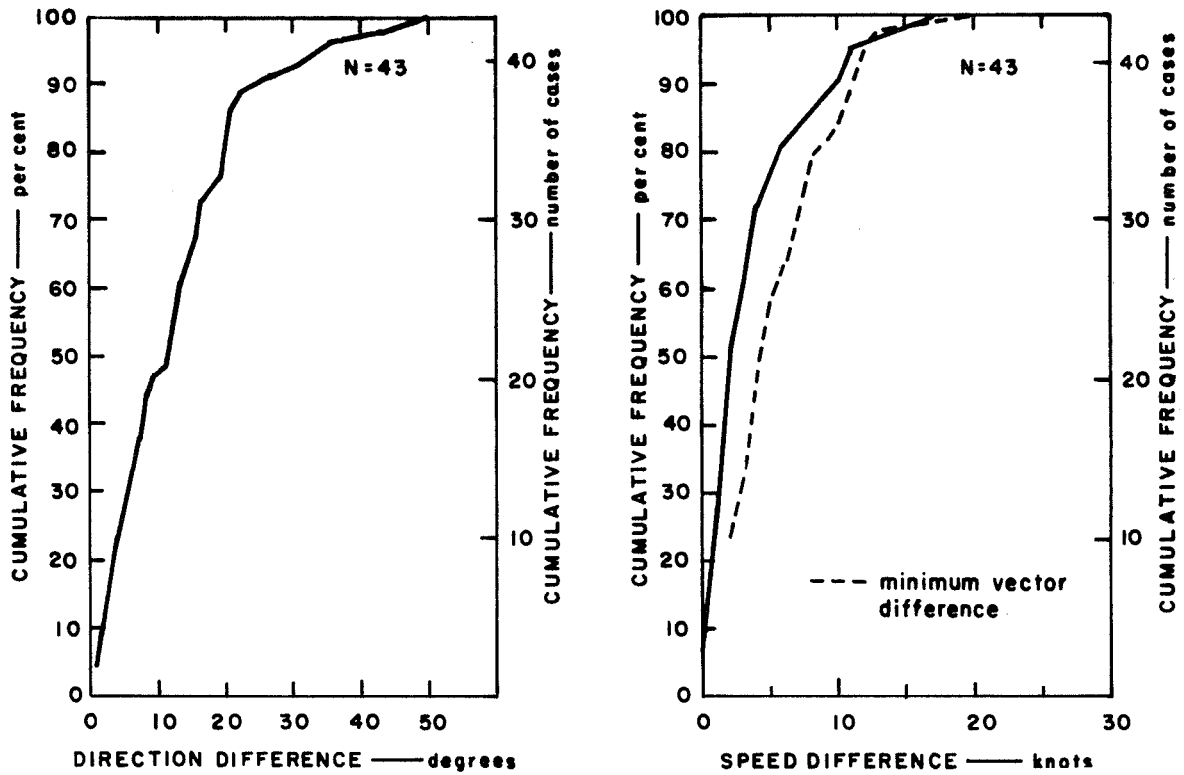


FIGURE 17 CUMULATIVE FREQUENCY OF DIFFERENCES BETWEEN CLOUD MOTION AND WIND AT LEVEL OF BEST FIT (minimum vector difference added)

exceed 60 nm or 2 hours of time difference. The cases, categorized as "high" clouds or "low" clouds, respectively (estimated from the motions and appearance in ATS photographs) are compared separately (see Figure 18). The 700-mb level was used as the break point between "low" and "high" cloud. In Figure 18(a), those cases located out to about 65° angle of view showed good agreement between the original cloud height class estimate of "high" clouds, the height of the level of best fit, and the cloud types reported by the surface observation. Only one case yielded a level of best fit (800-mb level) which can be considered to be incompatible with the ATS estimate and the cloud types.

At angles of view greater than 65°, the ATS cloud-height estimates and the levels of best fit do not agree; five cases with

Table 5

MEAN DIFFERENCES BETWEEN CLOUD MOTIONS AND WIND
AT THE LEVELS OF BEST FIT

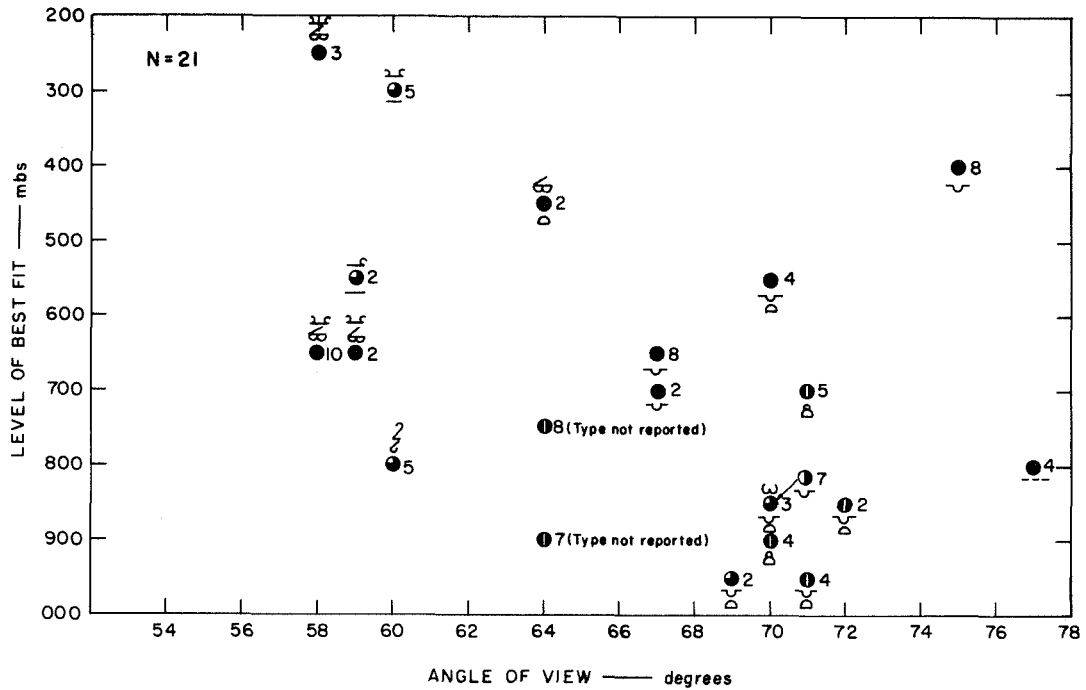
	Present Study (43 cases)	Serebreny, et al. (1970) (180 cases)
Mean (Scalar) Direction Difference	13.4°	5.77°
Mean (Scalar) Speed Difference	4.0 knots	3.15 knots
Mean Vector Difference (magnitude only)	5.9 knots	5.53 knots
Standard Vector Deviation, σ_v^*	7.1 knots	6.71 knots

*The standard vector deviation used in this report is based on the following formula:

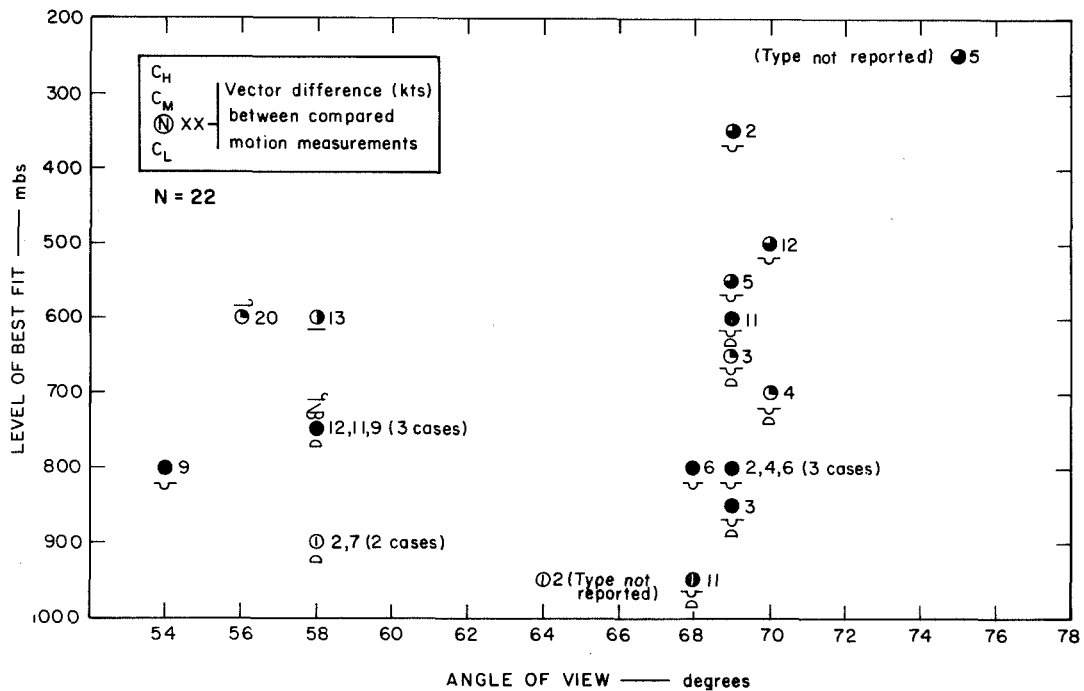
$$\sigma_v = \sqrt{\frac{\sum_{i=1}^n |R_i|^2}{N}}$$

where $|R_i|$ is the magnitude of the vector difference between ATS wind and balloon wind. If the directions are assumed to be randomly distributed, then σ_v is an estimate of the "error" that would not be exceeded in 68 percent of the cases.

levels of best fit above the 700-mb level were reported as low cloudiness. However, the low overcast prevents knowing if high cloud was also present at these stations. For the cases having a level of best fit below the 700-mb level, the reported cloud types are compatible, though not consistent with the original classification from the ATS photographs.



(a) CASES CATEGORIZED AS "HIGH" CLOUD FROM ATS PHOTOS



(b) CASES CATEGORIZED AS "LOW" CLOUD FROM ATS PHOTOS

FIGURE 18 LEVEL OF BEST FIT AND NEAREST REPORTED CLOUD COVER FOR 43 CASES WITHIN 60 nmi OF RAWINSONDE STATION

In Figure 18(b), the comparisons of cases located out to about 65° show good agreement between the initial estimate of "low" clouds using ATS data, the level of best fit, and the type of cloud reported by the surface observer. Beyond 65° angle of view, the estimate from the ATS photograph is consistent with the surface reports but levels of best fit are less compatible. Six cases, for which low stratiform clouds are reported, have levels of best fit above the 700-mb level.

The distribution in Figure 18 (considering both panels) indicates that most cloud height estimates were correct out to about 65° angle of view; beyond that point the estimates were correct in about 50 percent of the cases. The derived levels of best fit for cases having angles of view less than 65° were compatible with the separate cloud types in 13 out of 15 comparisons (87 percent). At angles of view greater than 65°, the levels of best fit were compatible in 14 out of 24 cases (58 percent). (Four cases in the sample did not have surface cloud types available.)

This decrease in "compatibility" demonstrates the comparatively greater difficulty of making cloud identification and measurement at the larger angles of view. Some of these difficulties are due to lack of resolution of cloud elements. Other difficulties stem from the measurement capability of the spacecraft and console systems.

D. Summation

The comparison of cloud height identifications (using the rather gross classification of "low" or "high") made by two investigators indicated rather good agreement for clouds viewed at less than 60° angle of view, despite a variety of synoptic conditions. During the six days the motion of the clouds, particularly the "low" clouds, agreed quite

well with the sense of the circulation implied by the surface and upper-air charts. The ability to identify or measure clouds at angles of view greater than 60° is highly influenced by cloud type, spacing between clouds, direction and magnitude of the cloud displacement and, not least, visible detail or configuration.

The tendency, when using ATS photographic data, is to rely on the amount and direction of displacement whenever identification is not clearly possible through cloud detail. The results seem to indicate that this is a reasonable approach to cloud identification, at least when cloud identity is based only on the sample stratification of "high" or "low" clouds.

The comparison of the motion of a given cloud as measured by two analysts yielded a speed difference of 10 knots or less in 82 percent of the comparisons and a direction difference of less than 35° in 90 percent of the cases. Agreements within 10° and 10 knots were achieved in 40 percent of the cases. The average speed difference was about 7 knots; the average direction difference was some 16° .

Although close agreement was obtained at all angles of view (45° to 78°), the largest disagreements in speed and/or direction were associated only with large angles of views (i.e., greater than 60°). In general, both the speed and direction differences tended to be small between 40° and 55° angle of view and then to increase markedly thereafter.

A comparison of cloud motion with the wind at the level of best fit, using rawinsonde data within 60 nmi of the measured cloud, indicated that 75 percent of the direction differences were less than 17° ; speed differences were less than 5 knots. The mean values were 13° and 4 knots, respectively. Minimum vector differences (magnitude) were less

than 8 knots in 75 percent of the cases; the average value was 6 knots. The range of direction and speed differences were about the same through all the angles of view involved (52° to 77°). Even with these differences, the distribution of the measurements over a widespread area seem to reflect the circulation in the area adequately, as expressed by the distribution of cloud cover.

The levels of best fit based on motion measurements associated with angles of view less than 65° were compatible in 87 percent of the comparisons with type of cloud reported at the surface. Beyond 65° angle of view, agreement was found in only 58 percent of the cases. Lack of resolution and inability to achieve the measurement accuracy required at large angles of view contribute to the loss of compatibility at large viewing angles.

The current SRI/NASA Electronic Display measuring system, applied at large angles of view, is such that a variation of one cursor unit, on the average, can increase or decrease the direction measured by 16° ; the speed can be changed by about 4 knots. This in turn can effect determination of the level of best fit in those instances when cloud motions are compared with rawinsonde data showing small changes of wind speed or large direction changes with height.

IV COMPARISON OF APOLLO 6 AND ATS III DATA

Task 2 was concerned with comparing ATS III photographs with photographic data secured by Apollo 6. On 4 April 1968 a camera aboard the unmanned Apollo 6 spacecraft took 70-mm color photographs of cloud cover and surface features. During a portion of the second orbit, cloud cover over the North Atlantic was photographed over a narrow swath extending from the coast of South Carolina to the coast of Mauritania in Western Africa. This section discusses the analyses of Apollo 6 photographs over the North Atlantic and compares them with other types of data. Specifically, cloud types shown by the Apollo 6 films were compared with ATS III cloud motions measured through the use of the SRI/NASA Electronic Display console. We also examined ESSA III photographs over the area of interest, but concluded that they did not provide any additional information; therefore, these are not presented or discussed.

One hundred and four frames of Apollo 6 color film were investigated, beginning with No. 831 ($32^{\circ} 37'N$, $78^{\circ} 46'W$, at 1326 GMT), and ending with No. 934 ($17^{\circ} 27'N$, $16^{\circ} 18'W$, at 1351 GMT). Black-and-white contact prints were made from the film containing the above frames; the prints were assembled as a mosaic (which required that each photograph be rotated 90° and overlapped about 50 percent). The mosaic was then photographed and prints made both to the original scale and at a reduced scale that corresponded to that of an enlarged or magnified section of the concurrent ATS III photograph.

An experiment was also conducted in which the 70-mm Apollo photographs were rephotographed on 16-mm color film with five stages of defocusing. The resulting films, especially the final stage of defocusing,

merge small cloud elements and blur the patterns to an extent nearly comparable to the ATS III photographs.

Eight ATS III Meteorological Spin-Scan Cloud Camera (MSSCC) photographs were selected for analysis: frames 8 (1256:41 GMT) through 15 (1522:50 GMT). Enlargements were printed from negatives that were made from positive-viewing transparencies on hand. The boundaries of the swath photographed from Apollo 6 were marked on the ATS photograph by identifying similar cloud patterns shown by the two types of photographs. The ATS III photograph was then given to meteorologists operating the display system, so they would know the specific area in which cloud-motion measurements were desired.

The eight ATS III photographs were entered in the storage disc in the display system, and by time-lapse viewing, the direction and speed of 55 cloud elements within the area viewed by Apollo 6 were determined.

A. Synoptic Situation and Cloud Types

Figure 19 shows charts of the 850- and 300-mb levels and locations of the 55 cloud elements measured from the ATS III films.

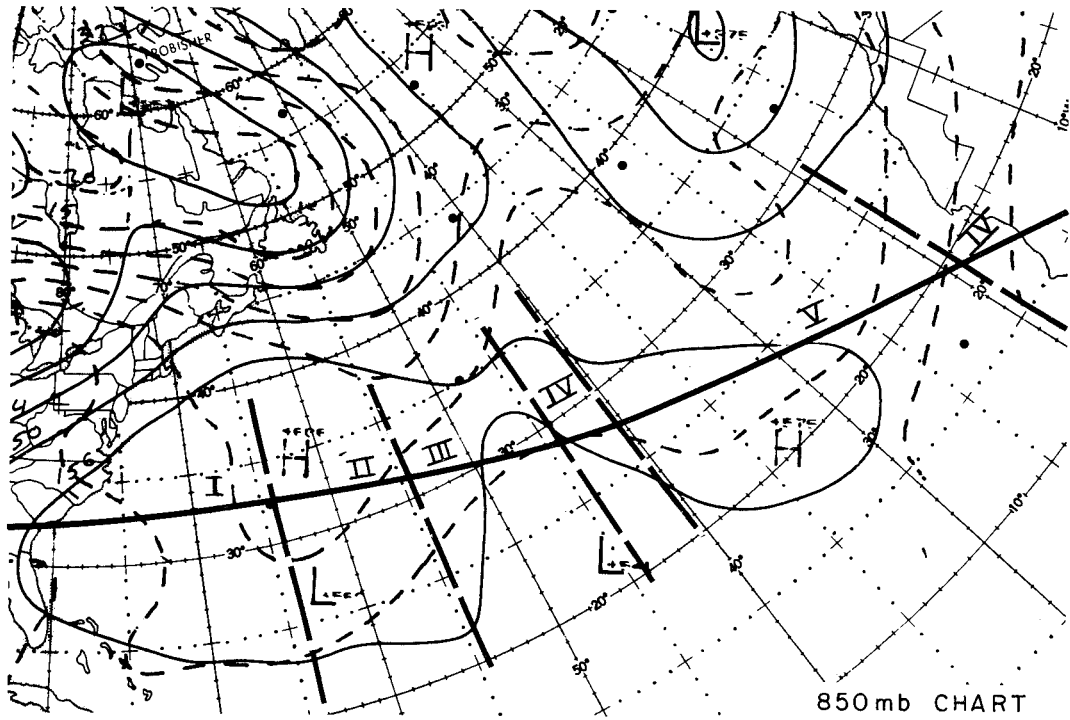
The indicated latitudes and longitudes are the midpoint positions of the distance over which the measured cloud elements traveled. This is not necessarily the same as the position on a given ATS III photograph, since different elements moved at different speeds and since the time period over which various elements could be followed varied due to formation and dissipation. The Roman numerals identify the areas along the track in which specific types, or combinations of types, of cloud cover predominated. The types of cloud cover, based on both the appearance of cloud cover in the Apollo 6 photographs and cloud-motion measurements from ATS photographs, are listed in Table 6.

Figure 19(a) shows 850- and 300-mb charts prepared by the NWP Unit of ESSA. The 850-mb chart shows high pressure over much of the North Atlantic along the Apollo 6 track but there is also an inverted trough between 45°W and 50°W. South of this trough (near 20°N) there is an "L" on the map, presumably denoting the location of a low-pressure area. There is another "L" at 26.5°N, 62.5°W, denoting an area of lower pressure near the southern edge of the high-pressure area over the Western Atlantic. The latter position labeled "L" corresponds roughly to an area of cloud in the ATS photograph that appears as a cloud vortex.

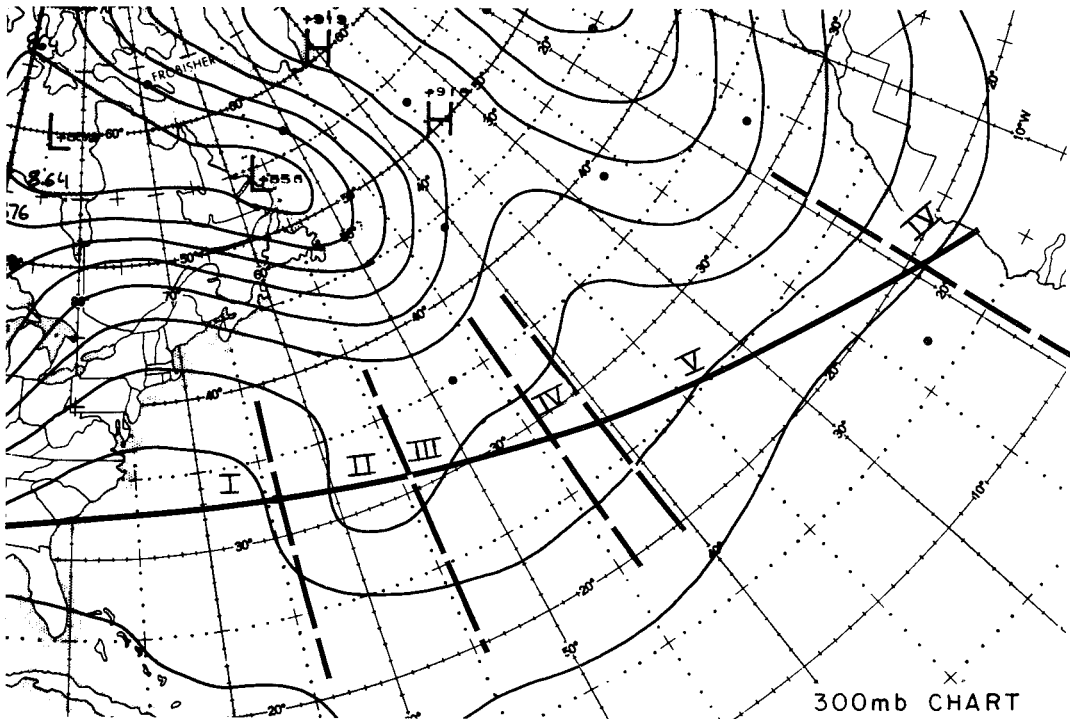
The 300-mb chart shows a trough across the Apollo track between 55°W and 60°W--the area of the cloud vortex--but the chart shows no evidence of a trough in the vicinity of the 850-mb level inverted trough near 45°W. Thus the latter is either a low level phenomenon or data are too sparse at upper levels for its identification. There were no closed lows south of the track until 1200 GMT, 6 April 1968, and even then there was no reflection of such a low circulation on the 700-mb chart. Reports from a Gull India flight along the 500-mb level showed a gradual change from moderate westerlies (20 knots) on 4 April 1968, to northeasterlies with speeds of 30 to 40 knots on 6 April in the vicinity of 23°N, 51°W or just to the east of the 300-mb trough in Figure 19(a).

Figure 20 illustrates the cloud cover shown by the ATS III photograph at 1338 GMT and the swath photographed from the Apollo 6 spacecraft. Roman numerals corresponding to those on Figure 19 identify the regions of similar cloud cover listed in Table 6.

Figure 21 is a comparison of cloud elements as shown by a reduced copy of a mosaic made from the high-resolution Apollo 6, 70-mm color film and by the ATS III camera system, which has a resolution of 2 nmi at the satellite subpoint. Careful inspection of the two types of



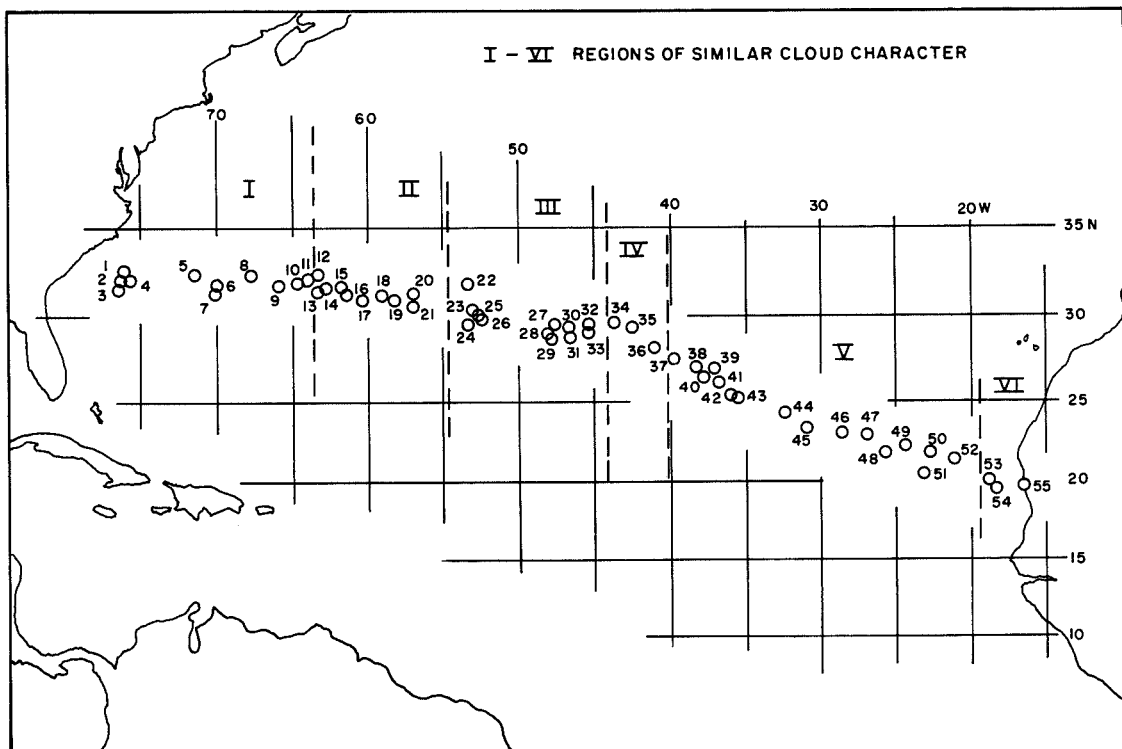
850 mb CHART



300 mb CHART

(a) SYNOPTIC SITUATION AND APOLLO 6 TRACK

FIGURE 19 SYNOPTIC SITUATION AT 1200 GMT ON 4 APRIL 1968 AND LOCATIONS OF CLOUDS MEASURED ALONG TRACK OF APOLLO 6



(b) CLOUD LOCATIONS

FIGURE 19 SYNOPTIC SITUATION AT 1200 GMT ON 4 APRIL 1968 AND LOCATIONS OF CLOUDS MEASURED ALONG TRACK OF APOLLO 6 (Concluded)

Table 6

CLOUD DISTRIBUTIONS ALONG TRACK OF APOLLO 6

Area	Cloud Types
I	Cumulus and stratocumulus
II	Upper clouds at the northern edge of a cloud vortex (probably altostratus)
III	Cirrus clouds with cumulus visible below
IV	Cirrus overcast
V	Scattered cumulus
VI	Jet stream cirrus

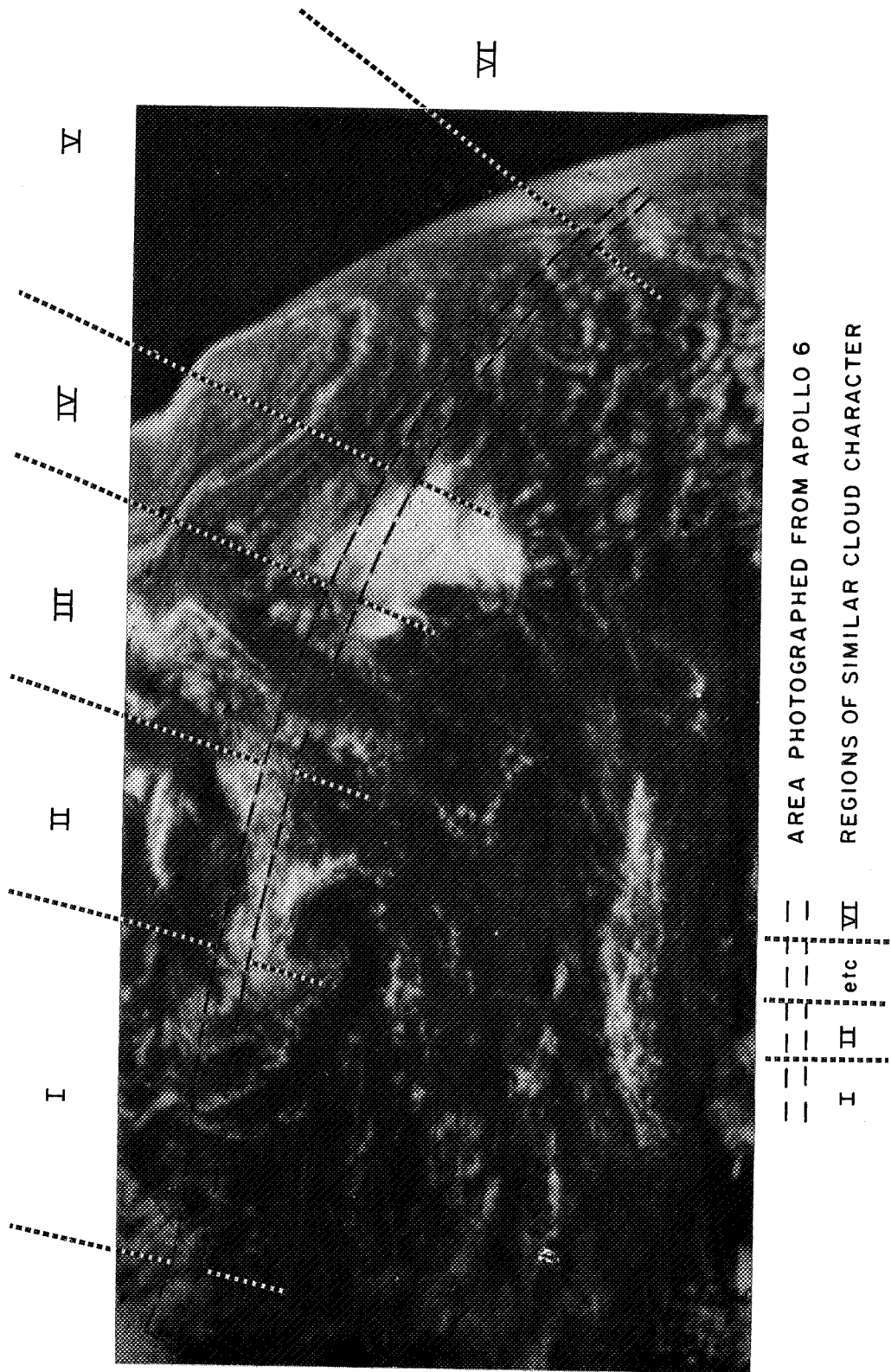


FIGURE 20 ATS III VIEW OF CLOUD COVER ALONG TRACK OF APOLLO 6

photographs shows that nearly all of the cloud patterns shown by the Apollo 6 can be identified in the ATS III photograph, despite the much lower resolution of the latter. Detail on specific cloud elements is, of course, "lost" in the ATS photograph. As an example, the rows of very small cumulus clouds in the area between cloud elements identified as 4 and 5 do not appear in the ATS III photograph.

B. Cloud Measurements

The direction and speed of the various cloud features are indicated on the overlay of Figure 22, together with an assessment of whether the clouds were at low altitudes or high altitudes. This assessment of altitude is not based solely on the photographs shown on Figure 21. This is because it is very difficult to determine cloud type and altitude from a single photograph. When a series of ATS photographs are viewed in time lapse, differential motion, knowledge of regional climatology, and the general synoptic pattern implied by the cloud configuration permit some differentiation between lower and upper clouds.

The accuracy of the measured motions depends on two main factors:

- The accuracy with which the photographs are registered with one another which can be done with extreme accuracy only when terrain features are visible.
- How well the cloud feature can be identified.

The ATS MSSCC with its 2-nmi resolution smears out cloud edges. In the case of the 4 April ATS III MSSCC photographs, there was a flaw in the pictures, as indicated by a marked discontinuity in the horizon on Figure 20. This flaw was near the northern edge of the area photographed by Apollo 6 over the western Atlantic, and thus some cloud elements at the northern edge of the Apollo 6 swath could not be measured. In addition,

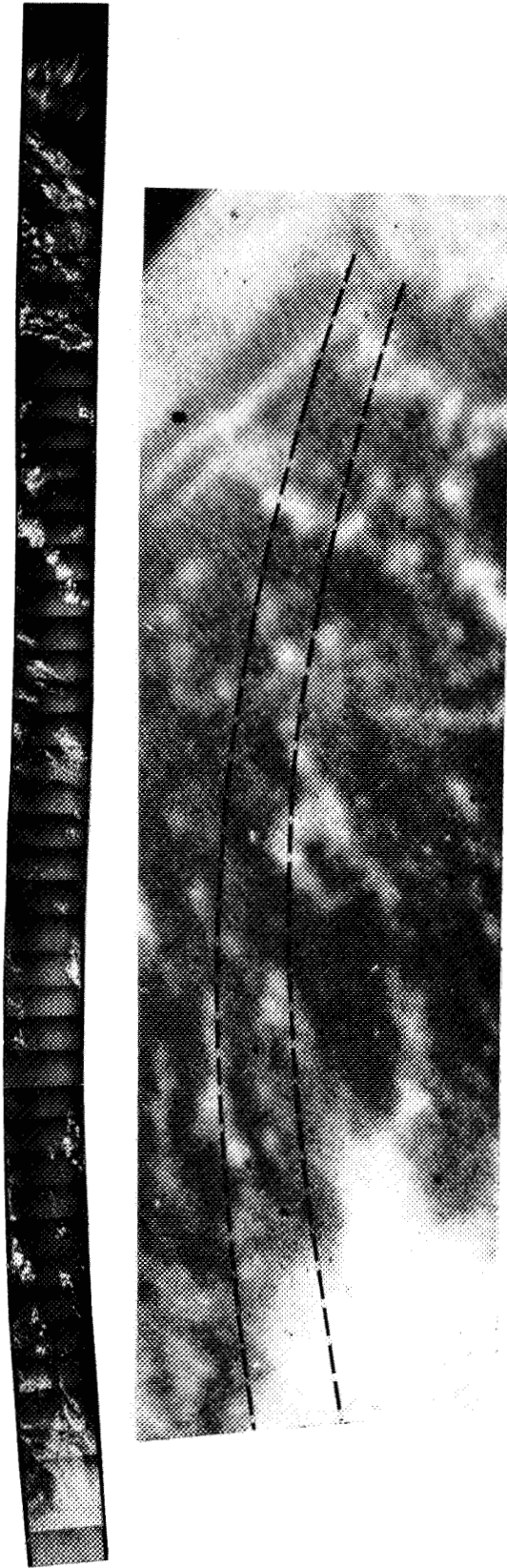
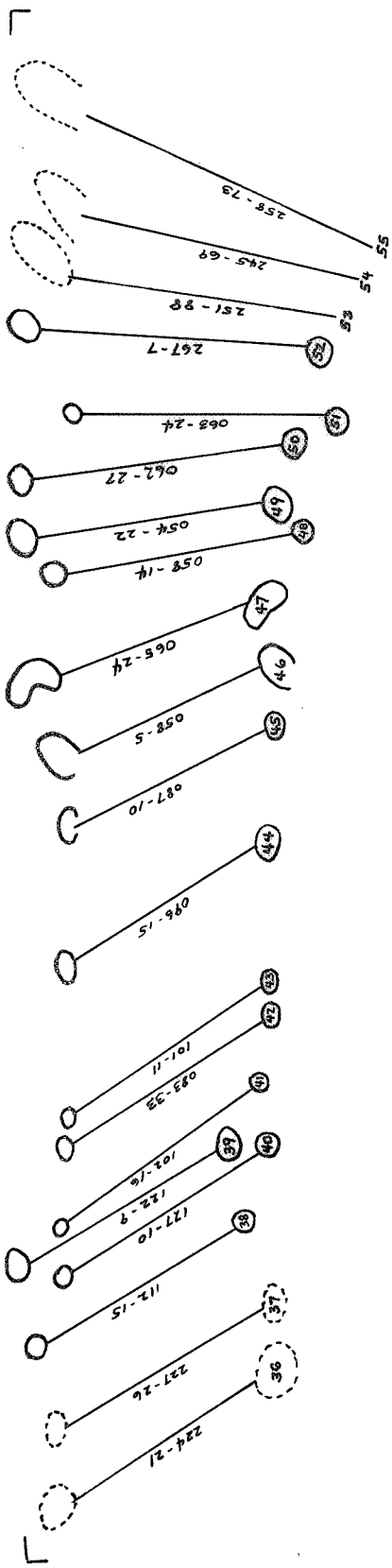


FIGURE 21 COMPARISON OF CLOUD ELEMENTS SHOWN BY APOLLO 6 AND ATS III PHOTOGRAPHS



L UPPER CLOUD () Wind direction - Wind speed
 LOWER CLOUD () Cloud identification number

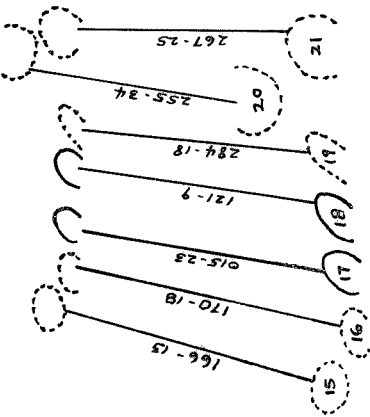
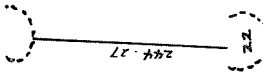
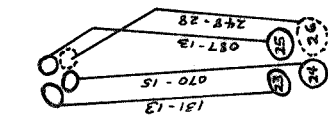
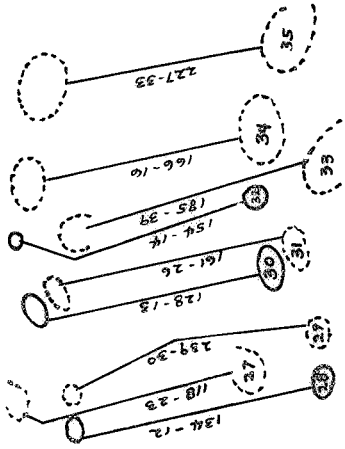
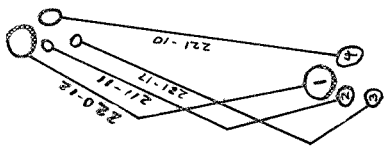
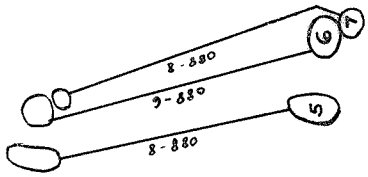
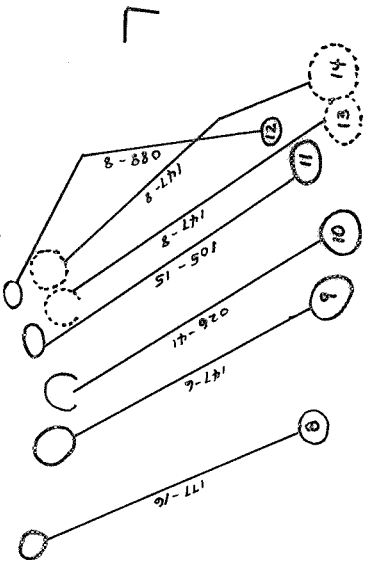




FIGURE 21 COMPARISON OF CLOUD ELEMENTS SHOWN BY APOLLO 6 AND ATS III PHOTOGRAPHS (Concluded)

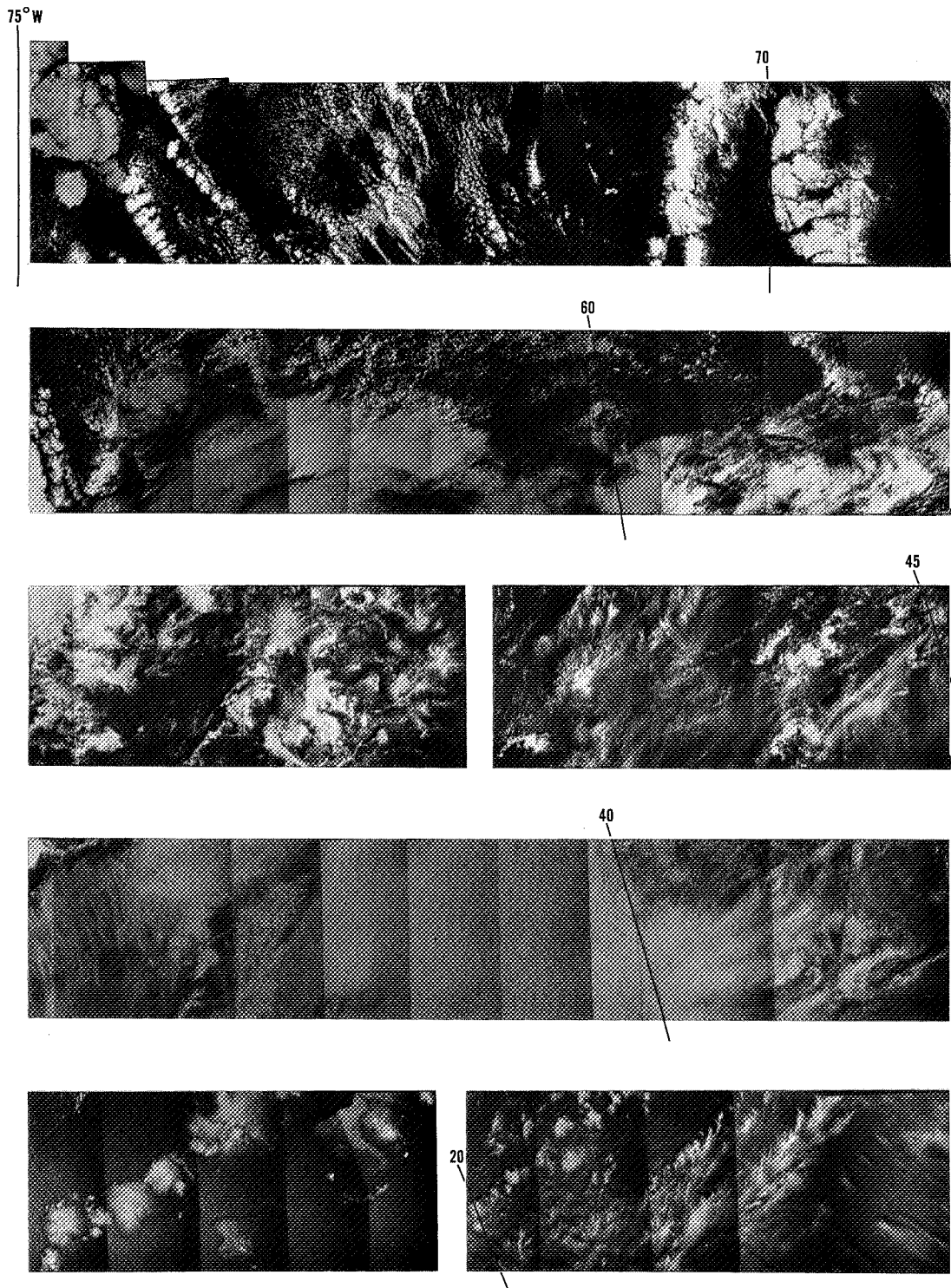
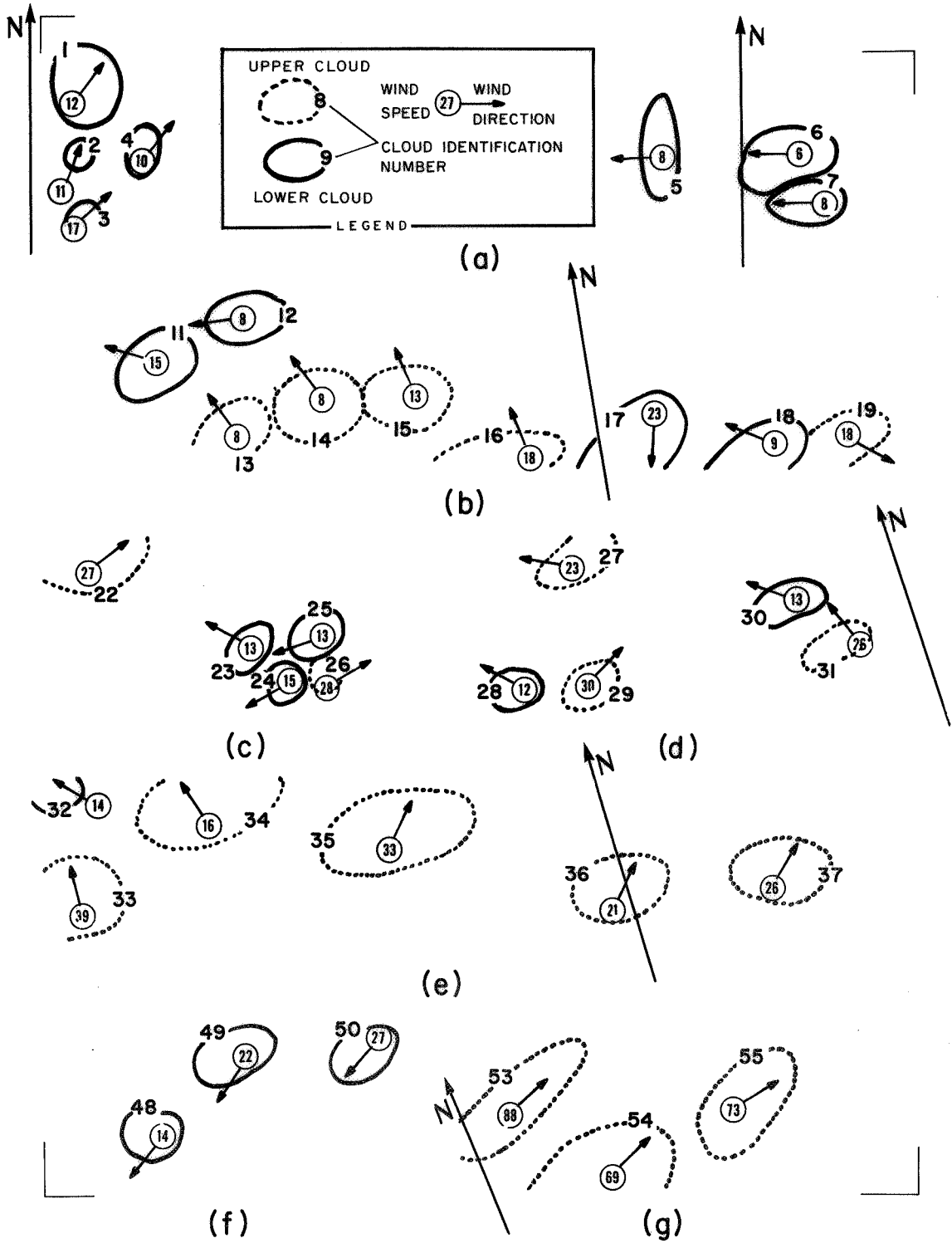


FIGURE 22 CLOUD MOTIONS SUPERIMPOSED OVER SELECTED SECTIONS OF APOLLO 6 MOSAICS



scan lines in several of the photographs appear to be missing, which caused further complications.

Figure 22 shows selected sequences of the Apollo 6 mosaic with superimposed cloud motions as measured from the ATS III photographs.

It should be noted that the indicated longitudes on Figure 22 do not agree completely with those on Figure 19. That is, cloud features 1-4 in Figure 22 are east of 75°W , while they are west of 75°W in Figure 19. The difference is that in Figure 19 the locations are the midpoint of the distance over which the cloud elements were followed; in Figure 22 the longitudes are those given in Table B-1 of Kaltenbach (1969). It is believed that, while the difference is not significant, the more westerly location is more nearly correct, since it locates the frames with Bermuda visible, in the correct geographical location.

Looking now at cloud heights and velocities, it is apparent that there are some differences in direction and speed over short distances. These differences may result from mesoscale structure of the atmosphere, effects of growth and dissipation of cloud elements, or measurement errors.

In Figure 22, the larger elements of the cumulus and stratocumulus are arranged in lines that have a vertebrae-like appearance. The larger of these lines are clearly evident in the ATS III photographs (see Figure 21). In fact, in the clusters (1-4) and (5-7) one can see brighter elements embedded in the organized amorphous cloud cover.

The measurements of the motions of the clouds show Elements 1, 2, 3, and 4 moving from a southwesterly direction while Elements 5, 6, and 7 were moving from the east. This apparently represents flow around the western portion of the Bermuda high.

The dominant cloud features in Figure 22(b) (see Elements 13, 14, 15, and 16) are the upper clouds at the northern rim of a cloud vortex centered south of the track. The low clouds to the right (Elements 17 and 18) are part of a band extending northeastward.

Some cirrus (Element 19) is evident at the right edge, and its motion is quite different from the low cloud (Element 18). In the ATS III photograph (Figure 21) this cloud complex is rather undifferentiated and one cannot distinguish the low from the high clouds. Only by obtaining measurements of cloud motion is it possible to distinguish the two levels.

Figure 22(c) shows examples of cirrus spissatus above low cumuli-form cloud cover. While it is not possible to distinguish the upper from the lower clouds in the ATS photograph (Figure 21) and the cloud elements tend to merge together even in the Apollo 6 photographs, motion analysis shows that Cloud Elements 22 and 26 are cirrus moving from the southwest at moderate speeds while Cloud Elements 23, 24, and 25 are cumulus moving from the east.

Figure 22(d) also shows a mixture of lower and upper clouds. In this case the velocity difference between the upper and lower clouds is not as marked as in the previous case. There is a considerable difference in the velocity of Cloud Elements 27 and 29. This difference apparently reflects a sharp change in flow over a short distance. The velocity of Cloud Element 29 is consistent with that of 22 and 26, while that of 27 is consistent with 31, 33, and 34. It is not known, however, whether these upper clouds are at different levels, so that it may be either vertical or horizontal wind shear that results in motions from different directions.

Figure 22(e) illustrates cirrus overcast associated with a well-developed cumulus cluster to the south. Here the cirrus is present in a rather extensive sheet that appears in the ATS III photograph as part of an extensive area of bright clouds. In the Apollo swath one views the northern rim of the cirrus sheet. Cloud-motion measurements of this cloud cover show diffluence of the cirrus. Elements 33 and 34 move from the south and southeast while Elements 35, 36, and 37 move from the southwest. The speeds are moderate in all cases.

Figures 22(f) and 22(g), respectively, show cumulus clouds moving from the northeast around the southeastern edge of the Azores high, and jet stream cirrus moving rapidly from the west. The cirrus are very close to the limb of the ATS photograph (see Figure 21), but their rapid motion made it possible to measure them with a reasonable degree of accuracy.

Some features of the cloud cover merit further discussion. For example, the cloud detail in Figure 22(a) that is lost in the ATS photograph but may be of extreme significance in a mesoscale sense is the difference in direction of the size distribution within the well-marked lines of cumulus (see Figure 23) on either side of a line A-A'. To the left of the line the cells seem to increase in size from south to north, to the right of this line the cells appear to increase in size from north to south.

These differences (not visible in the ATS III photographs) seem to imply the existence of increased instability in opposite directions on either side of the line as well as a possible difference in the thermal wind and wind shear on either side of the line. One might further speculate that this distribution of cumulus is a reflection of an eddy in the Gulf Stream, which results in a local small-scale redistribution of surface water temperatures.

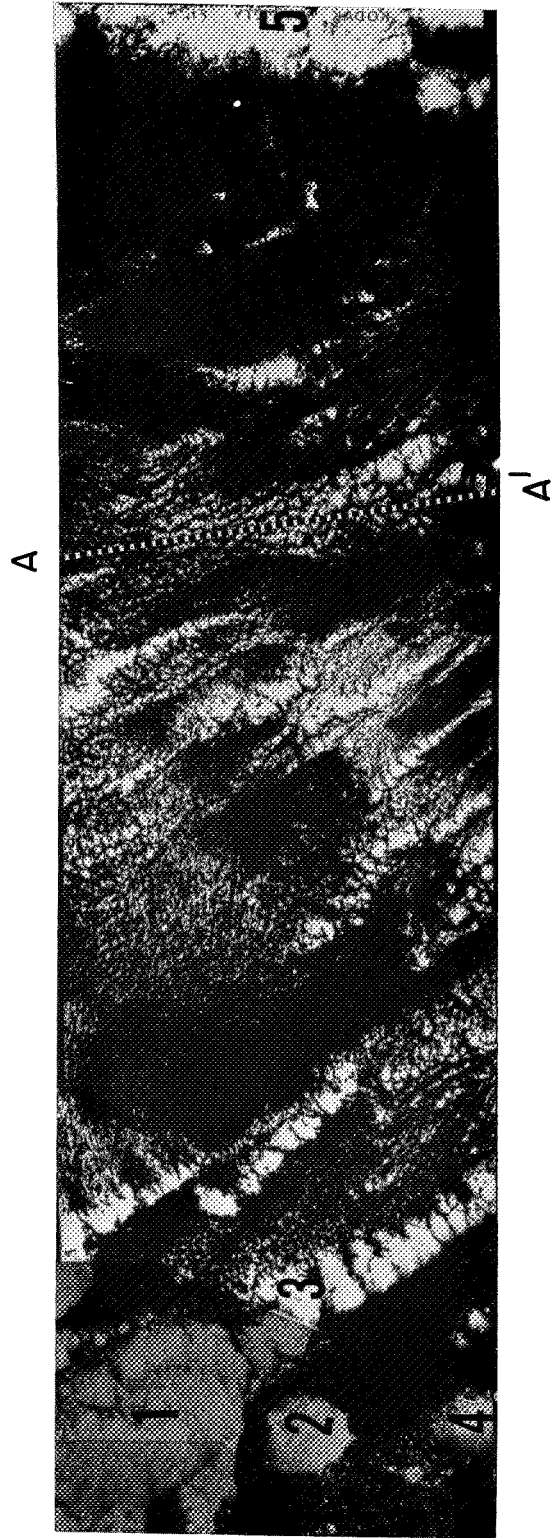
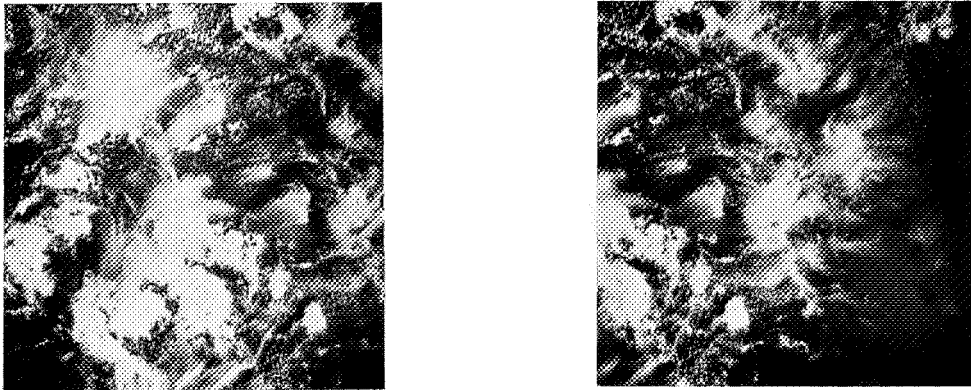


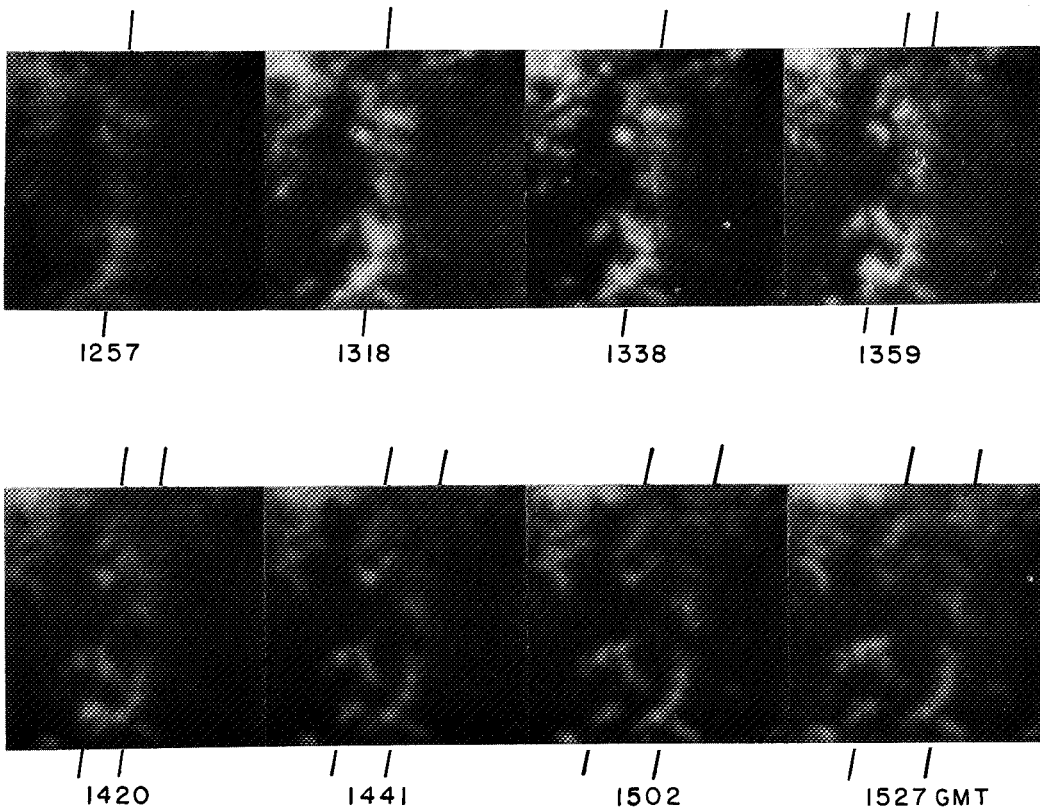
FIGURE 23 DETAILS OF CUMULUS CELL DISTRIBUTION

We were able only to obtain cloud-motion vectors for the largest of the cumulus bands. Elements 1, 2, 3, and 4 are west of the line A-A' and Elements 5, 6, and 7 are east of the line. In the former the motions are from the southwest, and in the latter from the east; in both cases the direction of motion is nearly perpendicular to the orientation of the rows of cumulus clouds. It is interesting to note that in most instances the longest axis of the individual elements of the clouds composing these bands is in the downwind direction of the measured motion.

Another interesting feature of the cloud cover in this series was the behavior of the elements in the vicinity of those labeled 23, 24, 25, and 26 [see Figure 22(c)]. In this area there was a band of cirriform clouds with a band of cumulus below. Figure 24 shows these two cloud layers as they were viewed by Apollo 6 and ATS III. Figure 24(a) shows two successive photographs from Apollo 6 that may be viewed with a stereoscope to show the altitude separation of the two cloud layers. The eight sections of ATS III photographs show what appears to be a single band at 1257 GMT, indicated by tick marks above and below the photographs, gradually becoming two distinct bands by 1527 GMT (see double set of marks). Note that nothing (shape, configuration, or brightness) in any of the ATS photographs differentiates low clouds from high clouds. In this instance such significant information could be derived only from the cloud-motion measurements available from ATS photographs. Near the southern end of the band the computed motion of the low clouds was from 87° at 8 knots, while the cirrus clouds were moving from 267° at 21 knots. As a matter of fact, five hours later, winds measured on a Gull India flight at $27^\circ\text{N } 50^\circ\text{W}$ were 270° , 20 knots at an altitude of 5770 meters. At that location, our cloud-motion measurement was 267° , 22 knots.



(a) STEREO PAIR OF APOLLO 6 PHOTOGRAPHS SHOWING CIRRUS OVER CUMULUS



(b) ATS III PHOTOGRAPHS SHOWING DIFFERENTIAL MOTION OF CIRRUS AND CUMULUS

FIGURE 24 DETAILS OF MOTION IN MULTIPLE LAYERS

C. Summation

The comparison of ATS III photographs (which have a resolution of only 2 nmi at the subpoint) with the very-high-resolution 70-mm color photographs taken by the Apollo 6 satellite showed that much of the detail visible in the high-resolution photographs was also detectable in the ATS photographs. It was possible to define the boundaries of the swath photographed from Apollo 6 on the ATS photograph so that cloud velocities within the swath could be measured from a series of ATS photographs. While in many instances it was not possible to differentiate lower from upper clouds on a given ATS photograph, motions of cloud elements provided clues as to whether the clouds were low or high. In one area in one of the ATS photographs, a band of cirrus was fused with a band of cumulus below it. Time-lapse viewing of a series of ATS photographs on the SRI/NASA Electronic Display System showed differential motion of the cloud elements, clearly indicating that there were clouds at two levels moving in opposite directions. This demonstrates that motion analysis, such as is possible using this system, is essential to understanding the nature of the cloud cover viewed by ATS satellites.

V COMPARISON OF CLOUD GROWTH RATES
WITH OBSERVED SEVERE STORM ACTIVITY

The objectives of this task were:

- (1) To identify cumulonimbus anvils on the SRI/NASA Electronic Display System's TV screen
- (2) To measure the motions and size changes of clouds identified as anvils
- (3) To determine whether growth rates and sizes of clouds were indicative of severe weather and were related to wind and wind shear at appropriate levels.

A contractual requirement was that two of the required six cases would be 19 and 23 April 1968. The remaining four cases could be any other days in April 1968 that appeared to have measurable anvils. The dates that were studied, together with the times of the ATS photographs examined on each date, are given in Table 7.

The following data were also analyzed in addition to the ATS cloud photographs:

- Radarscope photographs and RADU plotting charts showing radar echo distribution
- Severe storm reports tabulated in "Storm Data"
- Vertical distributions of temperature, moisture, and wind from rawinsonde ascents.

Table 7

GMT TIMES OF PHOTOGRAPHS USED IN CLOUD GROWTH STUDY

GMT Time on Date--April 1968					
17	18	19	23	28	30
	1510				
	1537				
	1605				
	1632				1649
	1700				1717
	1727				1744
1800	1821		1809		1811
1827			1836	1849	1839
1855			1904	1916	1906
1926			1931	1944	1934
1953			1959	2011	2001
2025		2019	2028	2039	2029
2057		2046	2056	2106	2056
2125		2114	2124	2134	2124
		2141	2151	2201	2151
		2209	2219	2229	2219
		2236	2246	2256	
		2304		2324	
		2331		2351	
		2358			

A. Measurement of Cloud Growth

The procedure followed to determine the size of a cloud element on a given ATS photograph was as follows: For each date selected for study, the portions of the ATS photographs showing the area of interest were entered on the display system's disc memory at maximum enlargement. The x and y cursors were then positioned on the edges of clouds that appeared to be associated with convective activity at as many locations as was deemed necessary to define the outline of the cloud being analyzed. These cursor values were entered on punched cards, and the latitudes and longitudes of the selected points were computed using the ATSWIND computer

program. These latitudes and longitudes were then plotted at convenient scales for computing anvil area and for comparison with radiosonde, radar, and severe storm reports.

To determine the accuracy of measurement of cloud size on the display system, three meteorologists made independent measurements of one cloud. The three sets of measurements were in perfect agreement on the windward edge of the cloud (where the edge was well-defined) but differed by a maximum of five x cursor units on the diffuse downwind end of the anvil. The anvil on the three sets of measurements averaged 30 cursor units in length so the uncertainty was $2.5/30$ or about 8 percent. The anvil was located near 32.5°N , where one y cursor unit is 3 nmi; hence, in terms of miles, the uncertainty in location of the edge was 7.5 nmi.

B. Discussion of Days Studied

The six days studied varied considerably in the extent and severity of weather within the areas examined. The intensity of weather associated with specific cloud areas was extracted from the storm data bulletins issued monthly from Asheville, North Carolina, and from remarks on the hourly RADU plotting charts. These data sources showed that some of the measured clouds were not even precipitating (no radar echoes) while other measured clouds produced tornadoes.

The number of clouds measured ranged from a minimum of two on 28 April to a maximum of eight on 23 April. The sizes of clouds measured varied from just under 200 nmi to over 20,000 nmi².

The number and size of the measured clouds depended on the distribution of cloud cover. If there was a widespread area of relatively uniform stratiform cloud cover it was difficult to isolate specific features to

study. Furthermore, two or more small clouds sometimes merged into a larger cloud; conversely, in some cases, a large cloud apparently split into two smaller clouds.

Table 8 lists the number of cells measured on each of the six days, the number of times each cell was observed, and the number of times the weather associated with the cells fell in each category.

The weather categories were defined as follows:

NE--No echo	No radar echoes in measured clouds
L--Weather of light intensity	Light to moderate rain or rain showers
M--Moderate intensity	Light or moderate thunderstorm
S--Severe weather	Tornadoes or funnel clouds, hail, strong winds, or heavy thunderstorms.

A series of photographs has been prepared to illustrate the cloud cover on each of the days studied. These pictures were made by photographing the portion of the display system's TV screen containing the area of interest. As presented in this report, the photographs are reduced from the TV presentation. The photographs do, however, illustrate such details as relative brightness and sharpness of edges that were available to the meteorologists measuring the clouds. Each cloud photograph has an overlay containing grid lines, ellipses demarking measured clouds, a letter identifying the cloud, and (in parentheses) a notation describing the weather category associated with the cloud.

1. 28 April 1968 [Figure 25]

Two cloud elements were measured. At the time illustrated, the weather accompanying both cloud elements was categorized as severe

Table 8

WEATHER CATEGORY ASSOCIATED WITH MEASURED CLOUD ELEMENTS

Date (1968)	Cloud Element	Number of Observations	Weather Category			
			No Echo	Light	Moderate	Severe
28 April	A	8			6	2
	B	7			3	4
17 April	A	6	6			
	B	6	6			
	C	7	7			
	D	4		4		
	E	4		4		
18 April	A	7		7		
	B	4		3	1	
	C	3		1	2	
	D	4	4			
19 April	A	6			5	1
	B	2			2	
	B	2				2
	C	5			5	
	D	6			6	
	E	3			3	
30 April	A	4		4		
	B	7	2	5		
	C	9		9		
	D	8	2	2	1	3
23 April	A	6			5	1
	B	9			1	8
	C	4				4
	D	4			4	
	E	3			1	2
	F	5			3	2
	G	4			3	1
	H	5			3	2
Totals	29	152	27	39	54	32

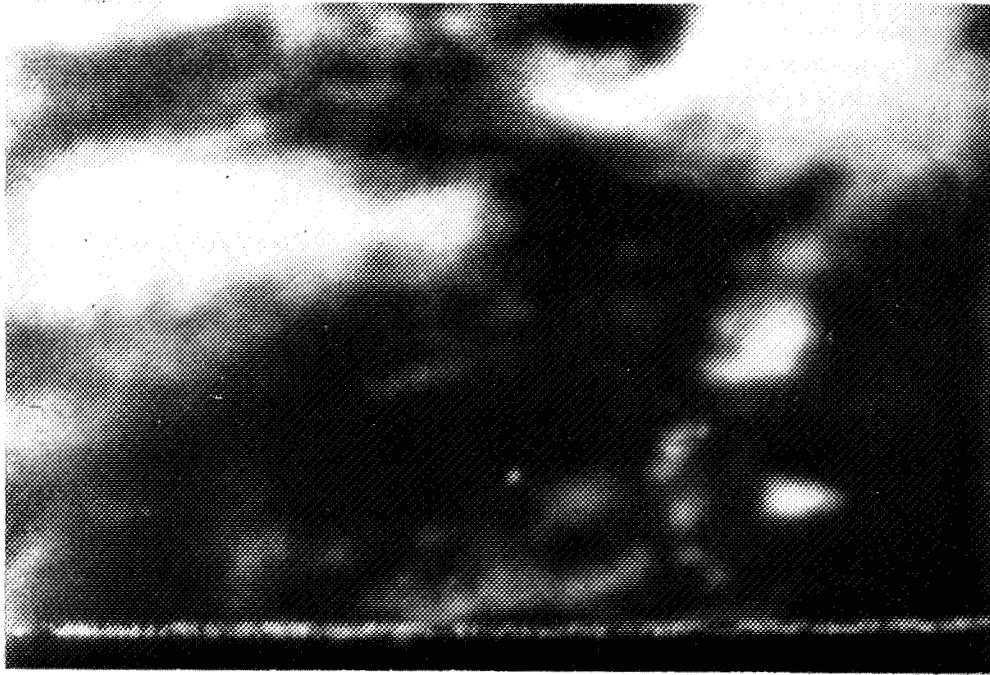
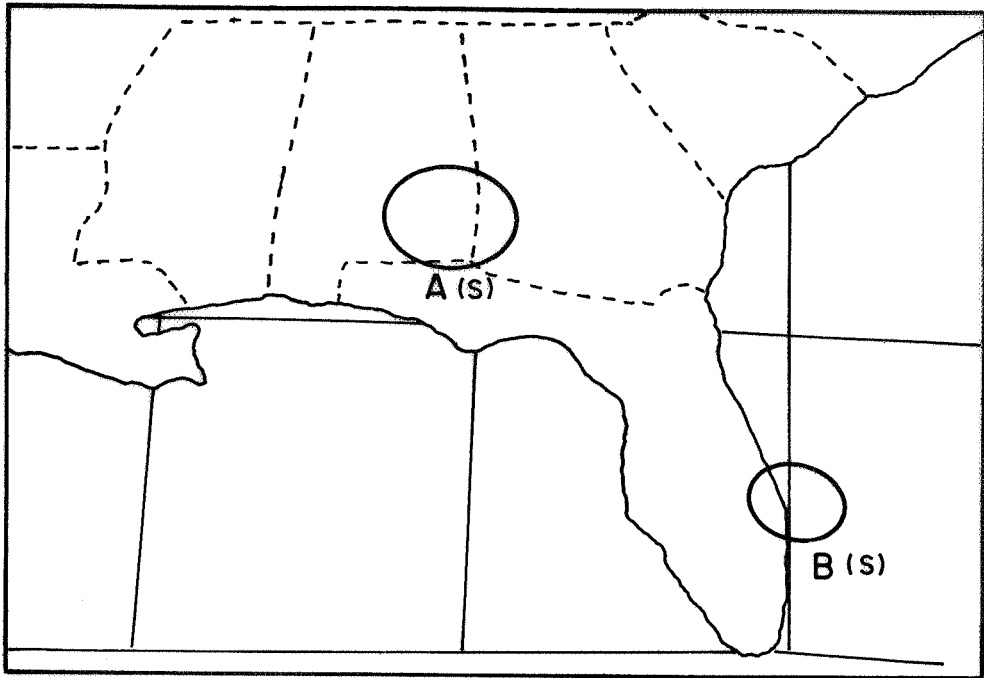



FIGURE 25 CLOUD COVER ON 28 APRIL 1968



2106 GMT

 LOCATION OF MEASURED CLOUD
A(s) CLOUD IDENTIFICATION AND ASSOCIATED WEATHER CATEGORY
WEATHER CATEGORY
 (NE) NO ECHO
 (L) WEATHER OF LIGHT INTENSITY
 (M) MODERATE INTENSITY
 (S) SEVERE WEATHER
WEATHER SYMBOLS
 T - TORNADO A - HAIL
 F - FUNNEL CLOUD ⚡ THUNDERSTORM
 W - WIND ⚡ LIGHTNING

LEGEND

(heavy thunderstorms were reported in both areas). Table 8 shows that Cloud Element A was only accompanied by severe weather on two of six observations, while Cloud Element B had associated severe weather on four out of seven observations. At the time illustrated Cloud Element A had reached its maximum size and decreased rapidly during the next hour; Cloud Element B increased in size during the next half hour then decreased slowly in size. Typical growth and decay curves for cloud elements such as this are illustrated in the discussion of the data for 23 April.

2. 17 April 1968 [Figure 26(a)]

Five cloud elements were measured. Four of these were south of a cold front that extended from central Illinois to northern Texas. The fifth cloud measured was behind the front and located over central Kansas. No radar echoes were associated with Cloud Elements A, B, and C, while only light rain was reported with Cloud Elements D and E. Table 8 shows that these weather categories prevailed throughout the period during which these cloud elements could be followed.

3. 18 April 1968 [Figure 26(b)]

Four cloud elements were measured. On this date there was a wave in southwestern Missouri on a cold front that extended from southern Ohio to southeastern New Mexico. The measured clouds were in the tropical air south of the front and were mostly brighter areas within an extensive cloud shield. Weather over the area at this time was not severe, as indicated by the lack of echo in Cloud Elements A, B, and C, and only light rain in Cloud Element D. Table 8, however, shows that during part of the time Cloud Elements B and C were followed, the associated weather was of moderate intensity.

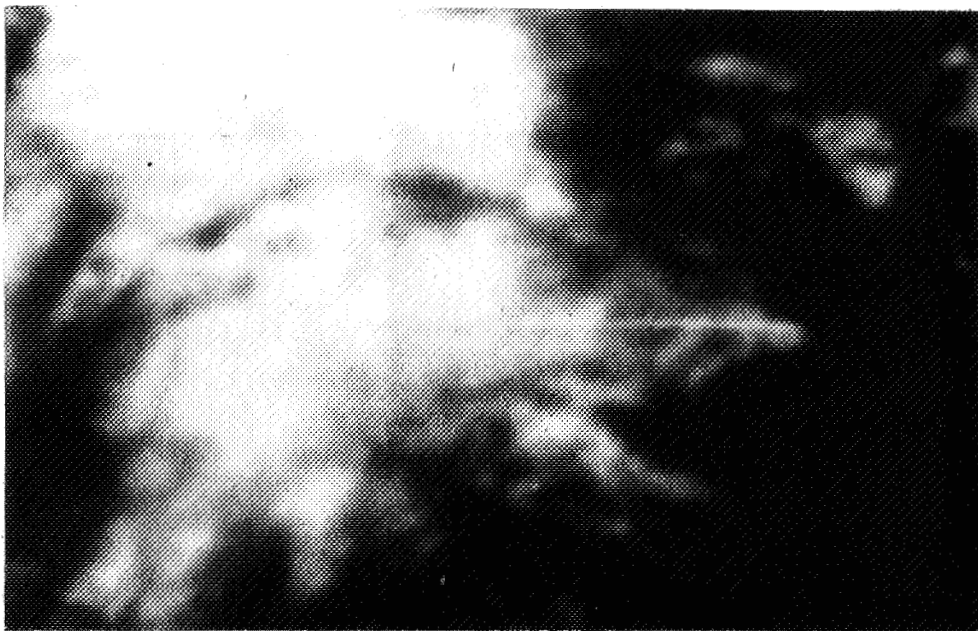
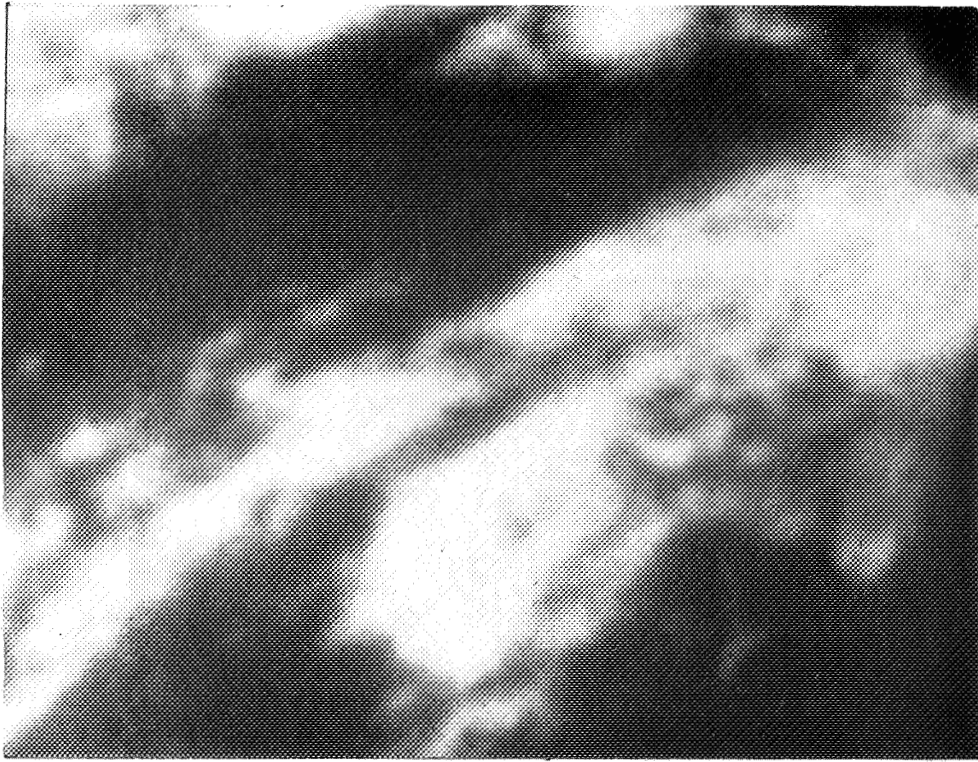
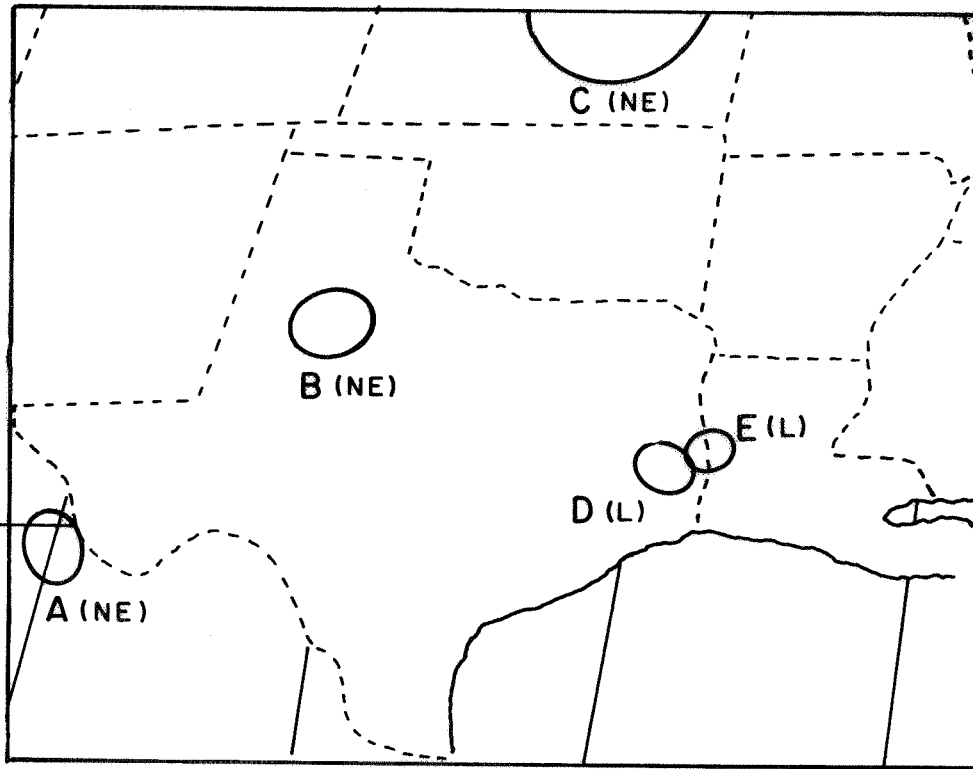
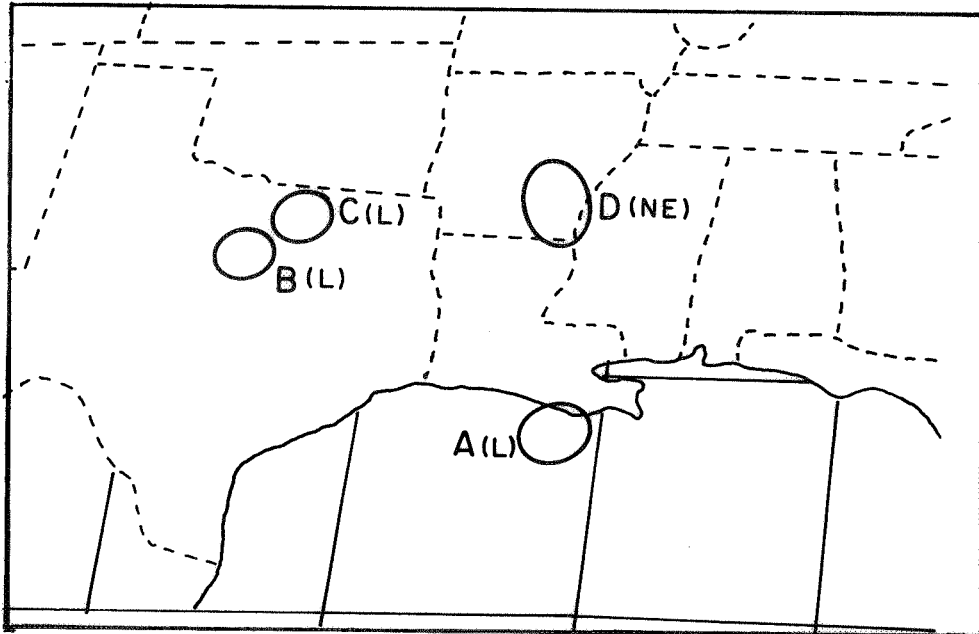


FIGURE 26 CLOUD COVER ON 17 AND 18 APRIL 1968



(a) 1926 GMT 17 APRIL 1968



(b) 1605 GMT 18 APRIL 1968

4. 19 April 1968 [Figure 27]

Six cloud elements were measured (two of which are outside the area covered by the photographs in Figure 27). Cloud Element A is just to the east of a low-pressure center and moved almost due north. The clouds further to the west were moving from the north with the circulation to the west of the low.

The cloud element labeled B at 2236 GMT and B' at 2331 GMT represents a situation where two elements apparently merged and the console operator followed one portion initially and the second portion in subsequent analyses. Cloud Elements A and B' had associated severe weather.

The cloud element labeled C grew very rapidly from its initial appearance at 2141 GMT to 2358 GMT, when sunset over the area prevented further measurement. Average growth rate during this period was computed to be 76.4 square miles per minute. In spite of this remarkable growth, there was no severe weather reported with this cloud (see Table 8) during the period it was analyzed.

Cloud Elements D and E, which are outside the area covered by Figure 27, had associated weather categorized as moderate throughout the period they were followed.

5. 30 April 1968 [Figure 28]

On 30 April there was a low-pressure area in the western Atlantic Ocean and a cold front moving southeastward across the northeastern part of the United States. Thunderstorms with strong winds and at least one tornado accompanied this cold front. Figure 28 shows two views of the cloud cover on this date and also shows the locations of measured cloud elements. The figure and Table 8 show that Cloud Element

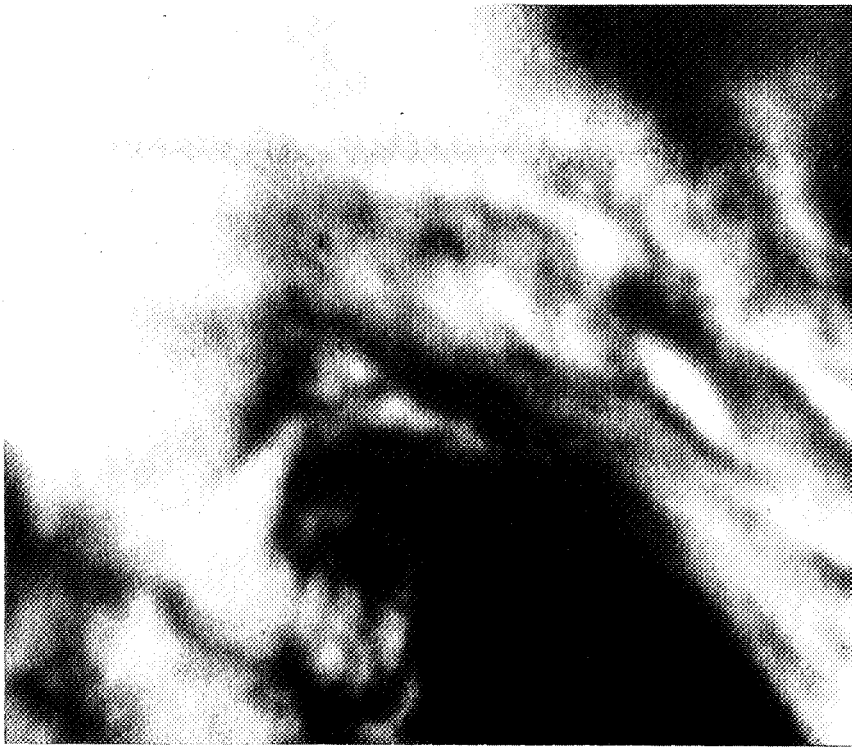
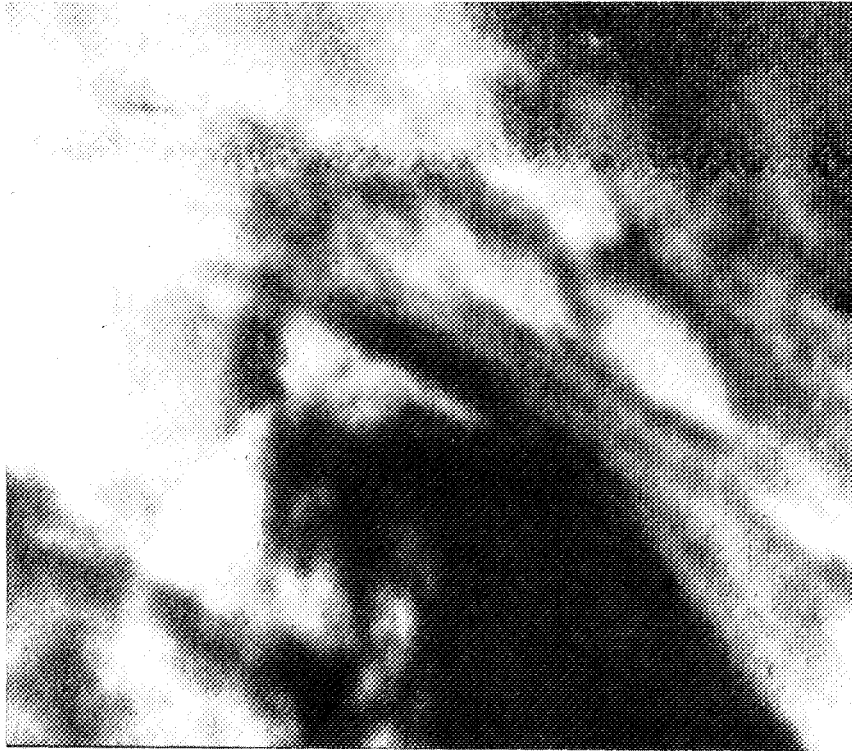
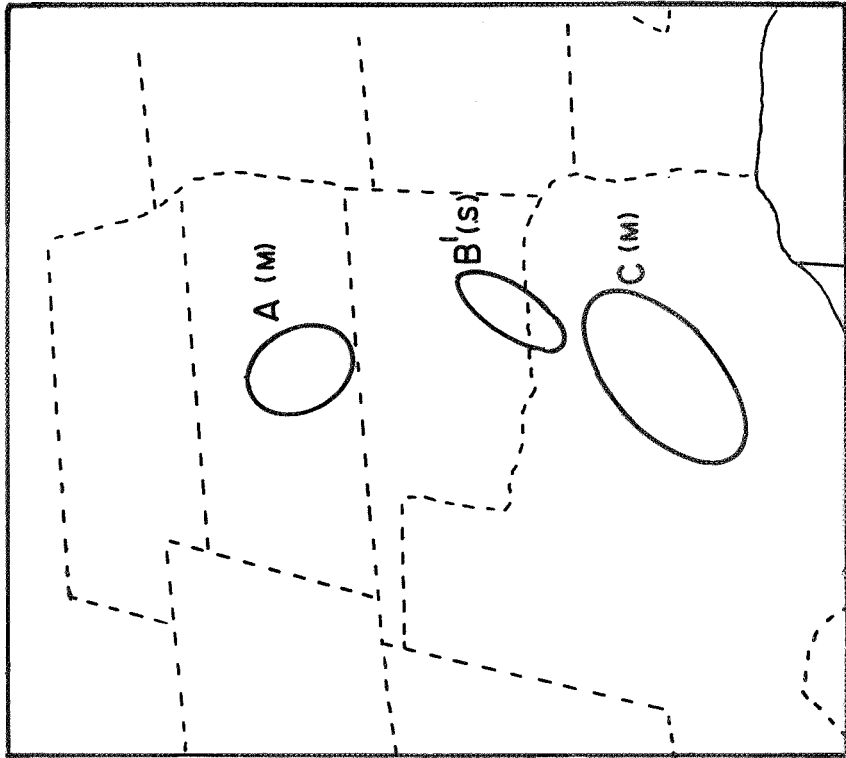
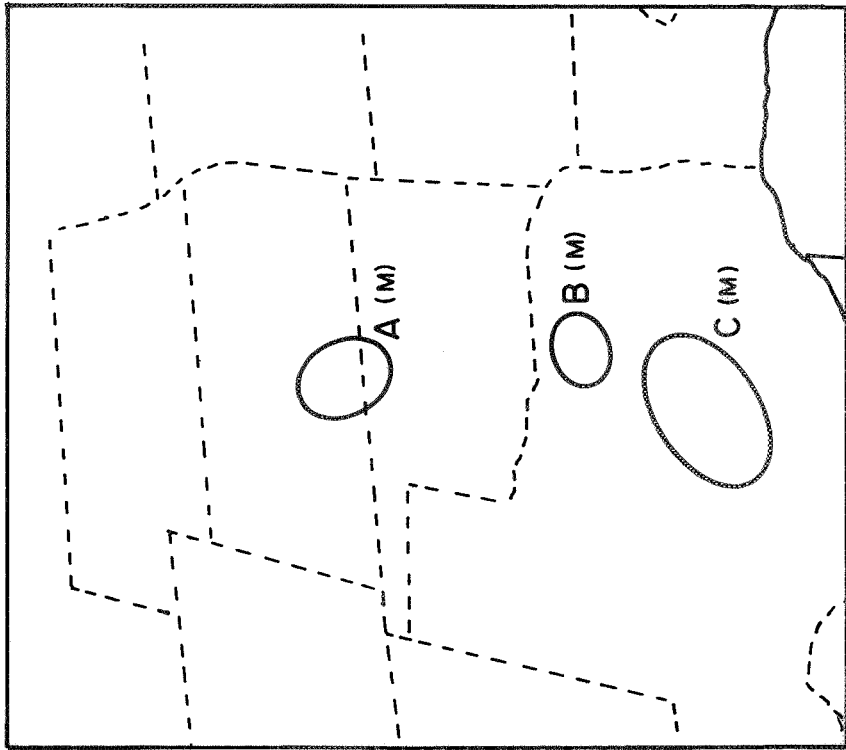


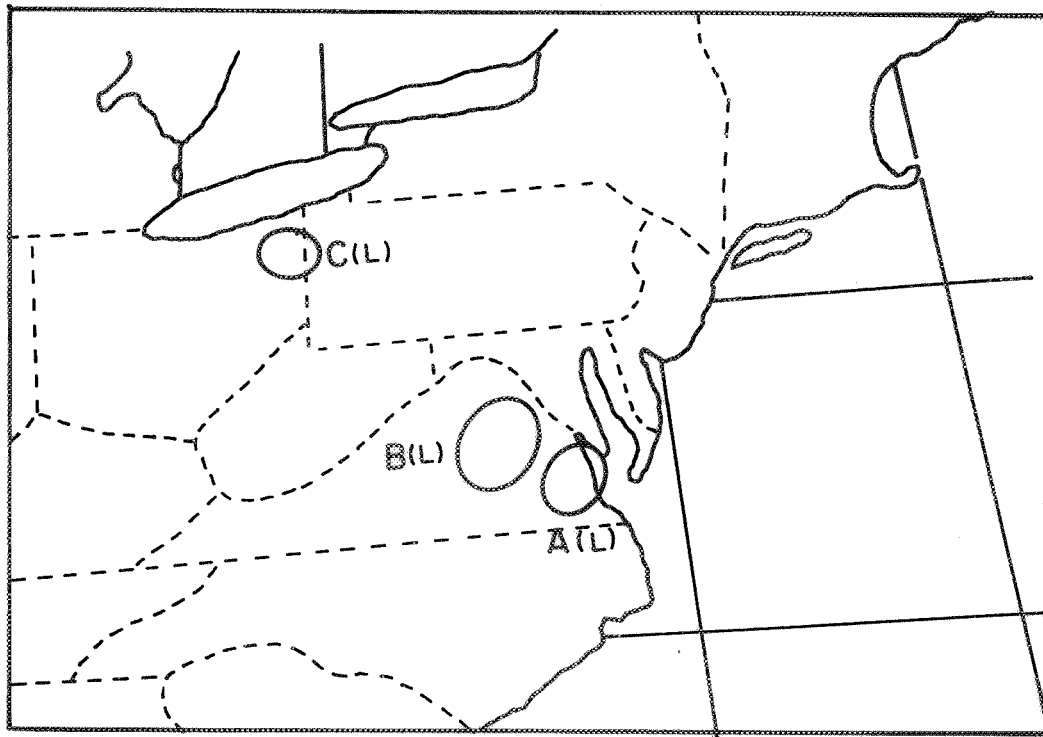
FIGURE 27 CLOUD COVER ON 19 APRIL 1968



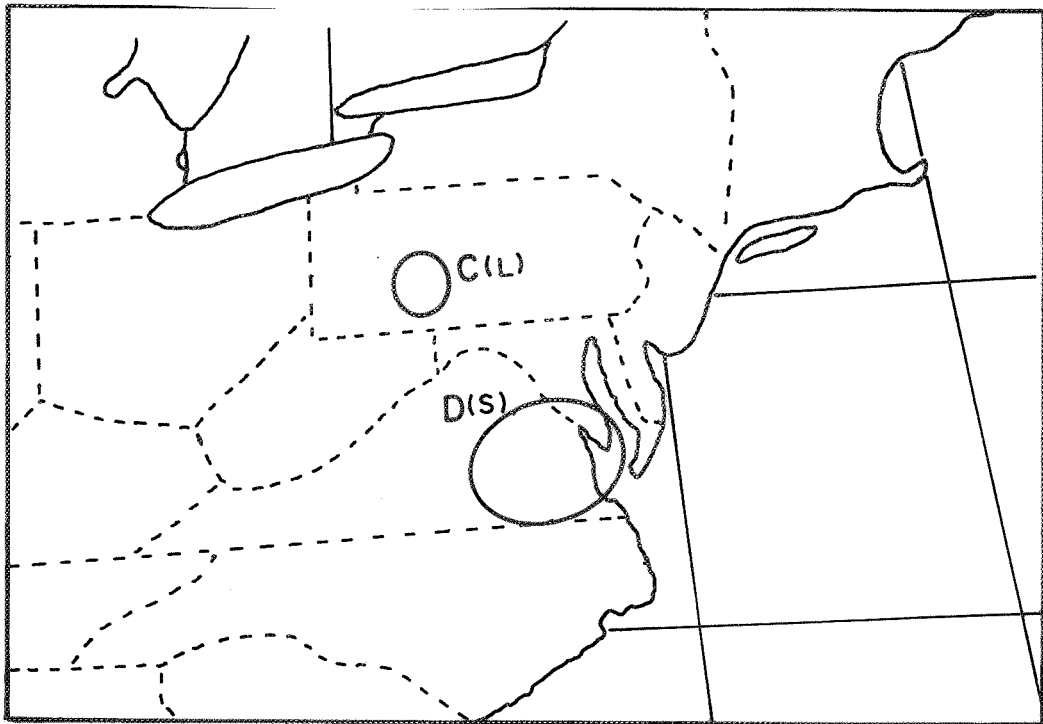
2331 GMT



2236 GMT



1744 GMT



2124 GMT

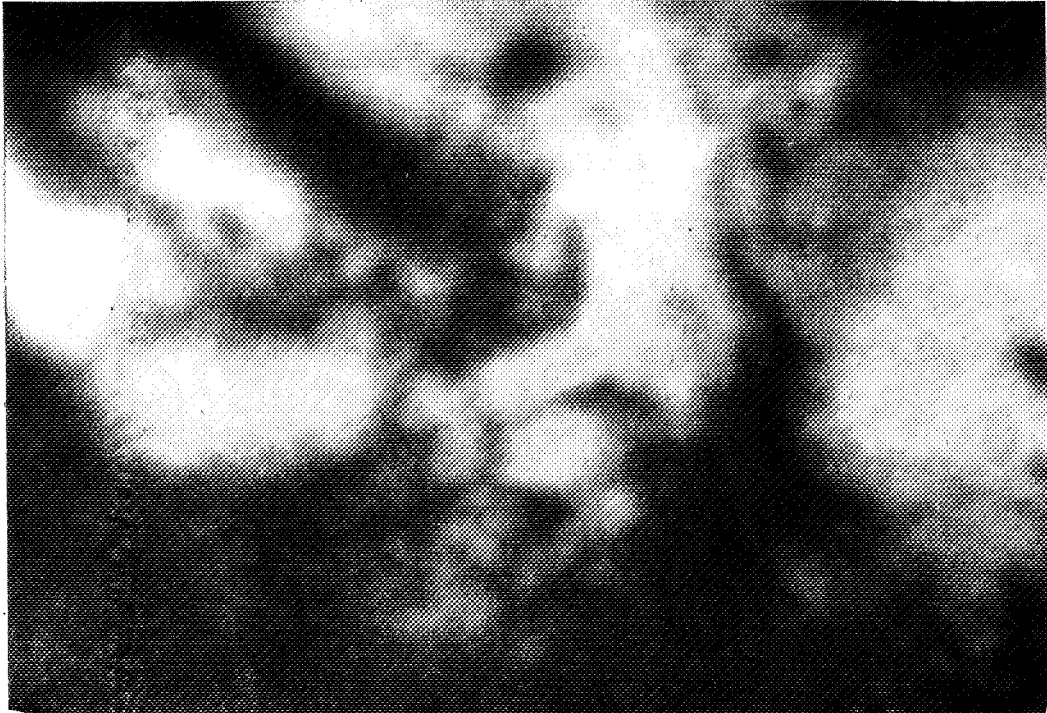
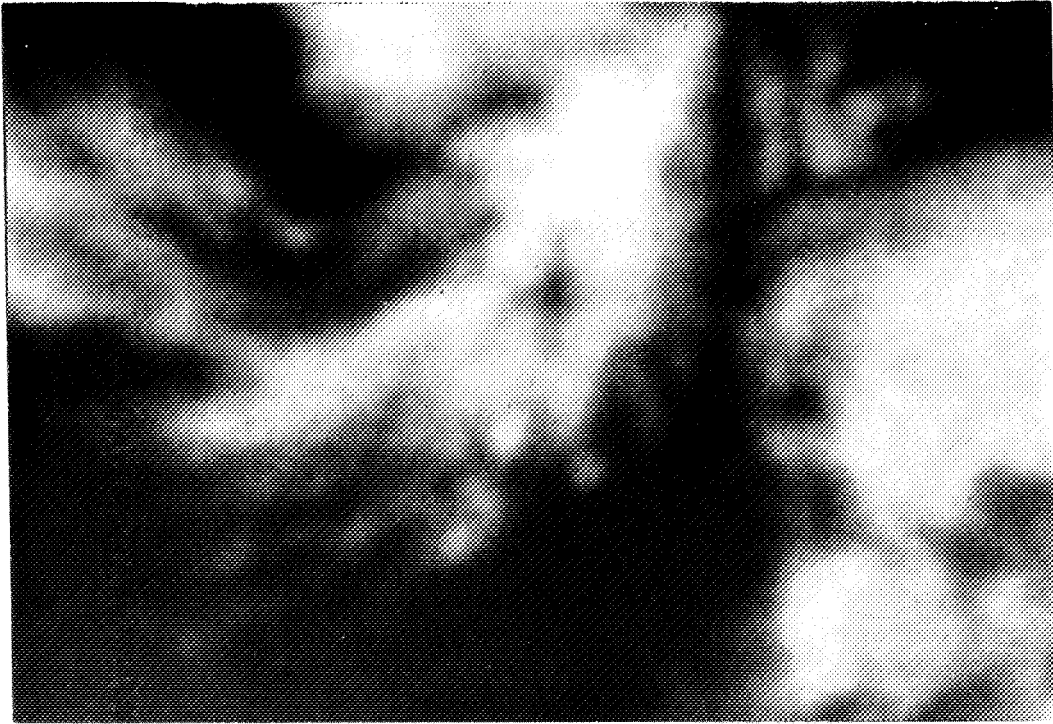


FIGURE 28 CLOUD COVER ON 30 APRIL 1968

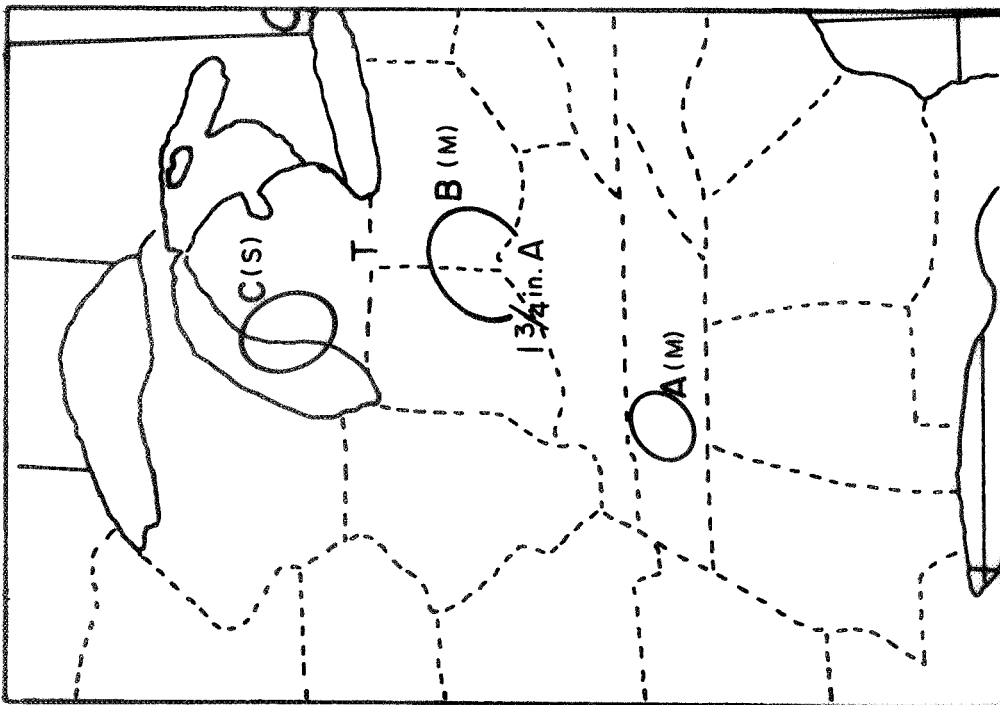
D (with which the tornado occurred) had severe weather during part of its life history and at other times had weather in the various other categories. This cloud element was the only one during the six days examined whose associated weather ranged through all four of the categories. Cloud Elements A, B, and C either had no echo or had weather categorized as being of light intensity.

6. 23 April 1968 [Figure 29]

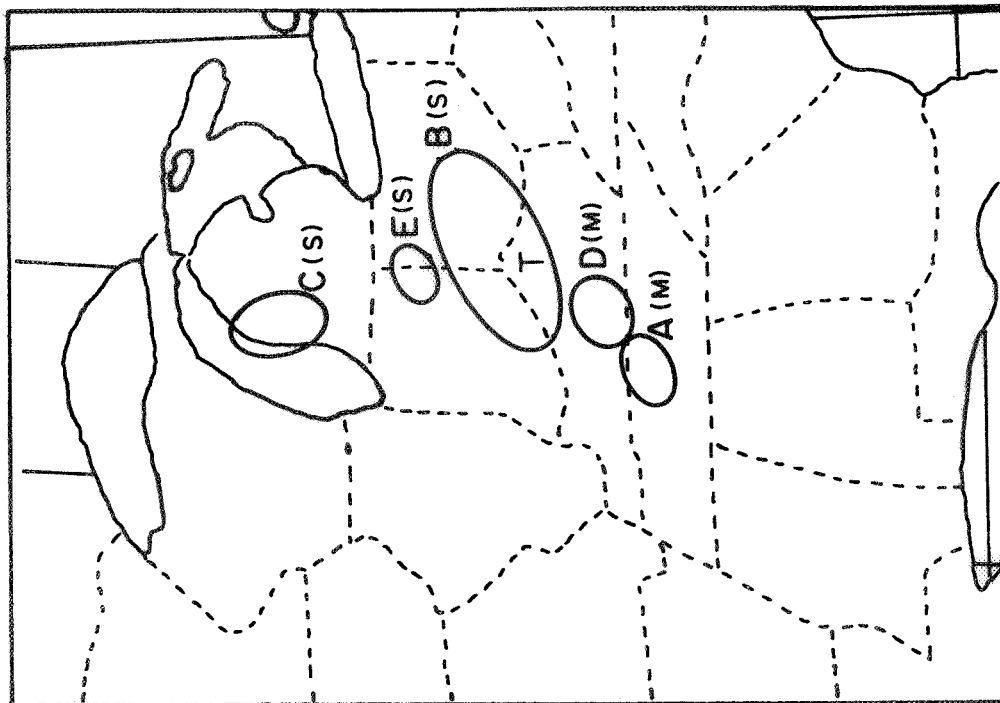
The data for 23 April are presented in detail because of the widespread occurrence of severe weather on this date. Eight of the ten photographs studied are shown in Figure 29. The locations of reported tornadoes, hail, windstorms, etc., are included on the overlay. Table 8 shows that on 23 April eight clouds were measured for a total of 40 measurements. Some of these clouds appeared on only three or four photographs, while one could be identified on nine frames. The associated weather at the time of 20 of these measurements was categorized as moderate; the remainder was categorized as severe. Severe weather also occurred with cloud elements that were not measured.

Reference to Figure 29 shows that three cloud elements were measured at 1809 GMT, two of which (A and B) had associated weather of moderate intensity, and the third (C) had severe weather. There was 1-3/4 inches of hail reported just to the southwest of Cloud Element B and a tornado reported between Cloud Elements B and C. The clouds with which the hail and tornado occurred were not measured because they tend to be part of clusters with no distinct edges.

Five clouds were measured at 1836 GMT. Cloud Elements A and D have associated weather categorized as moderate while severe weather was occurring with Cloud Elements B, C, and E. There was a tornado with Cloud Element B, as indicated by the T at the southern edge of the cloud.



1809 GMT



1836 GMT

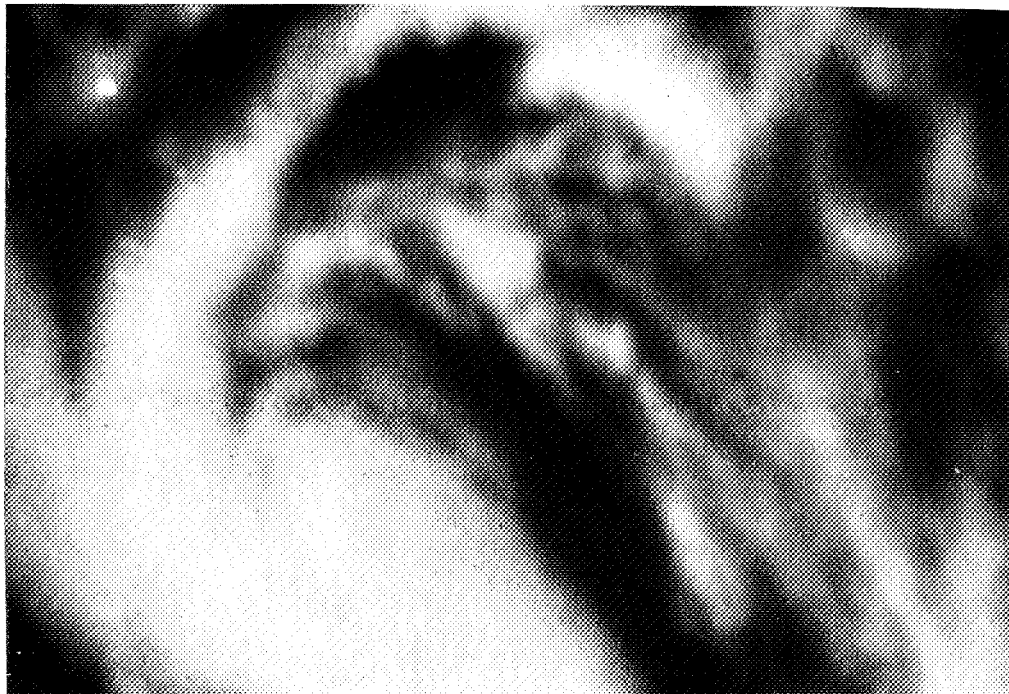


FIGURE 29 CLOUD COVER ON 23 APRIL 1968

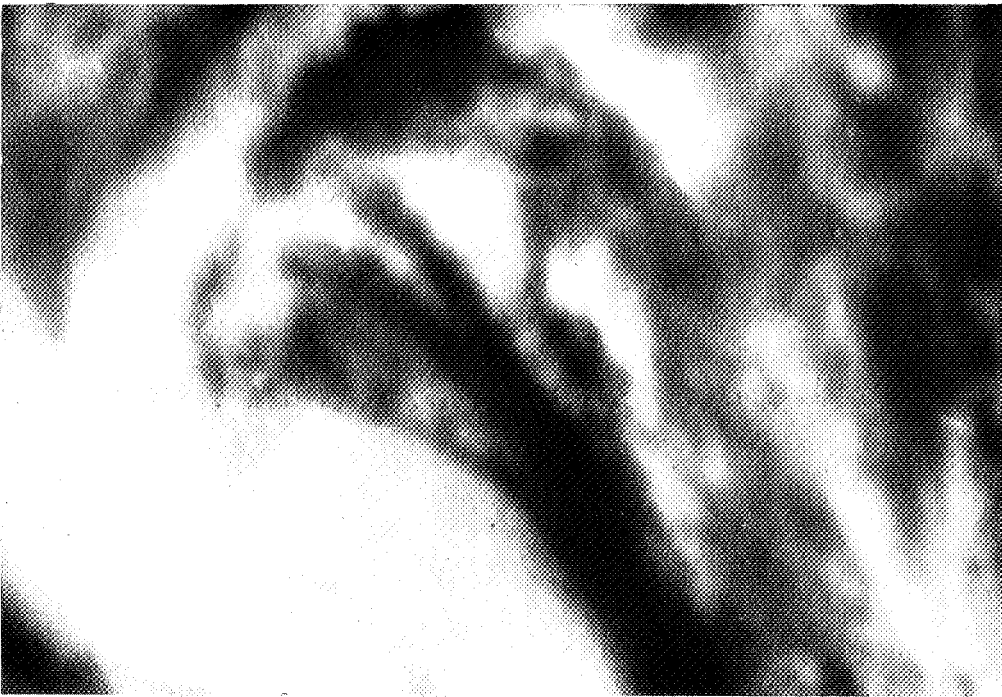
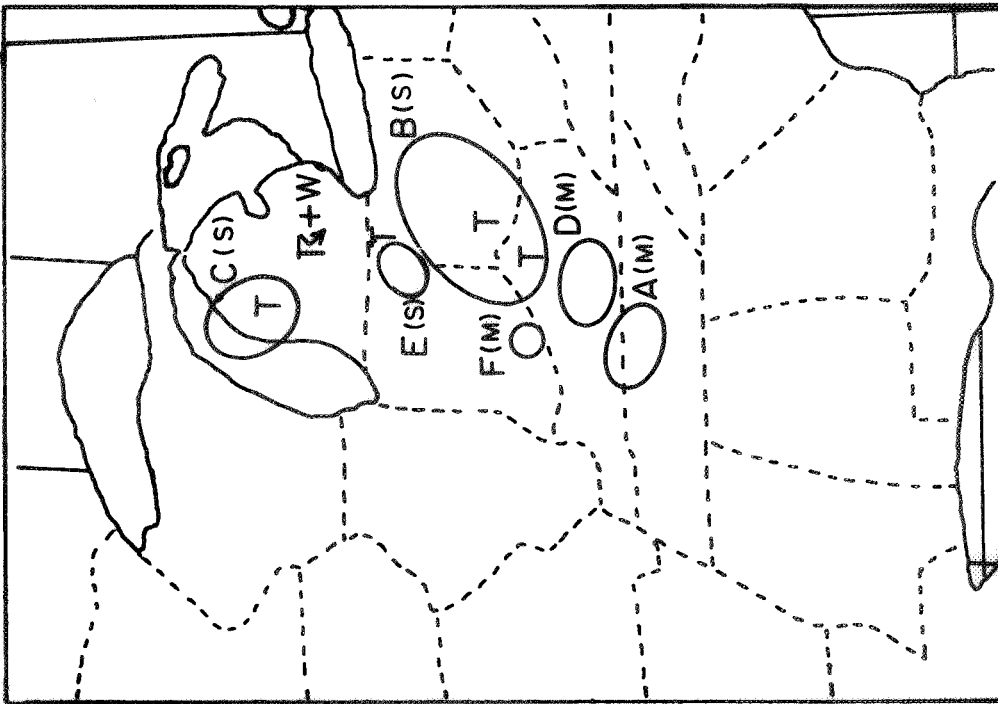
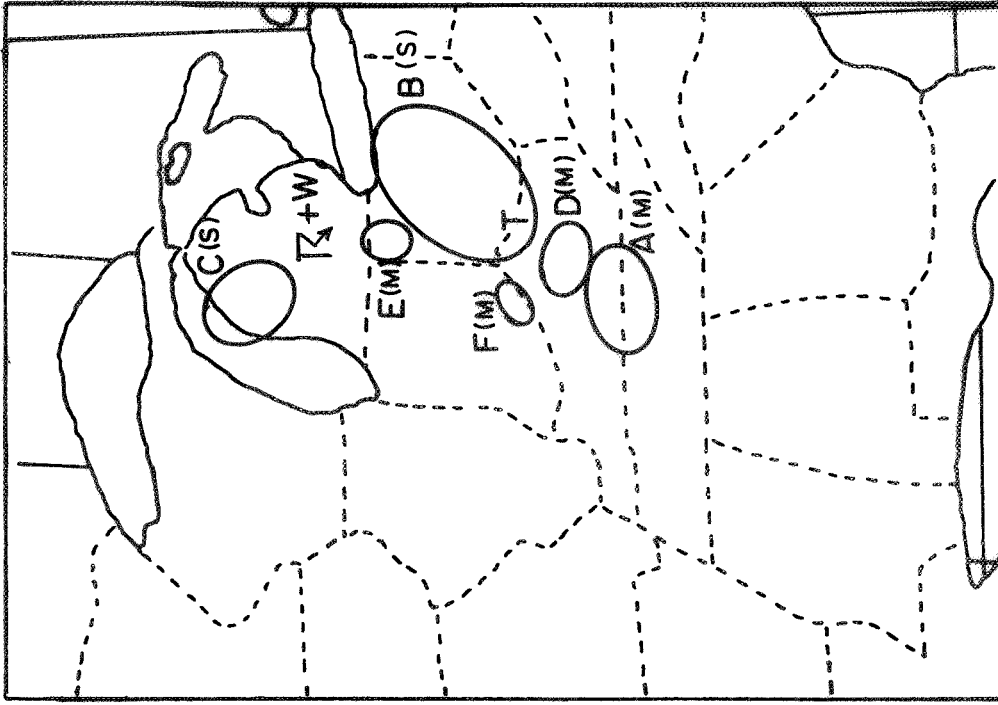


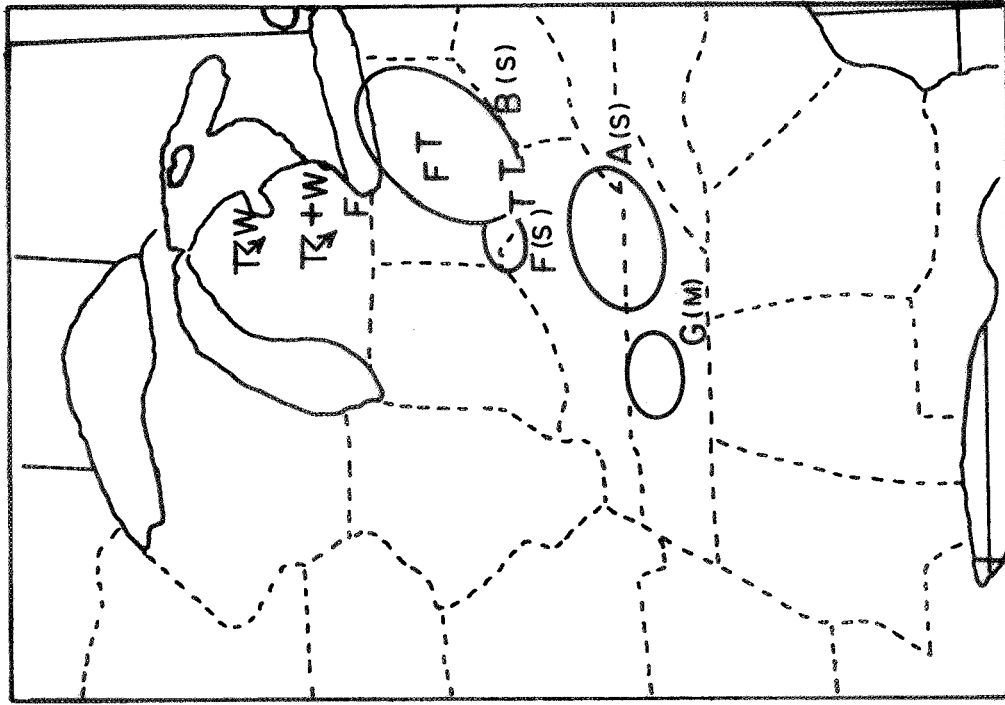
FIGURE 29 CLOUD COVER ON 23 APRIL 1968 (Continued)



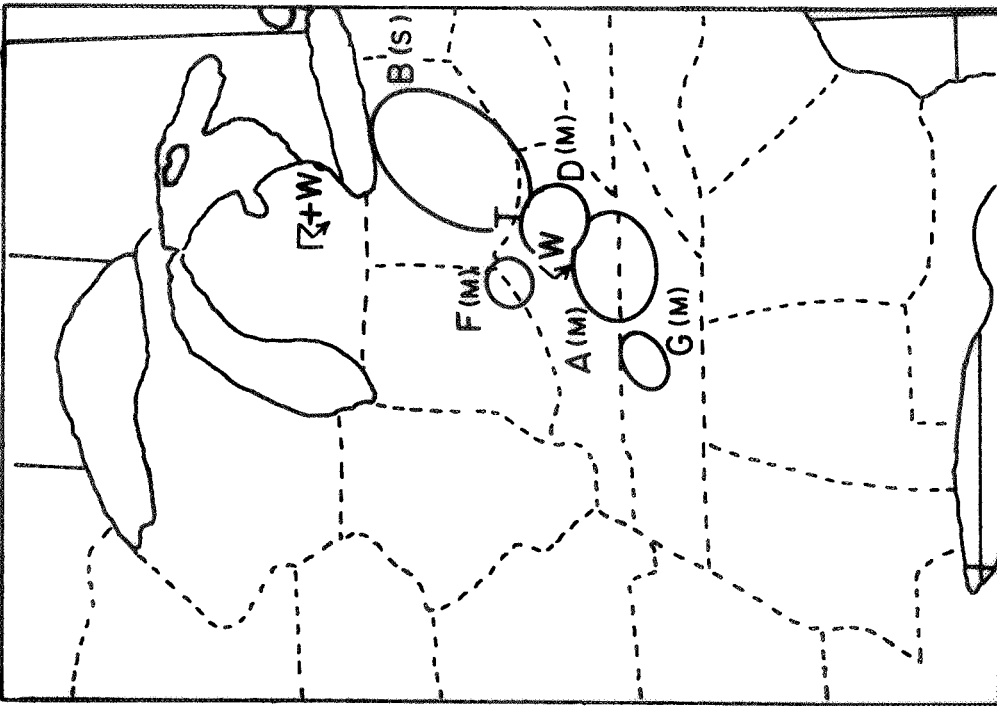
1904 GMT



1931 GMT



2028 GMT



1959 GMT

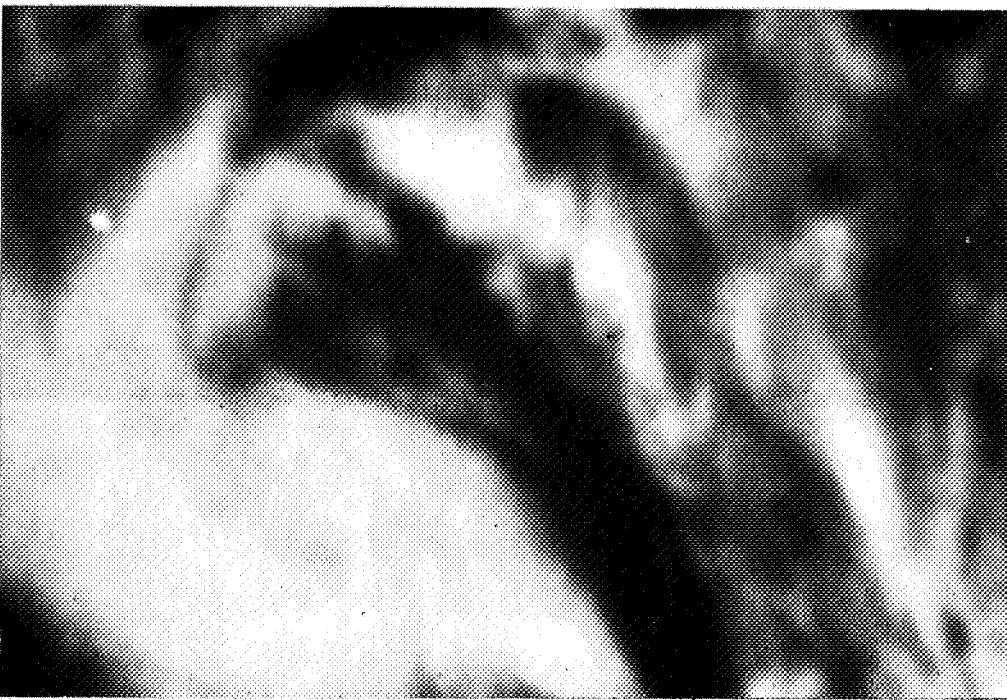
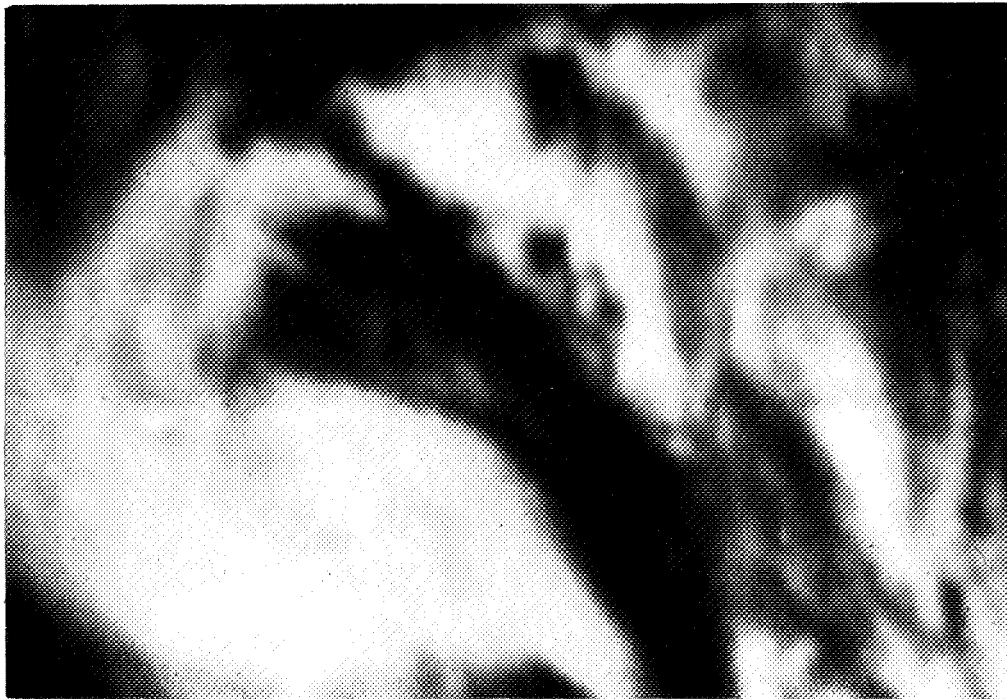


FIGURE 29 CLOUD COVER ON 23 APRIL 1968 (Continued)

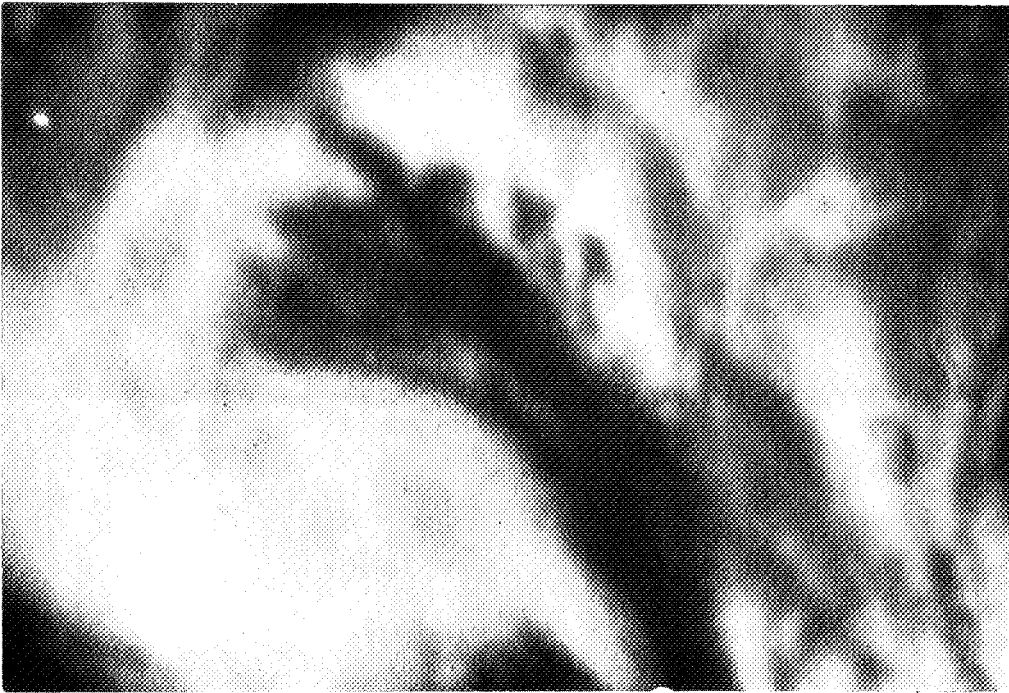
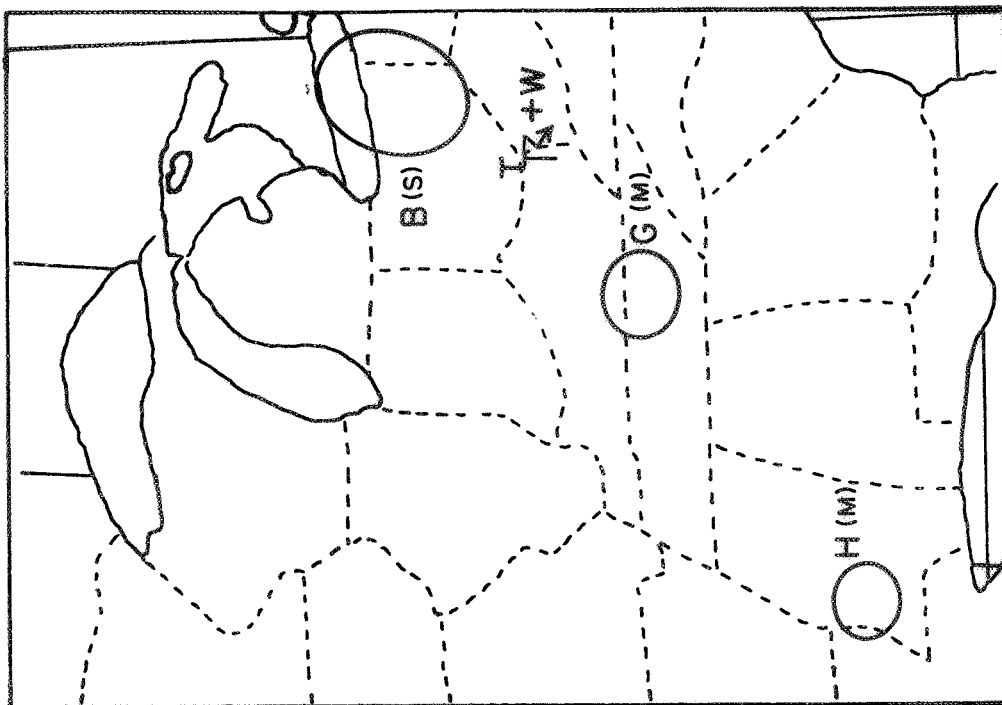
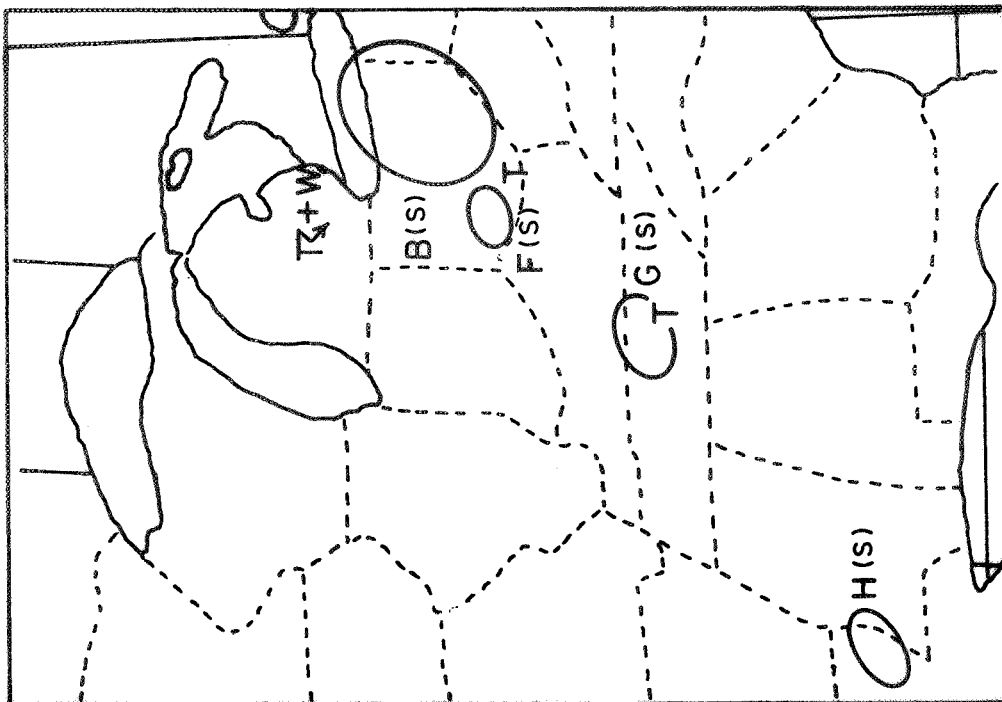


FIGURE 29 CLOUD COVER ON 23 APRIL 1968 (Concluded)



2124 GMT



2056 GMT

An additional cloud element, designated F, could be measured at 1904 GMT. There was weather categorized as moderate associated with Cloud Elements A, D, and F, while severe weather was associated with Cloud Elements B, C, and E. At this time there were two tornadoes associated with Cloud Element B, one tornado with Cloud Element C, a tornado just northeast of Cloud Element E, and a severe thunderstorm with strong winds southeast of Cloud Element C.

The photograph at 1931 GMT shows the same five measured cloud elements as the previous photograph. There are some changes in severe weather distributions since the previous photograph. The tornado in the center of Cloud Element B has apparently dissipated, as has the tornado northeast of Cloud Element E. Weather associated with Cloud Element E has decreased from severe to moderate.

At 1959 GMT, Cloud Element C has merged with the surrounding clouds and could no longer be measured. There are still reports of thunderstorms and winds in southeast Michigan in the area of cloud cover with no distinct cells. Cloud Elements A, D, and F have associated weather categorized as moderate; Cloud Element B has a tornado and a new cloud element, G, also with moderate associated weather, has been added.

The photograph at 2028 GMT shows two reports of thunderstorms and wind in Michigan associated with cloud cover that was not measured. Cloud Element B now has two tornadoes and a funnel cloud. A third tornado just to the southwest, because of the indefinite boundary of Cloud Element B, may or may not be associated with this cloud. Cloud Elements A, F, and G still have associated severe weather based on the classification as listed on the hourly radar summaries, even though there are no reported tornadoes with these clouds listed in the Storm Data bulletins.

At 2056 GMT there is still a report of a thunderstorm with strong winds in southeastern Michigan; Cloud Element B no longer contains a tornado but is still classified as severe, as is Cloud Element F. There is a tornado between Cloud Elements B and F, but the boundary of the specific cloud area with which it is associated is not distinct. This may be the tornado that was previously included within the boundary of Cloud Element B. A tornado is now reported with Cloud Element G and a new cloud element (H), also having associated severe weather, was measured on this photograph.

At 2124 GMT, Cloud Element B still has severe weather associated with it. Cloud Elements G and H only have weather classified as moderate and there is still a tornado in southern Ohio.

C. Cloud Size and Time Changes in Cloud Size Related to Severity of Associated Weather

Whether or not severe weather occurs with a particular cloud depends on a number of factors. Certainly if the synoptic situation is such that any lifting mechanism will rapidly carry moist air to high altitudes, isolated thunderstorms, tornadoes, hail, and so forth may be associated with scattered clouds of relatively small size. On other occasions, numerous convective clouds may form in close proximity. In such events the anvils from the individual clouds may merge and the resulting complexes appear as a single large cloud in ATS photographs. In the case of cold fronts or squall lines that have lifetimes of many hours, a well-developed cirrus canopy may be established, obscuring the formation of small new cells with which severe weather may occur. In this type of situation there may be an extensive area of old cloud, beneath which there may form a new vigorous convective cell producing severe weather. Unless this new cell protrudes above the old cirrus

canopy to such an extent that shadows or its brightness distinguish it from the lower cirrus, it may not be recognizable.

Thus, in many of the ATS photographs where resolution masks details of new cell formation in an area of cloud many hours old, only changes in size of the old cloud area are measurable. As a result, many of the old cells may be dying out and their cirrus plumes evaporating giving the impression of a general decrease in size while an embedded new cell that is not distinguishable may develop rapidly and produce a brief occurrence of severe weather. It is believed that this happened a number of times in cloud elements studied on the six days described previously.

Figure 30 shows time changes in cloud area and severity of associated weather on 23 April 1968. The figure shows a wide variety of sizes and rates of increase in area. The only cloud element that shows a size decrease during the period studied is Cloud Element B. Cloud Elements C, D, E, F, G, and H can be considered to have slow growth rates, Cloud Element A to have a moderate growth rate, and Cloud Element B to have a rapid growth rate between 1845 and 1930 GMT.

There is no marked tendency for the initially larger clouds to be more likely to have tornadoes (although at its maximum size Cloud Element B did have two tornadoes plus a funnel cloud). Also a cloud may have had associated severe weather when it was relatively small and only weather in the moderate category as it grew larger, e.g., Cloud Elements E, G, and H. Severity is not dependent on growth rates either. Therefore, size or growth rate does not seem to be a unique criteria for specifying whether a given cloud will or will not produce severe weather.

Similar figures were plotted for the other five days studied; however, because of the similarity of the relationships on the six days, it is felt that this one illustration suffices to categorize all six days.

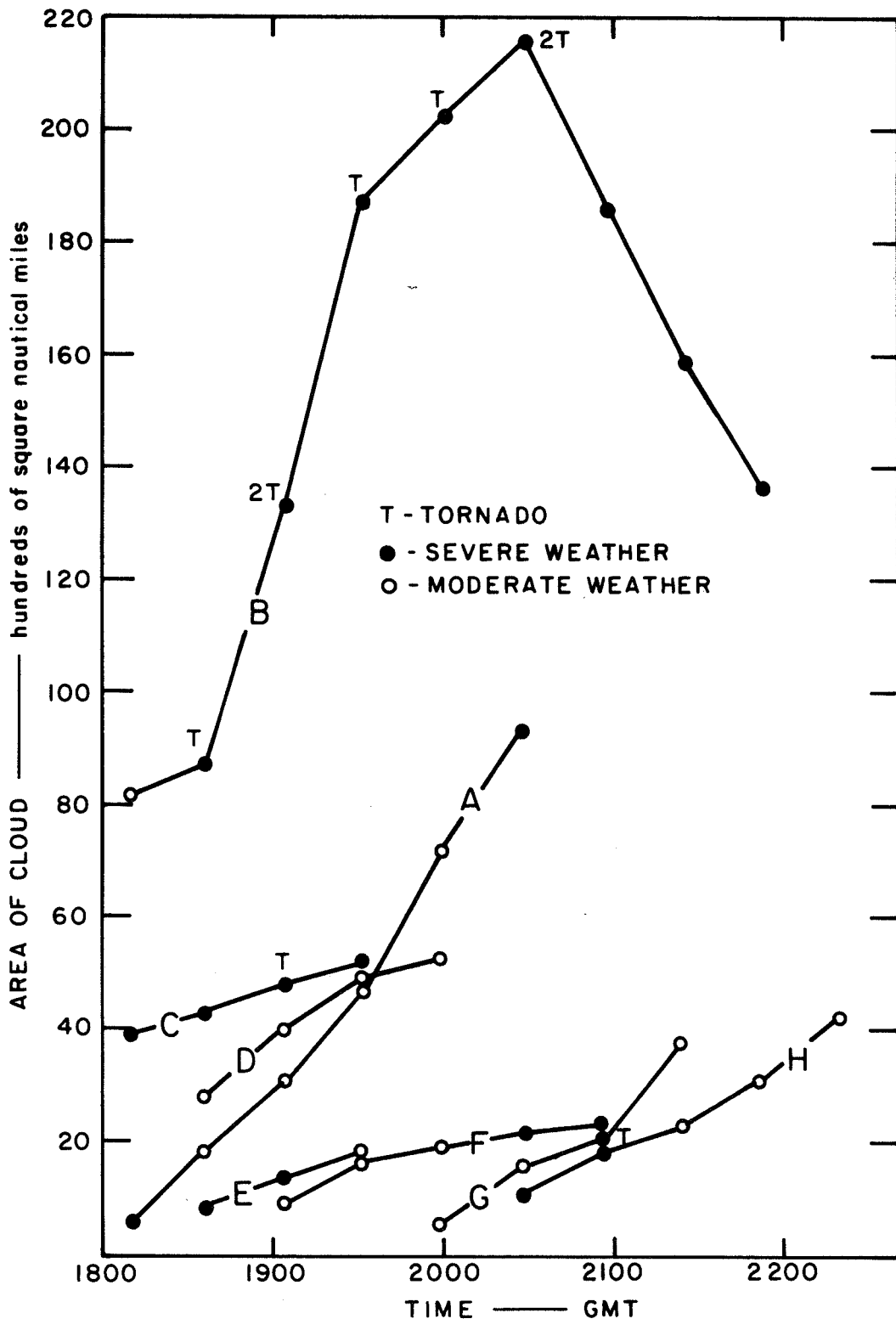


FIGURE 30 TIME CHANGES IN CLOUD AREAS AND SEVERITY OF ASSOCIATED WEATHER ON 23 APRIL 1968

Figure 31 provides information on the weather categories and size of cloud elements similar to that shown on Figure 30. The figure shows that measured cloud areas cover a wide range and on any given day there are cells of similar size with dissimilar weather categories:

- On 28 April, cloud elements with areas less than 1000 square miles had associated weather categorized as moderate, while cloud elements with areas ranging from about 1500 to 4000 square miles had associated weather in the moderate or severe category.
- On 17 April, the cell sizes ranged from 300 to 6000 square miles and the associated weather was of light intensity or reported no echoes at all. The larger clouds reported no echo.
- Data for 18 April show cloud areas from 600 to 3000 square miles with associated weather in each of three categories, though not of severe intensity.
- On 19 April, the sample of clouds associated with severe weather fall near the middle of the area range (1500 to 4000 square miles). Clouds associated with weather in the moderate category ranged from 300 to 9000 square miles. No lesser intensities were reported.
- On 30 April, clouds having areas of less than 2050 square miles were associated with weather in the light category or with no echo. Above this value the associated weather ranges in intensity from light to moderate to severe.

Data for 23 April have been discussed in detail previously. On this date, clouds larger than those on the other five days were measured. All of the cloud elements with areas greater than 9000 square miles had

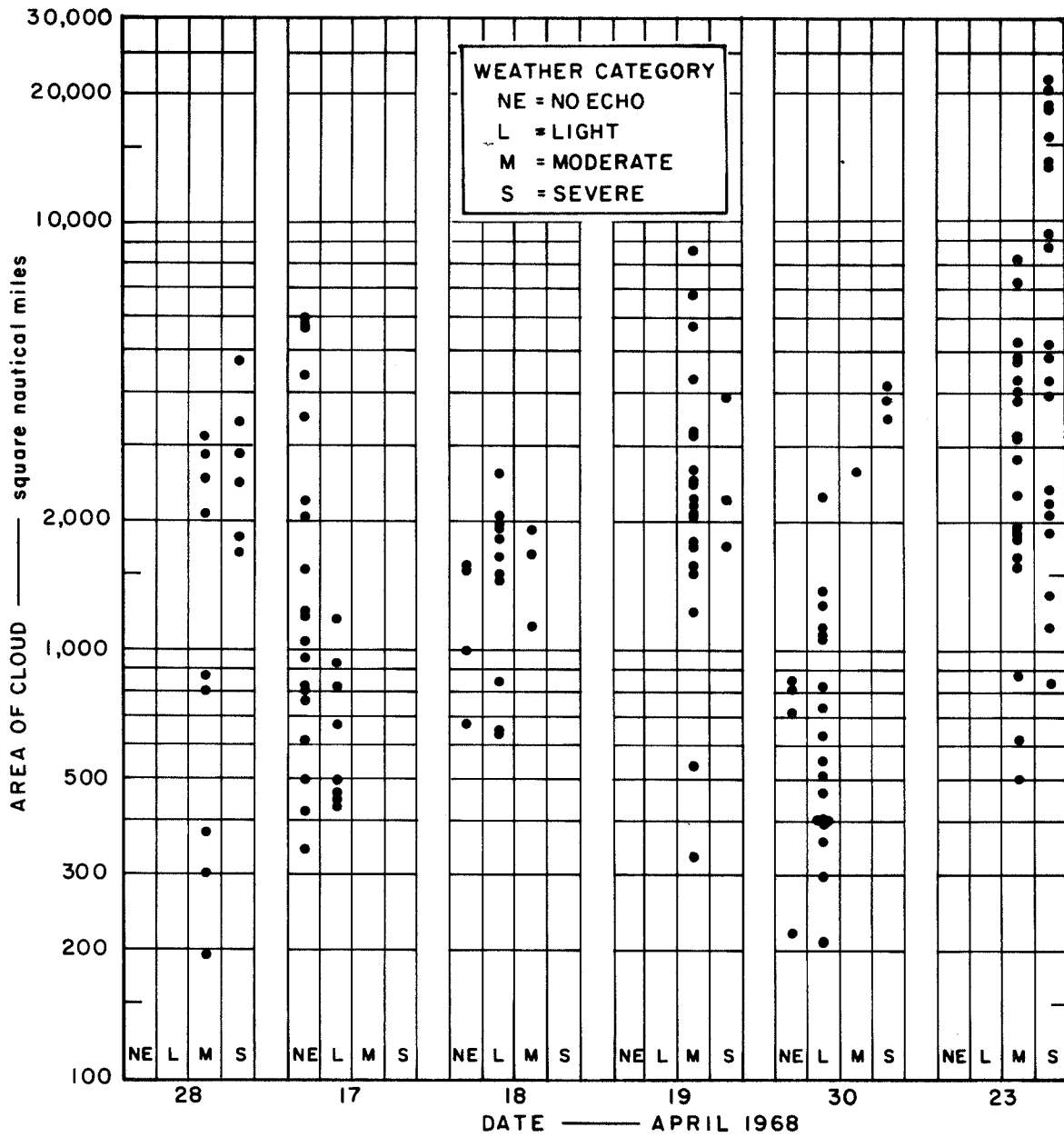


FIGURE 31 WEATHER CATEGORIES ASSOCIATED WITH CLOUD ELEMENTS OF VARIOUS SIZES

severe weather. This area would correspond closely to that of a circle of diameter slightly less than 2° of great circle arc (actually 1.8°). Other investigators (Boucher, 1967; Merritt and Smith, 1969) have noted a tendency for the largest (diameters of 2 to 2.5°) cloud areas identified as cirrus canopies to have associated severe weather. Clouds between 500 and 10,000 square miles in area were associated with either moderate or severe intensity. No lesser intensities were reported.

In this comparison of cloud size and severity of associated weather, the days were considered separately since we feel that there is probably enough difference in instability and type of cloud cover on the various days to completely obscure any weak relationship if the days were consolidated and treated as a single sample. For example, if data for all days were combined, the large clouds associated with no echo on 17 April (a day with rather stable conditions) would be mixed in with the clouds of comparable size on 19 April (when the associated weather was categorized as moderate). This would result in a graph showing absolutely no relationship between cloud size and associated weather.

Obviously the cloud size on any particular day must be related to an intimate knowledge of that day's synoptic situation (especially instability) if one hopes to have any chance of specifying whether a cloud of a given size may produce severe weather. Further, the cloud history of the area being examined must be known to determine whether earlier convective activity has produced cirrus canopies. Such canopies may obscure the development of new convective cells that could cause severe weather, whether the initial cirrus canopy were still increasing in size or were gradually dissipating.

D. Cloud Motion and Growth Related to Wind Shear

The direction of movement of the measured cloud elements was compared with the direction of the wind shear between the 900- and 300-mb levels. Data from the closest radiosonde station (in space and time) was used but in certain cases these data were up to six hours and several hundred miles from the measured clouds. Figure 32, which is a scatter diagram of the two sets of data, shows that the majority of the measured cloud elements moved in a direction to the left of the direction of the shear. That is, there is a clustering of points in the vicinity of a direction of movement of about 240° and a direction of shear of 270° .

A comparison of the distribution of points on this figure with the severity of weather shows that the more severe storms (coded 4 and 5) tend to have directions of motion closer to the direction of shear than the clouds with less severe weather.

Figure 33 compares average growth rates of measured cloud elements with the speed (in knots) of the wind shear between the 900- and 300-mb levels. The figure shows that growth rates are scattered over the entire range of observed speed shears. No correlation between growth rate and speed of wind shear is evident.

E. Summation

The comparison of growth rates of cloud areas with the severity of the attendant weather showed that neither size nor size changes in cloud area were unique indicators of weather severity. Of the largest clouds measured (in excess of 9000 square nautical miles), all had associated severe weather. Clouds smaller than this size were equally likely to have light to moderate associated weather or even no echo. The smallest cloud area measured (less than 200 square nautical miles) had associated weather in the moderate category.

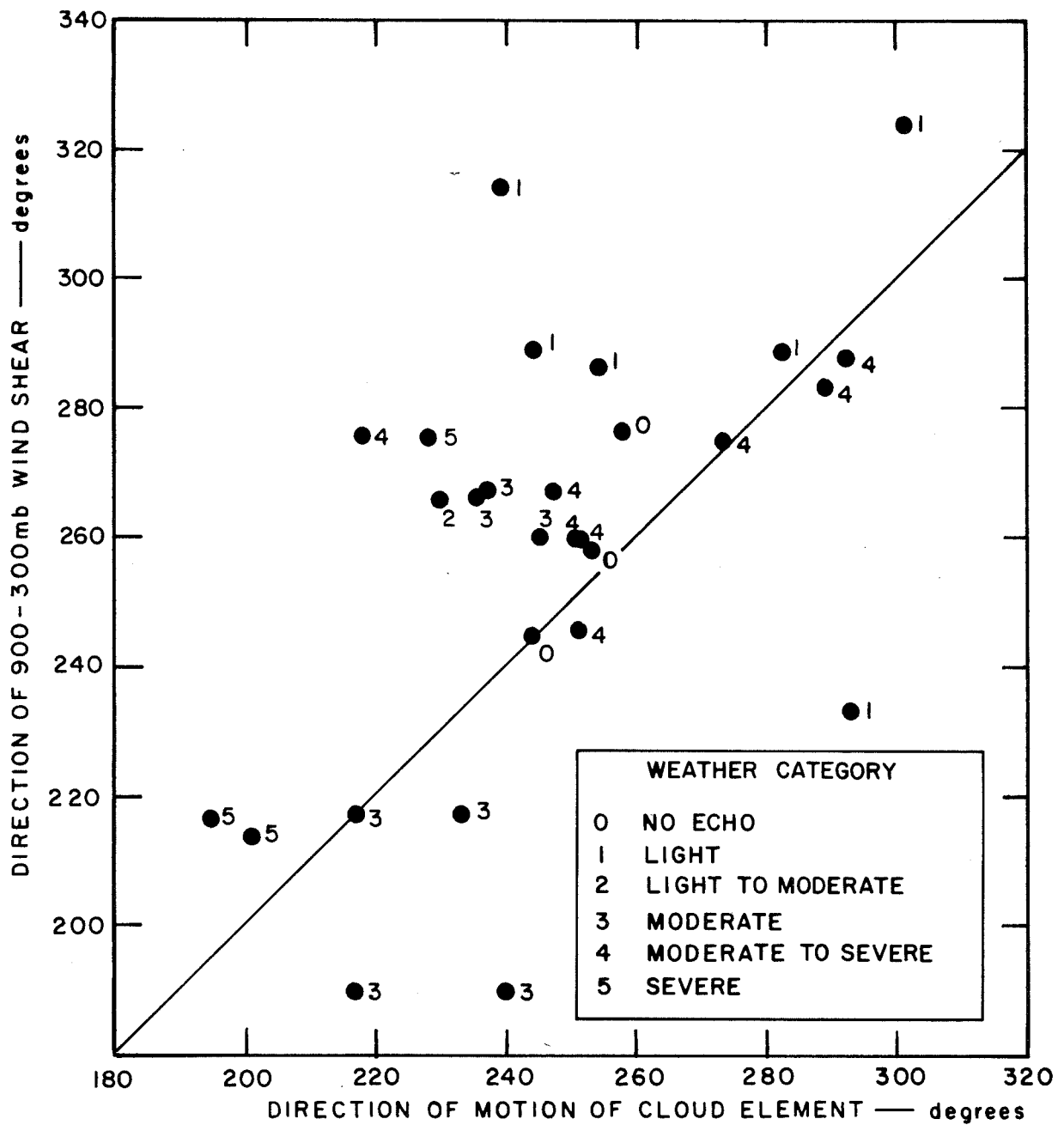


FIGURE 32 COMPARISON OF DIRECTION OF CLOUD MOTION AND DIRECTION OF WIND SHEAR

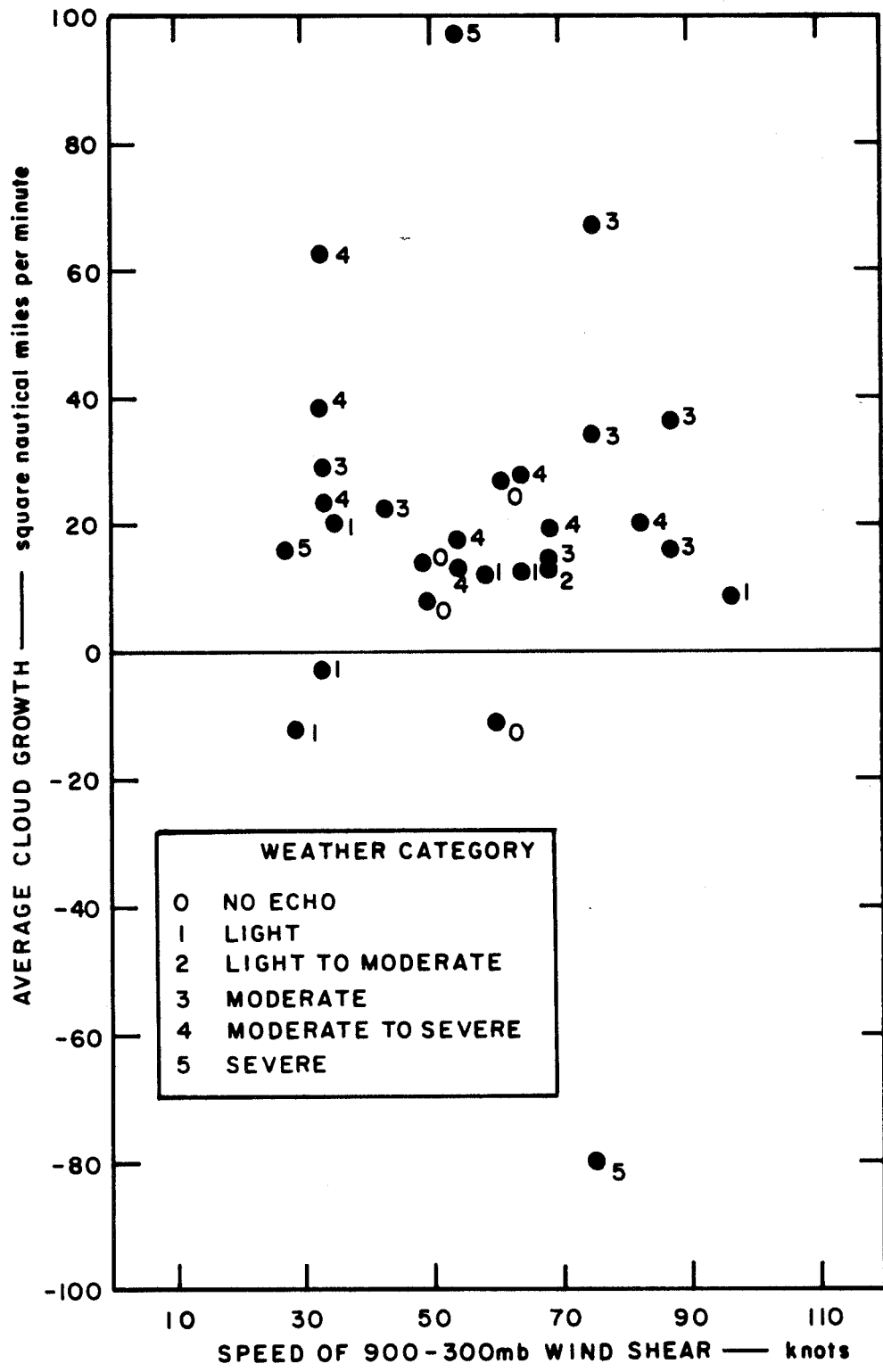


FIGURE 33 COMPARISON OF CLOUD GROWTH AND SPEED OF WIND SHEAR

No definite relationship was found between severity of weather associated with a cloud and wind shear but possible relationships may have been obscured by the distance (in space and time) between the measured cloud and the locations of measured winds.

REFERENCES

Anon., Storm Data, Vol. 10, No. 4, U.S. Dept. of Commerce, ESSA, Asheville, North Carolina (1968).

Boucher, R. M., 1967: "Relationships Between the Size of Satellite Observed Cirrus Shields and the Severity of Thunderstorm Complexes," J. Appl. Meteor., Vol. 6, No. 3, pp. 564-572.

Kaltenbach, J. L. (Compiler), 1969: "Science Report on the 70-Millimeter Photography of the Apollo 6 Mission," NASA S-217, Earth Resources Division, Science and Applications Directorate, Manned Spacecraft Center, Houston, Texas.

Merritt, E. S. and W. P. Smith, 1969: "Satellite-Observed Characteristics of Severe Local Storms," Preprints of Papers Presented at the Sixth Conference of Severe Local Storms. Boston Amer. Meteor. Soc., pp. 208-217 (Unpublished Manuscript).

Serebreny, S. M., W. E. Evans, R. G. Hadfield, and E. J. Wiegman, 1967: "Detection of Cloud Displacement Using Video Techniques," Final Report, ESSA Contract E-167-67-(n), SRI Project 6672, Stanford Research Institute, Menlo Park, California.

Serebreny, S. M., R. G. Hadfield, R. M. Trudeau, and E. J. Wiegman, 1969: "Comparison of Cloud Motion Vectors and Rawinsonde Data," Final Report, ESSA Contract E-193-68, SRI Project 7257, Stanford Research Institute, Menlo Park, California.

Serebreny, S. M., E. J. Wiegman, and R. G. Hadfield, 1970: "Further Comparison of Cloud Motion Vectors with Rawinsonde Observations," Final Report, ESSA Contract E-210-69(N), Stanford Research Institute, Menlo Park, California.

Shenk, W. E. and E. R. Kreins, 1970: "A Comparison Between Observed Winds and Cloud Motions Derived from Satellite Infrared Measurements," J. Appl. Meteor., Vol. 9, No. 4, pp. 702-710.

Evans, W. E. and S. M. Serebreny, December 1969: "Construction of ATS Cloud Console," Final Report, Contract NAS5-11652, SRI Project 7711, Stanford Research Institute, Menlo Park, California.